TRIBHUVAN UNIVERSITY

INSTITUTE OF ENGINEERING

PULCHOWK CAMPUS

THESIS NO: T07/079

Crash Reconstruction and Head Injury Assessment in Motorcycle-Truck Collisions: A Case Study

by

Hem Paudel

A THESIS

SUBMITTED TO THE DEPARTMENT OF CIVIL ENGINEERING

IN PARTIAL FULFILLMENT OF THE REQUIREMENTS FOR THE

DEGREE OF MASTER OF SCIENCE IN TRANSPORTATION ENGINEERING

DEPARTMENT OF CIVIL ENGINEERING

LALITPUR, NEPAL

MAY, 2026

COPYRIGHT

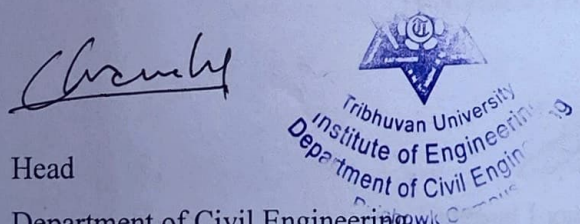

Head
Department of Civil Engineering
Pulchowk Campus, Institute of Engineering
Lalitpur, Kathmandu
Nepal

TRIBHUVAN UNIVERSITY

INSTITUTE OF ENGINEERING

PULCHOWK CAMPUS

DEPARTMENT OF CIVIL ENGINEERING

The undersigned certify that they have read and recommended to Institute of Engineering for acceptance, a thesis entitled **"Crash Reconstruction and Head Injury Assessment in Motorcycle-Truck Collisions: A Case Study"** submitted by Hem Paudel. in partial fulfillment of the requirement for degree of Master of Science in Transportation Engineering.

.....

Supervisor: Dr. Rojee Pradhananga
Assistant Professor
Institute of Engineering

.....

External Examiner: Mr. Hemant Tiwari
General Secretary
Society of Transport Engineers Nepal

.....

Program Coordinator: Mr. Anil Marsani
M.Sc. Transportation Engineering
Department of Civil Engineering

Date: ..11.May.2026.....

ABSTRACT

Road traffic crashes are a very serious public safety concern across the world and motorcyclists are disproportionately at risk of injuries and fatality. In Nepal, two-wheelers accounted 80.9% of vehicle registration in 2024, raising road safety issues in populated places such as Kathmandu valley. Despite this, comprehensive crash reconstruction and injury analysis of motorcycle-truck collisions remain largely unstudied in the Nepalese context. This study is based on a fatal motorcycle-truck crash in Kathmandu valley reconstructed through a dual-simulation framework Macroscopic reconstruction of vehicle dynamics was done using PC-Crash software and microscopic assessment of head injury using LS-DYNA. The crash involved a two-occupant motorcycle colliding with heavy truck resulting in riders' fatality and severe injuries to the pillion rider. Police records served as primary data sources complemented with road geometry and vehicle specifications.

The PC-Crash model reproduced pre-impact maneuvers, collision dynamics, and post-impact trajectories through iterative calibration against physical crash evidence, establishing pre-impact speeds of 34 km/h for the truck and 18 km/h for the motorcycle. The validated kinematic outputs were transferred to LS-DYNA as initial boundary conditions for finite element head impact analysis. Using a standardized pedestrian headform impactor and a two-component helmet model with appropriate material properties and contact definitions, the unprotected simulation produced a peak resultant acceleration of 190g and HIC_{15} of 1403, corresponding to AIS 4 (Severe). Introduction of the helmet reduced peak acceleration to 103g and HIC_{15} to 689 (AIS 2), representing a 50.9% reduction in injury severity. This study provides preliminary proof-of-concept evidence for a multi-scale simulation approach for crash analysis in the Nepalese context. Findings are indicative of head injury mechanisms in motorcycle-truck collisions and may inform future multi-scale investigations. Given the single- case scope, results should not be generalized or treated as independent policy directives: rather they establish a methodological foundation for more comprehensive studies.

Keywords: Motorcycle crash reconstruction, PC-Crash, Finite element analysis, Head injury assessment, Traffic safety, LS-DYNA, HIC criterion

ACKNOWLEDGMENT

I would like to express my sincere gratitude to my supervisor, Dr. Rojee Pradhananga, for her consistent guidance, constructive feedback, and unwavering support throughout the course of this thesis. Her expertise and commitment to academic excellence have been invaluable in shaping the direction and quality of this study.

I am equally grateful to our Program Coordinator, Mr. Anil Marsani, and to Dr. Pradeep Kumar Shrestha for their insightful suggestions, encouragement, and assistance during the various phases of this study. Their professional perspectives and timely guidance have significantly contributed to the refinement of the work presented herein.

I also extend my appreciation to my friends and peers, whose support, shared knowledge, and constructive discussions have greatly enriched my understanding of the subject matter and facilitated the successful completion of this thesis.

Name: Hem Paudel

Roll No: 079MsTrE007

TABLE OF CONTENTS

LIST OF FIGURES

LIST OF TABLES

LIST OF ABBREVIATIONS

ABS	Acrylonitrile Butadiene Styrene
AIS	Abbreviated Injury Scale
ATD	Anthropomorphic Test Device
CAD	Computer Aided Design
ELFORM	Element Formulation
EPS	Expanded Polystyrene
FE	Finite Element
FEA	Finite Element Analysis
FEM	Finite Element Modeling
GIS	Geographic Information System
HIC	Head Injury Criteria
KSI	Killed or Seriously Injured
LSTC	Livermore Software Technology Corporation
MADYMO	Mathematical Dynamic Model
NHTSA	National Highway Traffic Safety Administration
POI	Point of Impact
PTW	Powered Two-Wheeler
RTA	Road Traffic Accident
SMP	Shared Memory Parallel
WHO	World Health Organization

CHAPTER 1: INTRODUCTION

1.1 Background

Road traffic safety is a major concern in the present global context. Road crashes are one of the leading factors in injury, death, and property damage, affecting millions of lives worldwide. It has become a critical safety issue, causing significant economic and social impacts each year. The rapid rise in motorization and unplanned urbanization has escalated the complexity of overall traffic systems in developing countries, where road traffic safety measures often lag behind the pace of development (Wisutwattanasak et al., 2026).

According to the World Health Organization, Global Status Report on Road Safety, it was estimated that in 2021 there were 1.19 million road traffic crash deaths, representing 15 deaths per 100,000 population (WHO, 2023). Based on this study, Children and young people aged 5-29 years are the most likely to lose their life from road traffic injuries, with motorcycle riders and other powered two and three-wheelers causing 30% of all road traffic deaths and four-wheelers causing 25% of fatalities. The majority of road traffic crash deaths, around 92% occur in countries with low or middle incomes. The difference in death rates can be partly explained by the limited road safety infrastructure and insufficient enforcement of traffic regulations, even in the presence of relatively low vehicle density.

In recent years, the registration of motor vehicles has considerably increased in Nepal in relation to the rising transportation needs and economic growth. In 2024, Nepal registered a total of 242,441 vehicles, though overall registrations witnessed a general decline. Two-wheelers dominated the market, with motorcycles alone accounting for 80.9 percent (196,221 units) of total registrations, driven by their affordability, ease of use, and suitability for Nepal's challenging terrain. (Department of Transport Management, GoN, 2025) This trend highlights the increasing influence of two-wheelers in Nepal and their crucial importance in fulfilling the mobility demands. With the growth of the number of vehicles, the transportation environment experiences unprecedented pressure, and it plays quite a significant part in increasing the number of road traffic crashes.

Nearly 160,000 road traffic crashes occurred in Nepal from 2015 to 2024, killing 23,900 people and leaving 50,000 seriously injured (Ghimire et al., 2025; Nepal Traffic Police, 2024), an average of seven deaths and 83 injuries each day. The economic impacts have been estimated as 1.5-2% of the GDP, for the year 2021, which is higher than the national health expenditure (Asian Transport Observatory, 2025). In the Kathmandu valley, motorcycles are responsible for 70-80% of crashes, while they represent 68% of the total number of motorcycle crash fatalities in the country (Ghimire et al., 2025). The death rate of 28.2 per 100,000 is much higher than the Asia-Pacific average of 15.2, rising at 5.4% per year from 2016 to 2021, which puts Nepal well off track to meet the global Decade of Action target of cutting road deaths by 50% by 2030 (Asian Transport Observatory, 2025; WHO, 2023).

Crash severities vary from minor collisions causing vehicle damage to severe crashes resulting in fatalities and long-term disabilities. The severity of a crash depends on multiple factors, including speed, road conditions, driver behavior, and vehicle type. In Nepal, road crash often led to serious injuries due to inadequate emergency medical response, poorly maintained roads, and a lack of safety measures such as seatbelt and helmet enforcement.

Given the rising number of road traffic crashes, systematic crash analysis has become essential for understanding collision patterns, identifying high-risk conditions, and informing targeted safety interventions. However, conventional crash reporting and statistical analysis alone are insufficient for capturing the complex mechanics underlying individual crash events-particularly the biomechanical processes that determine injury severity at the occupant level. This limitation has driven growing interest in computational simulation as a complementary investigative tool. In crash reconstruction, software such as PC-Crash enables accurate modeling of vehicle trajectories and collision dynamics, while finite element analysis platforms such as LS-DYNA allow for detailed examination of structural deformation and occupant injury response under impact loading. Together, these tools provide engineers, researchers, and policymakers with a rigorous, reproducible method for understanding how crashes occur and why certain conditions produce fatal outcomes - forming the methodological foundation of the present study.

1.2 Problem Statement

Motorcycle collisions with heavy vehicles represent an extremely severe crash typology, which is due to the large difference in weight between the two vehicles (a fully loaded truck can be more than 20,000 kg while the motorcycle-rider combination is about 200-250 kg on impact, with almost all the kinetic energy transferred to the motorcycle and rider). This severity is supported by empirical evidence as shown in the research of Chang et al (2016) which found that the probability of being killed as a motorcycle rider around 80% higher when involved in a collision with a heavy vehicle than in other types of collisions, with 91-94% of heavy vehicle collisions resulting in severe injuries.

Structurally, this biomechanical vulnerability exists in the prevailing traffic condition of Nepal, where motorcycles and heavy goods vehicles run in undivided, mixed-flow carriageways within urban environments. However, thorough analysis of this crash type is markedly limited by Nepal's inadequate crash data infrastructure, which sees only 60% of traffic incidents recorded by official police, and features insufficient documentation of contributory factors in 58% of recorded crashes, and an absence of disaggregated data on crash typology by vehicle-type pairing (Bhatta et al., 2024; Khadka et al., 2022). The underreporting is so significant that WHO uses modelled estimates instead of known national figures. Given the lack of reliable statistical data, physics-based crash reconstruction, when systematically applied to documented real world crashes, is the most methodologically sound approach to understanding the mechanical causes of occupant injury in motorcycle-heavy vehicle crashes, and is the analytical framework used in this study.

Kathmandu valley, as the most densely populated and economically active urban region of Nepal, faces a severe and escalating road safety crisis driven predominantly by the rapid proliferation of motorcycles. Motorcycles constitute the primary mode of transportation in the valley, yet they remain the most vulnerable vehicle category in the traffic system, consistently associated with the highest rates of crash-related fatalities and serious injuries. Statistical records from the Metropolitan Traffic Police Division consistently indicate a disproportionate rise in two-wheeler-involved crashes over recent years, with a substantial proportion resulting in severe physical harm or death. While helmet use is mandatory for both motorcycle drivers and passengers(Government of Nepal, 1993) compliance rates among passengers remains critically low (Siebert et al., 2021), leaving them directly

exposed to head impact forces during collisions. Beyond helmet non-compliance, interacting factors including high traffic density, poorly maintained road surfaces, heterogeneous vehicle interactions, and risky rider behavior further compound the vulnerability of motorcyclists in this environment.

Despite magnitude of this problem, existing research in Nepal remains largely confined to broad statistical reporting of crash frequency and fatality counts. Detailed, case-level study on the mechanics of individual crash events remains scarce, and the biomechanical processes by which a collision translates into a specific head injury are not well understood in the local context. This evidential deficiency substantially undermines the capacity of policymakers, engineers, and road safety practitioners to identify the most consequential crash scenarios and design targeted, empirically grounded interventions calibrated to reduce preventable injury burden.

Computational simulation offers a rigorous and reproducible methodological framework for investigating crash mechanics at a resolution that is neither practically feasible nor ethically permissible through physical experimentation. PC-Crash, a widely validated multi-body dynamics platform (Steffan & Moser, 2011) enables accurate reconstruction of pre-impact vehicle trajectories and collision dynamics, while LS-DYNA's finite element analysis facilitates high-fidelity modeling of occupant head response, and injury assessment under impact loading condition (T. Nguyen & Dinh, 2025). However, the integrated application of these two platforms for motorcycle crash reconstruction has not been explored in the Nepalese context. Most simulation-based crash studies addressing South Asian Road conditions are either limited in scope focusing on vehicle dynamics alone without analytical injury assessment or are derived from crash databases that do not reflect the specific vehicle types, road geometries, and riding behaviors prevalent in Kathmandu valley.

This study addresses this gap by reconstructing one documented motorcycle-truck crash case from Kathmandu valley using a coupled PC-Crash and LS-DYNA simulation framework. By examining helmet conditions and their effect on key biomechanical injury metrics, including peak head acceleration and the Head Injury Criterion (HIC) the study aims to generate quantitative, case-specific evidence on head injury mechanisms in high-severity crashes. The findings are intended to establish a preliminary empirical basis from which more comprehensive multi-case investigations can be developed. Given the case-

specific character of the study, conclusions pertaining to helmet performance and enforcement policy should be interpreted as indicative rather than prescriptive, serving as a scientific foundation for future large-scale studies rather than as independent policy directives.

1.3 Objective

The primary objective of this study is to reconstruct, evaluate, and analyze a two-wheeler involved crash incident using numerical simulation tools.

Specific objectives:

1. To reconstruct a documented crash case involving two wheelers using simulation tools, ensuring realistic representation of collision kinematics and dynamics
2. To quantify the influence of helmet condition on head injury severity outcomes, providing analytical evidence relevant to safety interventions.

1.4 Scope of Study

In this study, the dual-simulation technique is used to reconstruct and examine truck-motorcycle collision situations. PC-Crash software is used to simulate vehicle paths and the general dynamics of a collision, whereas LS-DYNA is used to perform in-depth finite element modeling of essential parts of the system, such as the head, helmet, and truck structure, with detailed material properties and contact interaction models.

The study involves a number of major technical domains: the development of finite element models, mesh optimization procedures, contact definition procedures, and post-process procedures. Crash behavior and occupant injury are measured based on the kinematic parameters, biomechanical injury measure of peak accelerations and Head Injury Criterion (HIC).

It is clearly restricted to computational simulation and analysis. The experimental validation, broader traffic safety policies and epidemiological considerations are beyond the scope of this investigation as they are subjected to physical crash testing. Such a detailed methodology permits the detailed investigation of the collision dynamics and the mechanisms of injury by use of sophisticated numerical methods.

1.5 Significance of the Study

This study integrates PC-Crash and LS-DYNA to reconstruct motorcycle-truck crashes, enabling detailed examination of occupant kinematics and injury assessment that physical experimentation alone cannot provide. By quantifying head acceleration and Head Injury Criterion (HIC) values across varying helmet and impact conditions, it delivers precise, evidence-based prediction of injury severity.

The findings provide case-specific analytical evidence that may support future improvements in helmet standards and traffic safety enforcement in Nepal. Although based on a single-case simulation, the generated injury metrics contribute to the limited data-driven evidence available in the region. The dual-platform methodology also establishes a replicable framework for future crash reconstruction studies across South Asia.

1.6 Organization of Chapters

This thesis is organized in the following way:

CHAPTER 1: Introduction- includes an overview of the study background, the problem statement, objectives and scope of the study, and its significance.

CHAPTER 2: Literature Review- Includes previous studies relevant to crash reconstruction, finite element analysis, and primary factors affecting crash investigation.

CHAPTER 3: Research Methodology- Provides a detailed description of the overall study approach and the specific methods and techniques employed. This chapter explains the data collection procedures, analytical tools, and experimental or simulation processes used to address the study objectives.

CHAPTER 4: Result and Discussion- contains the interpretation and discussion of the study.

CHAPTER 5: Conclusion and Recommendations- provides an overview of major findings of this study and some suggestions concerning possible ways of future development.

References are provided at the end of the report.

CHAPTER 2: LITERATURE REVIEW

2.1 Overview of Relevant Literature

Road traffic crashes involving Powered two-wheelers (PTWs) represent a complex, multi-factorial safety challenge that spans vehicle dynamics, human behavior, infrastructure design, and assessment. The literature reviewed in this chapter is organized around five interconnected themes relevant as a case-specific reference: the characteristics and urban crash risks of two-wheelers; biomechanical injury criteria, specifically the Head Injury Criterion (HIC); the contributing factors to two-wheeler crash severity; injury patterns documented in PTW fatality studies; and crash reconstruction techniques, including simulation-based approaches using PC-Crash and LS-DYNA.

Globally, PTW users face disproportionately high fatality rates per kilometer traveled compared to car occupants, with head injury consistently identified as the primary determinant of fatal outcomes (Lin & Kraus, 2009; Van Elslande & Elvik, 2012). In Nepal specifically, the dominance of motorcycles in the vehicle fleet accounting for over 80% of new registrations in 2024, makes this a particularly acute national concern (Department of Transport Management, GoN, 2025). Despite this, simulation-based studies investigating motorcycle crash assessment in the Nepalese context remain extremely limited, representing a significant gap that the present study seeks to address.

Road traffic crashes are among the leading global causes of death and serious injury, with PTWs disproportionately involved (Sulaie, 2025). Studies conducted across more than 500,000 km of road in 80 countries found that fewer than one-third of roads meet a three-star safety rating, with the proportion dropping further on higher-speed corridors where injury risk is greatest (iRAP, 2021). Traffic congestion has also been shown to positively correlate with the frequency of killed or seriously injured (KSI) crashes, while having comparatively little effect on minor injury events (Kononen et al., 2011; C. Wang et al., 2011)).

2.2 Two Wheelers Characteristics in Urban Environment

In urban environments, limited road space forces various transportation modes; pedestrians, powered and non-powered two-wheelers, passenger cars, and public transport-to interact frequently, often creating risky situations that contribute to the high incidence of traffic crashes. PTWs, while integral to the traffic system, deviate from passenger car standards and require tailored safety measures (Van Elslande & Elvik, 2012). Regardless of geographic context, PTW users face disproportionately high road risks, with a much greater likelihood of being killed or severely injured per kilometer traveled compared to car occupants (van Elslande et al., 2015).

Fatal injury analyses have shown a strong correlation between head injuries and other severe trauma types such as chest injuries, internal organ damage, and limb injuries, among PTW crash victims (Marković et al., 2016). Helmets, particularly integral designs with full facial protection, have been shown to significantly reduce the risk of severe head injuries and fatalities (Thompson et al., 1999). However, helmet design features such as noise, ventilation, temperature regulation, field of vision, and size can influence rider perception and comfort (Orsi et al., 2012).

Given that head and neck injuries are among the most critical determinants of fatal outcomes in PTW crashes, many studies have focused on biomechanical injury criteria for these regions when evaluating motorcyclist impacts against roadside infrastructure (Lopez-Valdes et al., 2005). Helmets remain an effective countermeasure, reducing both the likelihood and severity of head injuries that could otherwise lead to long-term impairment or death (Gabella et al., 1994).

Recent research in motorcycle safety has employed the Head Injury Criterion (HIC) to quantify head injury risk and evaluate protective measures (Narayan Yoganandan et al., 2015). Experimental studies using Hybrid III headforms demonstrated that certified helmets can reduce HIC values by up to 92% compared to unhelmeted conditions, although the added mass may slightly increase rotational injury risk (Lloyd, 2025). Comparative analyses of HIC and BrIC across full-face, open-face, and half-coverage helmets highlighted the limitations of conventional helmet designs in mitigating rotational brain injuries (Chaichan et al., 2020; Radzuan et al., 2024). Furthermore, finite-element simulations have shown that motorcycle structural features, such as engine or air filter

positioning, can alter HIC_{15} values by ±21%, emphasizing the influence of vehicle design on head injury assessment (Mohd Jawi et al., 2021; Narayan Yoganandan et al., 2015).

In the South Asian context, and particularly in Nepal, the dominance of motorcycles in urban transport networks creates a road safety environment that is structurally distinct from those studied in high-income countries. Nepal's road network is characterized by narrow carriageways, mixed traffic composition, limited lane discipline, and inadequate roadside infrastructure conditions that amplify the crash risk for two-wheeler riders. Despite this, systematic biomechanical crash studies specific to Nepal remain scarce, with most available data limited to aggregate fatality statistics from Nepal Police annual reports and the Department of Roads. This absence of case-level, mechanics-based evidence represents a critical knowledge gap that the present study addresses through simulation-based reconstruction of a documented crash from Kathmandu valley.

2.3 Head Injury Criteria (HIC)

The Head Injury Criterion (HIC) is one of the most widely used biomechanical metrics for assessing the likelihood of head injury in impact events (Shunfeng Li, 2022). It quantifies injury risk based on the relationship between the magnitude and duration of the resultant linear acceleration experienced at the head's center of gravity during a collision (Fernandes, 2012).

Originally developed in the early 1970s through animal studies, cadaver experiments, and anthropomorphic test device (ATD) tests, the HIC is rooted in two principal head injury mechanisms: (1) inertial brain injury, resulting from rapid acceleration or deceleration that causes the brain to move relative to the skull, potentially leading to diffuse axonal injury, intracranial hemorrhage, or concussion; and (2) localized skull trauma, arising from concentrated impact forces capable of fracturing the skull and directly damaging brain tissue.

The Head Injury Criterion (HIC) can be calculated mathematically from the linear acceleration of the head's center of mass over a specific time interval during impact. The most common formulation is shown in Equation 2.1.

$$HIC=Max_{t1,\,t2}\left[(t_2-t_1)\left(\frac{1}{t_2-t_1}\int_{t_1}^{t_2}a(t)dt\right)^{2.5}\right] \quad \text{…..……(2.1)}$$

Where:

a(t) = resultant linear acceleration at the head's center of gravity (in g, 1 g = 9.81 m/s²),

t_1, t_2= start and end times of the chosen time interval (seconds),

$t_2-t_1 \leq$ the evaluation window (e.g., 15 ms for HIC_{15} or 36 ms for HIC_{36}).

The exponent 2.5 reflects empirical correlation between acceleration severity and injury probability

The calculation seeks the time interval that produces the maximum value of the criterion, reflecting the most severe acceleration pulse within the impact.

A study by Qiu et al (2020) leveraged NHTSA's injury risk functions to link HIC values to AIS-based injury severity. Their findings are shown in Table 2.1 below;

Table 2.1 AIS Based Injury and Corresponding HIC Ranges

AIS Level	**HIC Range**
None or Minor	HIC < 250
Moderate (AIS 2)	250<HIC < 750
Major (AIS 3)	750<HIC < 1250
Severe (AIS 4)	1250<HIC < 1750
Critical/Fatal	HIC > 1750

2.4 Factors Contributing to Two-Wheeler Crashes

The severity of two-wheeler crashes is influenced by a combination of behavioral, environmental, and vehicle-related factors (D. V. M. Nguyen et al., 2021). The body of literature reviewed consistently identifies a core set of variables that significantly elevate crash severity risk. Table 2.2 summarizes the significant factors identified across key studies, each supported by empirical evidence linking the factor to increased injury severity or fatality likelihood.

Table 2.2 Overview of the Factors Contributing to Two-Wheeler Crashes

Authors	Significant Factor
(Keall & Newstead, 2012)	Higher level of congestion
(Al-Zubaidi et al., 2022)	aggressive driving, speeding, and no traffic control
(Brown et al., 2021)	speed, distraction, and observation error
(Rifaat et al., 2012)	alcohol impairment and speeding
(Tay & Rifaat, 2007)	type of vehicles, road characteristics, the type of collision
(Naqvi & Tiwari, 2017)	Collision type, time of the day, number of vehicles
(Ahmed et al., 2016)	helmet non-use and clothing entanglement
(Waseem et al., 2019)	not wearing a helmet, speeding, running a red light
(Seyfi et al., 2023)	helmet use, motorcycle age, road surface condition,
(Gabella et al., 1994)	helmet use, hitting a fixed object, and motorcycle speed
(Shaheed & Gkritza, 2014)	helmet use, speeding, riding on a dry road surface
(Shankar & Mannering, 1996)	helmet use, motorcycle displacement, rider age, speed

In these studies, helmet non-use and excessive speed are the two most frequently reported variables in crash fatality outcomes, and they are universally present across geographic contexts in South Asia, North America and Europe. The secondary and significant contributors are the conditions of the road surfaces, the characteristics of the vehicles, and the time-of-day effects. It is worth noting that the combination of such factors, such as travelling at high speed on the poor road surfaces without a helmet, results in the cumulative risk that would be significantly larger than either factor used individually. These results are directly used in the parametric focus of the current study that testing the combined impact of the helmet condition and the velocity at impact on the severity of head injuries during a reconstructed motorcycle-truck crash.

2.5 Types of Injuries Experienced in Two-Wheeler Crashes

One of the most vulnerable road users is two-wheeler riders and passengers who are not shielded by the structural protection of enclosed vehicles and instead exposed to the entire force of collision loads. Having no internal restraint systems, they are highly prone to a variety of injuries, and the trauma distribution is dependent on both biomechanics of the

collision and the protective equipment. Table 2.3 provides a summary of injury patterns by major post-mortem and clinical studies of two-wheeler fatalities.

Table 2.3 Injury Patterns Observed in Two-Wheeler Crashes

Authors	Injury Types
(Yaqoob Md et al., 2016))	Distal Portion of The Lower Limb
(Ainy et al., 2016)	Head and Neck; Chest and Abdomen; Lower Limbs
(Kual et al., 2005)	Head and Neck; Upper and Lower Extremities
(Lin & Kraus, 2009)	Head Injury
(Mätzsch & Karlsson, 1986)	Head and Upper Body Extremities
(Ankarath et al., 2002))	Head, Chest and Abdominal Injury
(Wyatt et al., 1999)	Head Neck and Chest
(Unal et al., 2018)	Head/Face/Neck, Chest and Bone Fractures
(Faduyile et al., 2017)	Head Injury
(Ramli et al., 2014)	Head, Thorax and Abdominal Injury
(Larsen & Hardt-Madsen, 1988)	Head, Thorax and Abdomen

As a striking fact, the accumulation of evidence across studies across several continents and decades bears witness: head injury is the most common type of injury in the case of two-wheeler fatalities, as evidenced by its presence as a primary finding in most of the above studies (Fernandes, 2012). This trend is universal irrespective of the geographic setting, which justifies the urgent need to protect the head as a way of minimizing mortality. The second cluster of injury is chest and abdominal trauma, indicating the susceptibility of the thoracic area to both frontal and lateral impacts. Although lower limb injuries are common in non-fatal crashes, they are less often mentioned as a leading cause of death. The results of this study give biomechanical rationale as to why the study is devoted to the mechanics of head injuries and the importance of helmet protection in defining the crash survivability rates.

2.6 Crash Reconstruction Techniques

Crash reconstruction is a scientific method of inquiry for examining and understanding the dynamics of motor vehicle collisions. It is a methodical study of physical evidence, environmental conditions, vehicle dynamics, and occupant biomechanics to ascertain how

and why a collision or crash occurred. The primary purpose of crash reconstruction is to establish the chronology of the events prior to, during, and after the impact enabling better analysis of causative factors and identification of potential injury mitigation measures.

These techniques are applicable across traffic safety research, legal proceedings, insurance claims, and vehicle safety enhancement. Reconstruction methods range from simple hand calculations to advanced computational simulations, depending on analysis complexity and purpose. Broadly, crash reconstruction strategies can be categorized into traditional and simulation-based approaches.

2.6.1 Traditional Method of Crash Reconstruction

The reconstruction of crashes has traditionally been based on the physical evidence and the measure of the site and application of mathematical tools to comprehend how and why the road crash took place in the step-by-step approach to the case. It is a decades-old process that is regarded as one of the primary ways when the advanced simulations are unavailable. Trained engineers or investigators conduct systematic data collection and analysis.

A conventional crash investigation commences with scene examination assessing road geometry, traffic control devices, vehicle rest positions, and the surrounding environment. Special attention is given to skid marks or tire tracks, which are analyzed using friction-drag equations to estimate pre-braking speeds. In addition to road signs, the condition of the vehicles is also of great assistance in re-assembling the crash. Vehicle damage patterns assist in identifying the point of impact, direction of force, and approximate speeds. Conservation of momentum and energy principles are applied to compute pre- and post-impact velocities.

Eyewitness testimonies and driver interviews complement physical evidence. They provide a clear image and help in verification of evidence on the body. Investigators typically produce diagrams illustrating vehicle trajectories and event sequences. The crash situation can be re-created step by step by combining measurements and illustrations. Despite their importance, traditional techniques are limited. The quality of the reconstruction process is also dependent on the evidence available and the experience of the investigator. Only using hand methods crash investigators might not be able to study all the details of the complex multi-vehicle or high-speed crashes. Nevertheless, these methods remain in use globally, particularly in areas with limited access to simulation software

2.6.2 Simulation Based Reconstruction Techniques

Simulation-based methods have become the predominant approach in advanced crash reconstruction, with tools such as PC-Crash, MADYMO, and Ansys LS-DYNA used to reproduce crash phenomena based on the laws of physics and vehicle dynamics (Pérez-Zuriaga et al., 2023). These platforms support two- and three-dimensional analysis, enabling visualization of vehicle and occupant movement before, during, and after impact through physically grounded algorithms.

Software such as PC-Crash and LS-DYNA offer high-fidelity modeling of vehicle kinematics, collision mechanics, and injury assessment. They accommodate a broad range of crash types from low-speed impacts to complex multi-vehicle scenarios, and deliver outputs applicable to engineering analysis, forensic investigation, and legal proceedings.

2.7 Overview of Simulation Software

2.7.1 PC Crash

PC-Crash, developed by Dr. Steffan Datentechnik GmbH, is a physics-based crash reconstruction software widely used to understand and replicate crashes involving vehicles, pedestrians, and roadside objects. The software is designed to support road crash reconstruction through mathematical models to determine the sequence of events integrating multiple modules for vehicle configurations, crash dynamics, graphical outputs, and 3D animations (Steffan & Moser, 2011).

PC-Crash combines kinematic time-forward vehicle dynamics simulation with a momentum-based collision model to accurately simulate vehicle interactions. This enables reconstruction from the moment of driver reaction through to the final rest positions of all vehicles in a single run. Users may specify speed, mass, braking intensity, steering input, and road parameters to create realistic crash scenarios.

The collision model is based on the Kudlich-Slibar approach, in which post-collision vehicle movement parameters are calculated from pre-impact conditions. Assuming infinitesimal collision time, the model applies a single impact vector while ignoring external forces such as tire-road interaction during the impact itself.

The software is particularly valuable for visualizing crash scenarios through detailed 3D animations, which are especially useful in legal contexts, insurance assessments, and expert

analyses. Integration with tools such as MADYMO enables further analysis of occupant kinematics and injury risk estimation. While PC-Crash can produce accurate results, the quality of input data and user expertise are critical factors in its reliability.

The specific selection of PC-Crash was based on its proven impact modeling in momentum-based models, and the strength of its multi-body system dynamics, which are essential to provide accurate pre- and post-collision kinematic analysis. The simulation capability of the software to simulate vehicle paths and their parameterized input values and its detailed database of vehicles, provide realistic representations of local conditions. Moreover, its ability to export time-resolved kinematic data of detail to be integrated with Finite Element Modeling adds depth to the analysis of injuries. The availability of PC-Crash within the institutional research environment, along with its established use in forensic crash reconstruction, further supported its selection over other reconstruction tools.

2.7.1.1 Model Overview

The software employed in this study simulates the crash between two vehicles based on the momentum model (Urquhart, 2015a), with the coefficient of restitution as a key variable used as shown in Figure 2.1. This method, based on the work of Kudlich (1966) and Slibar (1966), “focuses on the percentage change in momentum at the moment of collision and relative force transmission between vehicles”. For full impacts, the model assumes that the common velocity at the contact point is identical, indicating a complete transfer of momentums. Conversely, sliding impacts, such as sideswipes, have zero contact velocity, resulting in different post-impact dynamics. Given specified pre-impact velocities and positions, the model accurately computes post-impact velocities, trajectories in accordance with momentum-exchange principles applied in collision analysis.

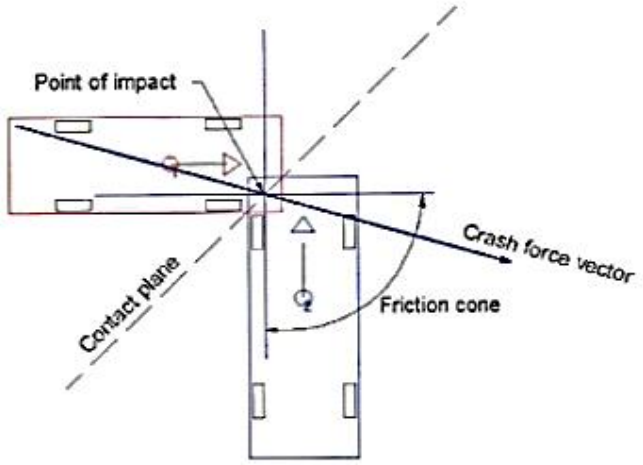

Figure 2.1 Momentum Model (Source:PC-Crash Manual, 2023)

"An impact often consists of two stages: compression and restitution. Under full impact, both vehicles have the same velocity at the instant of impact, which marks the end of the compression phase, after which the vehicles separate during the restitution phase" (Dr. Steffan Datentechnik., 2023). The coefficient of restitution, as defined in the software is the ratio of the restitution impulse to the compression impulse as in Equation 2.2 and total impulse is sum of compression impulse and restitution impulse as in Equation 2.3 (Urquhart, 2015b).

$$\varepsilon = Sr/Sc \qquad \text{…..…….(2.2)}$$

Total impulse can be given by;

$$S = Sc + Sr = Sc(1 + \varepsilon) \qquad \text{…..…….(2.3)}$$

Where;

ε – Coefficient of Restitution

Sr- Restitution Impulse

Sc- Compression Impulse

To determine the resulting force vectors, Figure 2.2 provides a schematic sketch of this method, and the PC-Crash manuals (Steffan & Moser, 2011) present a more in-depth derivation the force vectors

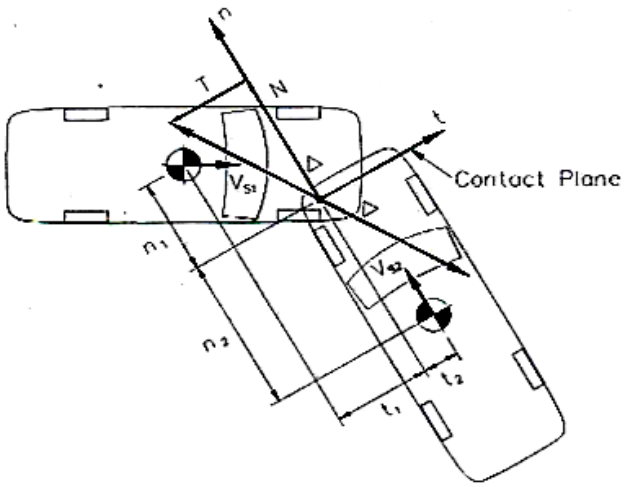

Figure 2.2 Geometric Schematic Impact Model Showing Contact Plane (Source: PC-Crash Manual, 2023)

2.7.1.2 Multibody Model Overview

A Multibody pedestrian model is a chain of interrelated parts (e.g. head, torso, pelvis) connected by articulated joints. The properties of each segment include geometry, mass, contact stiffness, and friction coefficients, typically modeled as ellipsoids of degree n (Moser et al., 1999). The volume of bodies and joints directly influences computational time, thus, there is a need to construct a balance between model detail and efficiency. The models presented in this paper present pedestrian and occupant models with 20 bodies and 19 joints to balance accuracy and computational efficiency (Moser et al., 1999). A typical multibody model can be seen in Figure 2.3.

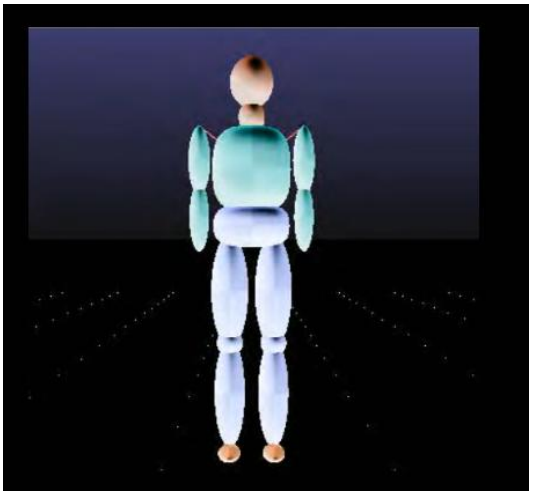

Figure 2.3 Multibody Pedestrian Model (Source: PC-Crash Manual, 2023)

External forces such as gravity, contact, friction, and joint reactions are calculated on each body at every time step in a multibody system simulation (Q. C. Wang et al., 2012). The motion of each body is then obtained by solving the equations of motion, which are based on force balance and conservation of angular momentum. Each body is assigned a mass and an associated symmetric mass tensor, usually represented as an ellipsoid for contact calculations, though the tensor itself is not restricted by this shape. The equations are solved numerically using an explicit Euler integration scheme with a typical time step between 0.1 and 1 milliseconds.

2.7.1.3 Multibody Contact Model Overview

The forces between two multibody elements, or between a body and another object, are calculated using contact models represented by a linear stiffness function (Dr. Steffan Datentechnik., 2023). The coefficient of restitution determines the elasticity of the contact, whereas friction is calculated using a specified contact friction coefficient applied after computing the normal force as in Equation 2.4 and 2.5. This approach allows simulation of full impacts, partial sliding, and sliding contacts. After defining the general body parameters, the model automatically computes the penetration depth, point of impact, and orientation of the contact plane.

$$\vec{F}N, \text{Approaching} = \lambda * S \qquad \ldots\ldots\ldots\ldots\ldots(2.4)$$

$$\vec{F}N, \text{Separating} = \varepsilon^2 * \lambda * S \qquad \ldots\ldots\ldots\ldots\ldots(2.5)$$

Where:

$\vec{F}$n, approaching = Contact normal force if bodies are approaching

$\vec{F}$n, separating = Contact normal force if bodies are separating

S = Stiffness coefficient

λ = Penetration depth

ε =Coefficient of restitution

Three different impact configurations are possible:

A Ellipsoid to Ellipsoid Contacts

When dealing with ellipsoid-to-ellipsoid contacts, the contact point is assumed to lie on a line between an ellipsoid surface point and a point on the other ellipsoid. These points are defined such that their tangential planes are parallel and the separation between them is minimized. The precise point of the contact is obtained through the stiffness characteristics of the bodies that come into contact with each other. The component of the contact force acting tangentially is found by using the lower coefficient of friction between the two ellipsoids, and the direction of this component is parallel to the relative velocity vector.

B Ellipsoid to Vehicle Contacts

PC-Crash vehicles are represented as rigid bodies to facilitate multibody contacts between pedestrians. They are depicted in several triangular polygonal faces on their surface. Vehicle geometry is defined as key dimensions, and imported as detailed 3D models. The model assumes that the point of contact lies in the polygon of the surface of the vehicle in the absence of deformation. The contact point must be within the triangular polygons. The vertical distance between the point of the ellipsoid when the tangential plane is normal to vehicle surface and the plane itself is used to calculate penetration depth. Tangential contact forces depend on the friction coefficient between the ellipsoid and the vehicle and their relative speed. These forces are applied to the vehicle model to analyze post-collision behavior.

C Ellipsoid to Ground Contacts

The ground surface in PC-Crash is represented by multiple 3D slope polygons., where each polygon has a friction coefficient linked to it. Contacts between ellipsoids and the ground polygons are modeled similarly to those between ellipsoids and vehicles. Unlike vehicles, ground polygons are treated as fixed and do not move in response to applied forces.

2.7.2 Ansys LS-DYNA

Ansys LS-DYNA is a general-purpose finite element analysis (FEA) software originally developed by the Livermore Software Technology Corporation (LSTC), which was acquired by Ansys Inc. in 2019. The software is particularly well-suited to highly nonlinear transient dynamic problems, including large deformations, material failure, and complex contact interactions, making it a leading tool for high-speed impact and crash simulations.

Originally developed for defense applications, LS-DYNA has since become widely adopted across numerous engineering disciplines. It is commonly employed in automotive crash testing, aerospace and defense modelling, manufacturing processes such as metal forming and stamping, and biomechanical studies involving human injury mechanisms. In civil engineering, it is also applied to assess the structural behavior of buildings, bridges, and dams under extreme loading conditions. Its ability to replace costly physical testing with accurate virtual simulations has made it an invaluable resource across these fields.

The software offers both explicit and implicit solvers, enabling simulation of a broad range of physical phenomena including structural, thermal, fluid, and electromagnetic problems. Its advanced multi-physics coupling allows engineers to model real-world scenarios involving multiple interacting systems with high fidelity. LS-DYNA incorporates an extensive material model library capable of representing metals, plastics, foams, composites, and biological tissues. Advanced contact algorithms facilitate the modelling of complex interactions between numerous geometric and material components. The software is optimized for High-Performance Computing (HPC), enabling large-scale models to be executed efficiently. It is fully compatible with widely used pre/post-processing tools including LS-PrePost and Ansys Mechanical, streamlining the overall simulation workflow. Ongoing development by a global community of engineers and researchers continues to maintain LS-DYNA's position as a state-of-the-art solution for advanced engineering analysis.

2.7.2.1 Finite Element Modeling

The Finite Element Method (FEM) is a widely used numerical method for solving differential equations in physical systems, particularly in structural mechanics, heat conduction, and fluid dynamics problems. FEM works by dividing a complex and continuous domain into smaller, manageable subdomains called finite elements as shown in Figure 2.4 (Johansson & Nilsson, 2025). Each element consists of nodes where governing equations are solved to determine variables such as displacement or velocity. These local solutions are then combined to form a global solution representing the entire structure or system. FEM is particularly effective at simulating complex geometries, nonlinear material behavior, and various boundary conditions. (N. Ottosson & H. Petersson., 1992).

Computational FEM employs either an implicit or explicit solution method. Implicit solvers are generally used for slow-moving or steady-state problems and involve solving a large system of equations that relate the current and predicted future states This approach provides stability but requires more computational effort. In contrast, explicit solvers are typically employed for highly dynamic problems involving large deformations or contact interactions. (Harish, 2019).

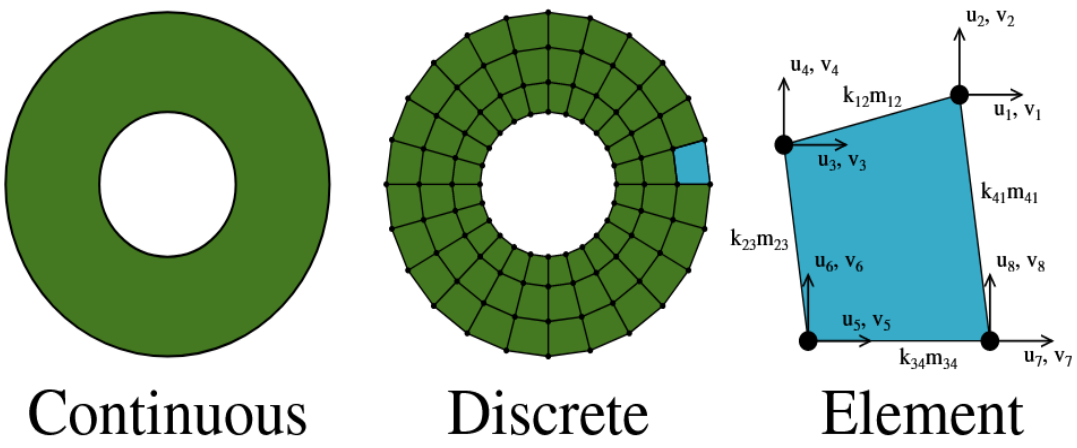

Figure 2.4 Discretization of A Continuous Domain Into Quadrilateral Elements (Source: Johansson & Nilsson, 2025)

2.7.2.2 Element Formulations

Element formulations in the Finite Element Method (FEM) vary according to four aspects: dimensionality, order, geometry, and integration scheme. Dimensionality is the level of abstraction of an element, i.e, beam elements (1D), shell elements (2D), and solid elements (3D), depending on the context and precision needed. The element order determines how many nodes the element has and the order of the shape functions defining interpolation over the element(Johansson & Nilsson, 2025). Three popular geometries of solid elements are tetrahedral, pentahedral, and hexahedral elements, with hexahedral elements being commonly employed in crash simulations because of their superior accuracy-to-cost ratio and resistance to volumetric locking under large deformation (LS DYNA user manual, 2021).

The integration scheme determines the way internal forces and strains are evaluated. In LS-DYNA, Gauss Quadrature is used with the options being one-point integration, partial, and complete depending on the level of computational efficiency and accuracy desired. The full integration tends to be more accurate, but can cause problems such as element locking in elements of low order and increased computational expense. To overcome that, LS-DYNA also provides selective reduced integration, where accuracy is preserved allowing stable calculations with less computational effort (Okereke & Keates, 2018).

2.8 Relevant Literatures Using PC Crash and Ansys Ls-DYNA

Motorcyclists face a disproportionately high risk of severe head injuries in road crashes. To enhance the accuracy of crash reconstructions, Santos et al (2023) emphasized the integrated use of PC-Crash for vehicle motion simulation and injury analysis, alongside finite element (FE) modeling for structural deformations analysis, enabling reliable speed estimation. LS-DYNA, in particular, has gained wide applicability in crash and injury modeling due to its advanced FE capabilities. Kirkpatrick et al(2003) provided a comprehensive account of its utility in incorporating detailed safety studies into crash simulations.

Various researchers such as Narayan Yoganandan et al. (2015) have employed these tools to assess injury indices such as the Head Injury Criterion (HIC), femur force, and lower leg force. Wan et al (2020) observed significant variation in injury patterns among two-wheeler users, with motorcycle riders experiencing higher HIC and femur force values in side

impacts due to greater mass and rotational radius. Both motorcycle and bicycle riders exhibited elevated HIC values in rear-end collisions, indicating a higher head injury risk. LS-DYNA has also been applied to car-pedestrian collisions for HIC based injury severity evaluation by Ruan et al.(2003) and to automate pedestrian head impact result visualization (Parab et al., 2020).

PC-Crash and LS-DYNA simulations have further been used to assess helmet effectiveness. Thai et al.(2021) reported that all helmet types significantly reduced linear acceleration and HIC values, with full-face helmets providing the greatest protection, followed by open-face and half helmets. Ho et al.(2025) demonstrated that helmets substantially reduce head injury severity in vehicle-motorcycle collisions, particularly at impact angles that would otherwise result in direct head-vehicle contact. LS-DYNA based studies have validated its utility in predicting injury severity, Kimpara et al.(2006) tested a cadaver-validated FE head model that accurately predicted brain response metrics such as HIC; and examined the effects of material properties and impact location on HIC; and other researchers have investigated helmet design parameters; such as foam stiffness and shell thickness that significantly reduce peak accelerations.

2.9 Research Gap and Study Justification

This study addresses a dual empirical and methodological research gap. Empirically, the motorcycle crash burden in Nepal is one of the highest in South Asia, with two-wheelers responsible for 68% of all motorcycle related fatalities and injuries (Kathmandu Post, 2023), a motorcycle fatality rate of 28.2 per 100,000 population, (nearly double the Asia-Pacific average) and motorcycle fatalities increasing at 5.4% per year from 2016 to 2021 (*Asian* Transport Observatory, 2025). This is exacerbated by a lack of adequate crash data infrastructure, with only 60% of crashes documented in police reports, as well as fewer than half of crashes reporting contributory factors and no disaggregated motorcycle-heavy vehicle crash data (Bhatta et al., 2024; Khadka et al., 2022; WHO, 2023). In Europe, China, and Vietnam, simulation-based crash reconstruction has been used in motorcycle crash dynamics and occupant injury analysis as seen in other studies (Ho Trong et al., 2026; Santos et al., 2023), but no similar studies have been done in Nepal. This study directly tackles both dimensions by using a dual-simulation reconstruction framework for a documented fatal motorcycle-truck collision in Kathmandu valley, and supporting the

methodological feasibility of this approach in the Nepalese crash data environment while also providing mechanistic injury causation evidence that the existing statistical record is unable to provide.

The reviewed literature points to three consistent findings: head injury is the principal cause of death in two-wheeler crashes, helmet use is the most effective protective measure available to riders, and coupled PC-Crash and LS-DYNA simulation is a well-validated method for analyzing crash dynamics and occupant injury together. Despite this, a significant gap exists in studies specific to Nepal's context. Studies examining the specific collision pattern between motorcycles and heavy trucks under Kathmandu valley conditions are limited, and the integrated multi-scale framework combining vehicle dynamics with occupant injury assessment remains rare in the literature.

This study addresses this gap directly by reconstructing a real motorcycle-truck collision from Kathmandu valley through the coupled PC-Crash and LS-DYNA framework, with the aim of understanding head injury mechanisms and quantifying the protective role of helmet use. The results offer preliminary biomechanical data applicable in road safety studies in Nepal. Since the study was conducted using a single-case study, the findings can be viewed as a methodical demonstration of the proof of concept and a prelude to the generation of an evidence base of helmet regulation and engineering decisions.

CHAPTER 3: METHODOLOGY

3.1 Research Design

This study adopts a case-study-based computational simulation approach to investigate the head injury severity in a motorcycle-truck collision in Kathmandu valley. The study is structured as a two-stage simulation process: in the first stage, macroscopic crash reconstruction using PC-Crash, to simulate the entire collision process influencing the pre-impact vehicle kinematics, impact dynamics and the post-impact trajectories. The simulation takes into consideration the mass properties of the vehicles, the initial velocities, the braking behavior, the road friction coefficients and the impact geometry. The quantified boundary conditions of the next stage are key output parameters such as impact velocity, impact angle, and acceleration-time histories. In second stage, PC-Crash output parameters are transferred in LS-DYNA as input loading conditions. A finite element model of the motorcyclist's head is subjected to the derived impact velocity and force-time histories, acceleration time histories enabling quantification of injury metrics including Head Injury Criterion (HIC).

This dual-scale methodology allows the study to bridge the gap between vehicle-level collision dynamics and occupant-level injury assessment within a single, integrated analytical framework. The overall methodological workflow is illustrated in Figure 3.1.

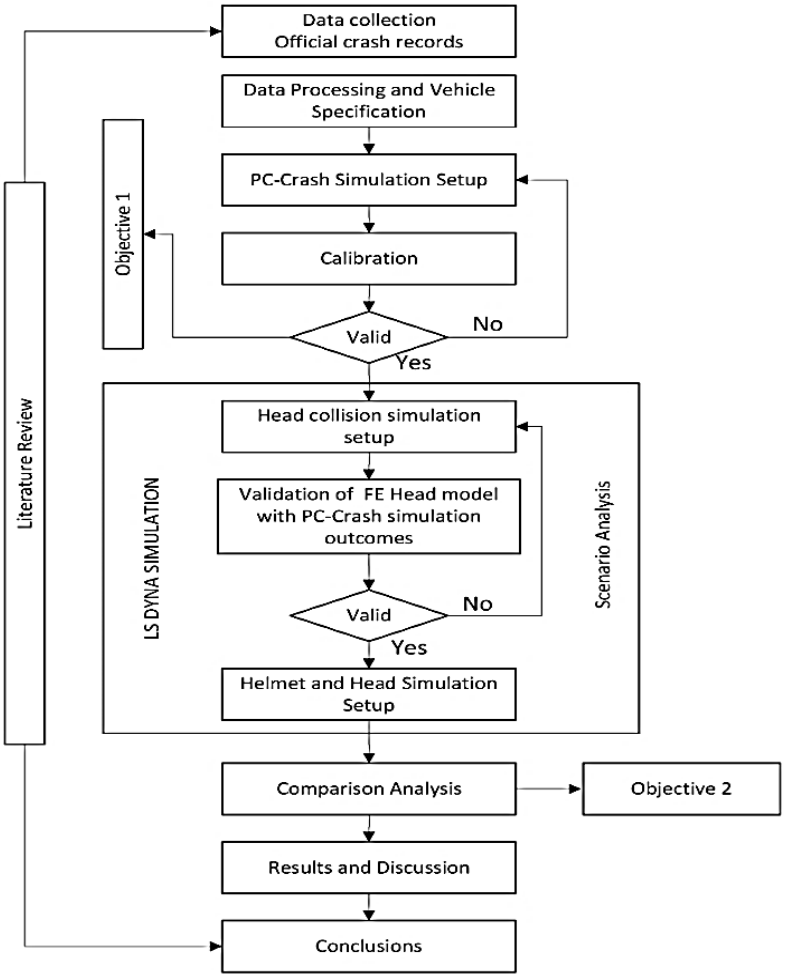

Figure 3.1 Methodological Workflow

3.2 Data Acquisition

Nepal currently lacks a centralized, publicly accessible, and well-organized crash database. In this analysis, crash data was manually collected and summarized from police department records. These sources were very helpful in obtaining the information about the crash type, time and date of crash, rider description, vehicle description, helmet use, reported injuries or fatalities, and contributing factors. While many records lacked precise geographic information such as exact locations, road names, or coordinates some did include such details. Despite these spatial data limitations, the dataset was adequate for examining crash types and influencing factors. Additional information on relevant road geometry and vehicle specifications was also gathered, enhancing the contextual understanding of each case.

3.3 Data Review and Scope Definition

Following initial data acquisition, a comprehensive data review was conducted to assess the quality, consistency, and completeness of the acquired information. Key variables, including vehicle types, rider demographics, crash timing, reported injuries or fatalities, and collision dynamics were systematically identified and examined. Particular emphasis was placed on detecting and handling missing values, poorly described entries and inconsistencies among sources. Records lacking essential inputs required for simulation such as sufficient crash details or vehicle specifications were excluded from further analysis. Where vehicle specifications were unavailable, further efforts were made to obtain the necessary information from police reports, institutional, and official sources.

Of the crash cases obtained from police records, one case was identified as meeting all inclusion criteria: availability of vehicle manufacture and model, crash location identifiable from records, sufficient description of occupant positions and injuries, and documented post-impact rest positions. This case- a motorcycle-truck collision- on an urban road in Kathmandu valley was selected as the subject of full reconstruction and FE analysis. The characteristics of the selected case are summarized in Table 3.1 below. Detailed examination of the occupant-level injury data from this case informed the subsequent decision regarding the appropriate subject for biomechanical simulation, as discussed in the following paragraphs.

Table 3.1 Selected Case Summary

Parameter	**Details**
Crash Type	Motorcycle-Truck Collision
Location	Urban Arterial Road
Occupants	Motorcycle Rider + Pillion Passenger
Rider Outcome	Fatal at collision site
Pillion Outcome	Severe cranial trauma, AIS 3-4, survived
Helmet Status-Rider	Helmeted
Helmet Status-Pillion	Unhelmeted
Simulation Focus	Pillion Passenger Head Injury Assessment

The selected case involved a motorcycle carrying two occupants that collided with a heavy truck. According to official crash reports and medical records, the motorcycle rider sustained fatal injuries at the collision site despite wearing a helmet, while the pillion passenger survived with severe cranial and bodily trauma. The finite element analysis

focuses on the pillion rider on the grounds of both biomechanical tractability and simulation validity. The motorcycle rider sustained non-survivable head trauma, indicating that impact forces exceeded the structural failure threshold of the skull, a condition where helmet energy absorption is already overwhelmed and HIC-based differentiation between helmeted and unhelmeted outcomes becomes physically meaningless. Simulation of non-survivable impacts cannot yield quantifiable insight into helmet protective mechanisms within the clinically relevant injury range.

The pillion rider sustained severe cranial trauma and associated injuries without helmet protection, placing the injury outcome within the AIS 3-4 range of the Abbreviated Injury Scale-the biomechanical regime in which HIC_{15} demonstrates the greatest discriminatory sensitivity between injury severity classifications (Qiu et al., 2020). The absence of a helmet protection in this documented case provides an appropriate and well-defined baseline condition from which the protective benefit of helmet use can be systematically quantified through comparison with subsequent helmeted simulation scenarios. Furthermore, the documented survival of pillion passenger with severe but non-fatal injuries provides a clinically verifiable reference point for validating simulation outputs, specifically by comparing HIC_{15} values derived from the unhelmeted simulation against the AIS 3-4 injury classification recorded in medical documentation.

The scope of the study was defined accordingly: non-location-specific simulation and analytical injury analysis of the selected crash case, using PC-Crash for vehicle dynamics reconstruction and LS-DYNA for occupant head injury assessment.

3.4 Reconstruction Process from Crash Report Evidence

Reconstruction was done systematically to ensure each crash scenario was accurately imported into PC-Crash. This involved careful data entry, scene modeling, as well as matching the vehicles and parameterizing the crash simulation to precisely recreate the incident.

3.4.1 Location of the Incident

This reconstruction process began by identifying the vehicle impact. After confirming the road layout and direction of travel, an appropriate area was selected to capture all of the

events preceding the crash, typically covering around 10 seconds before impact. This timeframe allowed tracing vehicle motion using safety beacons or crash data.

3.4.2 Road Layout

The selected area covered all activities described in the incident report. In some cases, investigators submitted detailed overhead digital maps, but in the majority of reconstructions, detailed maps were manually created using high-resolution Google Maps satellite imagery. The road structure was then designed in PC-Crash using these images and its built-in modeling tools Any relevant roadside barriers, fixed objects, or other obstructions present at the crash scene were also incorporated into the road layout to accurately represent the crash environment.

3.4.3 Vehicle Type Involved

The case evidence provided the make, model, and year of every vehicle involved in the incidents. These vehicles were imported into the reconstruction environment using PC-Crash's built-in vehicle database. Most of the time, an exact match of make, model, and year was found. Where no exact match existed, the closest match was selected and manually adjusted for weight, wheelbase, and other physical characteristics. For two-wheeler crashes, a multibody model from the PC-Crash database was used. The model was then tuned by adjusting parameters such as body dimensions, mass distribution, and posture to fit the descriptions from police and case records.

3.4.4 Occupants

Vehicle occupants, including drivers, were included in the reconstruction model. Masses were assigned at occupant positions, assuming 70 kg per adult and 45 kg per child when specific weights were unavailable. Vehicle mass, particularly for the striking vehicle, was adjusted to include occupants and any cargo or load present during the crash, based on records or reasonable assumptions.

3.4.5 Point of Impact (POI)

Once the vehicle setup and crash environment modeling were complete, the point of impact (POI) was estimated using scene photographs showing tire marks, debris, and road surface

damage. Since dimensions and orientations of the vehicles were already defined, determining the POI was not as challenging. An important aspect of this calculation was the contact angle between the vehicles, which was determined by direction and degree of crush damage and photographic clarity. Post-collision mechanical inspection reports were also used to confirm observed deformations, improving reconstruction validity.

3.4.6 Vehicle Speeds

In PC-Crash, where direct speed measurements were not possible, pre-impact vehicle speeds were estimated by iterative parameter approach. Preliminary estimates were based on background information, such as displayed speed limits, the current traffic flow, and existing case history. These initial values were taken as the initial input of the simulation and gradually improved by comparing the motions of vehicles simulated with physical data found at the crash scene, including final rest positions, points of contact identified, and distribution of roadway marks or debris.

The approximate speeds were then implemented in PC-Crash to determine the pre impact trajectories of the vehicles. The simulations were performed in an iterative way by adjusting the speed inputs and starting points, until the modeled kinematics were close to the dynamics of the crash we were observing. Simulated tracks, collision geometry and position after impact were compared to documented scene data to verify alignment.

3.4.7 Post Impact Positions/Rest Positions

After the point of impact (POI), PC-Crash automatically estimated the after-collision trajectories and the ultimate rest position of the vehicles involved. In simpler, particularly two-vehicle crashes, these estimates often aligned well with scene evidence such as road markings and photographic damage patterns. Police reports detailing occupants' final locations post-crash were also used to verify and refine simulations, ensuring consistency with recorded outcomes.

3.5 Finite Element Modeling

This study developed a finite element (FE) head model as a central tool for analyzing head injury mechanisms in motorcycle-truck collisions. The modeling process followed a structured sequence: CAD preprocessing to refine anatomical geometry, meshing to

discretize the model, material modeling to represent tissue properties, contact definition to capture external interactions, parameter initialization to set boundary and loading conditions, and solver configuration to conduct dynamic simulations. The impact velocities and boundary conditions obtained from PC-Crash reconstructions were applied as initial boundary conditions in the FE model, defining the kinematic loading experienced by the head during collision.This systematic approach ensured a reliable framework for simulating traumatic impacts and assessing injury outcomes.

3.5.1 CAD Model Preparation

The CAD geometries of the headform, helmet and the truck impact section were developed to realistically represent their actual shapes while maintaining computational efficiency. The headform was taken from the standardized Ansys LS-DYNA pedestrian impactor library, which provided a validated and reproducible basis for the study. Small geometric details and gaps were simplified or removed to create clean, watertight surfaces that support stable meshing. The truck impact surface was modeled as a rigid shell to realistically capture its much greater stiffness compared to the human head.

3.5.2 Meshing

The Ansys LS-PrePost was used to mesh all the components considering carefully the quality of the elements that would be used in the dynamic impact simulations. Regions of high sensitivity to contact and local deformation, e.g., the headform skin and truck impact surfaces, were given finer meshes to sample the detailed responses. Less important regions used coarser meshes to ensure that the ability to compute did not affect the global accuracy. The truck was simulated as a stiff shell with a thickness line to the real structure, which gives the truck behavior and the stiffness a real appearance.

3.5.3 Material Modeling and Contact Definitions

All components were assigned material models reflecting their mechanical behavior under dynamic loading. The helmet components comprising the outer shell, foam liner, and rigid inner structure were assigned constitutive models appropriate to their respective roles: elastic formulations for the shell, crushable foam models for the energy-absorbing liner, and rigid material definitions for the inner structural elements (Fernandes, 2012). The truck impact surface was modeled as a rigid body, consistent with its substantially greater

stiffness. Specific material property values including elastic modulus, density, and Poisson's ratio for each component are tabulated in the Results chapter (Table 4.2 and Table 4.3), derived from published literature and validated headform specifications.

Contact interactions between the headform, helmet and the truck impact surface were defined using Contact algorithms in LS-DYNA, with tied constraints applied at bonded interfaces where required. Contact parameters were validated using pre-processing diagnostic tools to minimize initial penetrations while maintaining numerical stability. This approach ensured realistic impact response without compromising model integrity.

3.5.4 Initial Parameters and Boundary Conditions

Before the execution of the simulation, intensive checking of the finite element model was done to achieve numerical stability and geometric integrity, especially focusing on detecting and fixing interface anomalies, e.g. overlapping and penetration of components. Geometric differences were determined and then corrected systematically using node projection methods and then with a careful positional readjustment to provide correct inter-component contact. Contact definitions were all carefully validated with high level pre-processing diagnostic facilities and LS-DYNA contact parameters then optimized to ensure that minimum initial penetrations were possible without the loss of computational stability. All these preparatory actions created a strong and sound finite element model that is in a position to give correct results during the impact simulation analysis.

In order to achieve an efficient simulation of the crash scenario, the use of both boundary and loading conditions was simplified and representative. Instead of simulating the complete sequence of collisions, initial velocities calculated by simulating PC-Crash were applied directly to the model to display the speed of impact at contact point. This opposing structure was completely restrained, and it was far stiffer than the object that struck it. This method minimized the cost of computation and retained the necessary physics of the impact so that the model could still generate credible results to analyze the dynamic response and possible injury outcome

3.5.5 Solver Setup and Processing

The simulation was executed using LS-DYNA's explicit solver with Shared Memory Parallel (SMP) processing, appropriate for the short-duration, high-rate dynamics of the impact event. The simulation duration was set to capture the full impact pulse, typically on the order of 10-15 milliseconds, sufficient to encompass the peak acceleration response and subsequent rebound phase. The time step was automatically calculated by LS-DYNA based on the Courant stability criterion, governed by the minimum element characteristic length and material wave speed. Output data including nodal accelerations, contact forces, and element stresses were requested at intervals sufficient to resolve the temporal profile of the impact pulse.

Post-processing was conducted in LS-PrePost, where resultant head acceleration was plotted as a function of time to identify peak values and the acceleration-time pulse profile. HIC_{15} values were calculated from the resultant acceleration history using the standard formulation, and the results were assessed against the AIS-based severity thresholds summarized in Table 2.1.

CHAPTER 4: RESULT AND DISCUSSION

4.1 General

The results outlined herein encompass the quantitative outcomes of the motorcycle-truck crash reconstruction. The analysis is structured in two stages: first, crash reconstruction using PC-Crash to reproduce vehicle kinematics and calibrate the scenario against physical evidence; and second, finite element (FE) modeling using Ansys LS-DYNA to examine head impact mechanics and quantify injury criteria. The results are discussed alongside their implications for injury assessment and crash reconstruction validity, consistent with the methodology described in CHAPTER 3:

4.2 Case Background

The case examined involves a motorcycle carrying two occupants that collided with a heavy truck on an urban road in Kathmandu valley. According to official crash reports and medical records, the motorcycle rider sustained fatal injuries at the collision site despite wearing a helmet, while the pillion passenger survived with severe cranial and bodily trauma. The truck's pre-crash behavior involved acceleration, a lane-change maneuver into the oncoming lane, driver reaction, and braking all of which were incorporated into the simulation to realistically reconstruct vehicle motion prior to impact. The motorcycle's approach trajectory on the right lane was similarly parameterized from available evidence.

As discussed in Section 3.3, the finite element analysis focuses on the pillion rider, whose survivable but severe head injuries present the most analytically productive scenario for investigating the biomechanical effect of impact conditions and protective equipment. The results of both the PC-Crash reconstruction and the LS-DYNA head impact simulation are presented in the sections below.

4.3 Reconstruction with PC-Crash

The PC-Crash reconstruction combined official crash reports with roadway geometry, vehicle data, and environmental details to create a realistic virtual environment. Reconstruction accuracy was ensured through a three-step verification process: comparing simulated trajectories and rest positions with scene evidence, matching collision points with observed damage, and refining dynamics through iterative adjustments. This systematic approach provided a reliable kinetic foundation for subsequent finite element analysis.

4.3.1 Scene Mapping

High-resolution Google Maps satellite imagery was imported into PC-Crash via the Extras > Mapping/GIS option and scaled to actual ground dimensions. This provided a georeferenced background map over which the road network was overlaid with a spatial precision. The road surface was modeled using PC-Crash road-building tools (Draw > Road Section). As detailed roadside data were unavailable, the surrounding was modeled as a uniform open landmass. The resulting crash site layout is shown in the Figure 4.1.

Figure 4.1 Layout of Crash Site

4.3.2 Vehicle Modeling and Dynamics

Vehicle make, model, and year information was retrieved from the police case files and matched the PC-Crash vehicle database. When exact vehicle models were unavailable, similar models were selected and modified in terms of mass, size, and wheelbase. Occupant and loading conditions were considered to realistically reflect crash dynamics. For two-wheeler, a multibody rider model was calibrated to the reported weight (70 kg) and height (170 cm). Physical properties and vehicle dynamics were further tuned using PC-Crash's customizable input interface to reproduce the distinct characteristics of each vehicle involved.

4.3.2.1 Vehicle Setup and Data

The Truck model was imported into PC-Crash using DSD database that most accurately matched the police record specifications. These models were positioned in the recreated crash scene at reported precrash positions, forming the baseline configuration in future simulation and calibration. Realistic dynamic behavior parameters such as curb weight, center of gravity, ABS settings, wheelbase, and axle positions were adjusted to reflect behavioral tendencies such as rollover or off-center impacts, and the other configurable geometry and suspension parameters were kept through a standard input interface as shown in Figure 4.2 and Figure 4.3.

Spring and damping coefficients were specified per-wheel, a preset stiff suspension configuration was used to represent the mini-truck behavior, and occupant and cargo masses were not compensated. Given that the reconstruction included the truck's pre-impact acceleration phase, engine power and torque characteristics were incorporated to improve kinematic accuracy. Tyre characteristics such as type, dimensions and lateral spacing (in the case of the truck) were modeled using linear tire model shown in Figure 4.4 to provide a computationally efficient and consistent representation of braking and final vehicle positions.

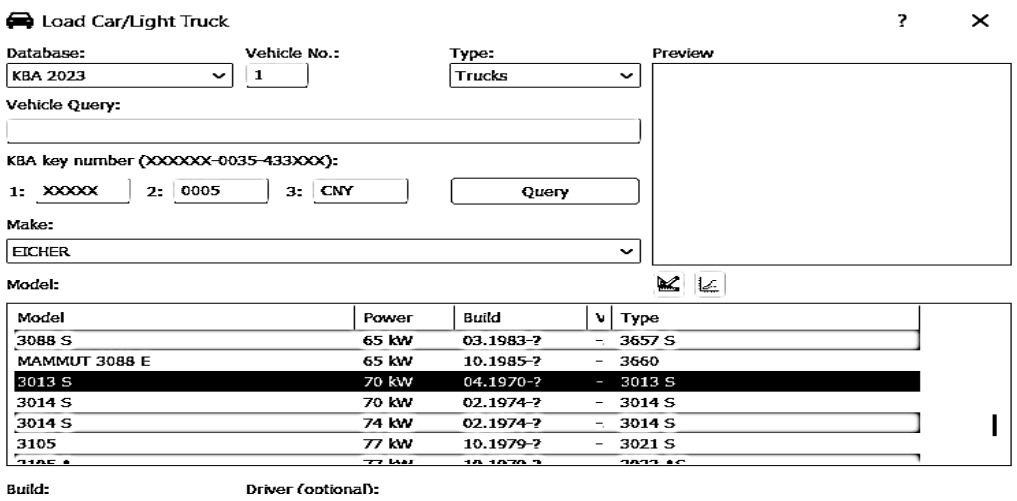

Figure 4.2 Vehicle Model Selection From PC-Crash

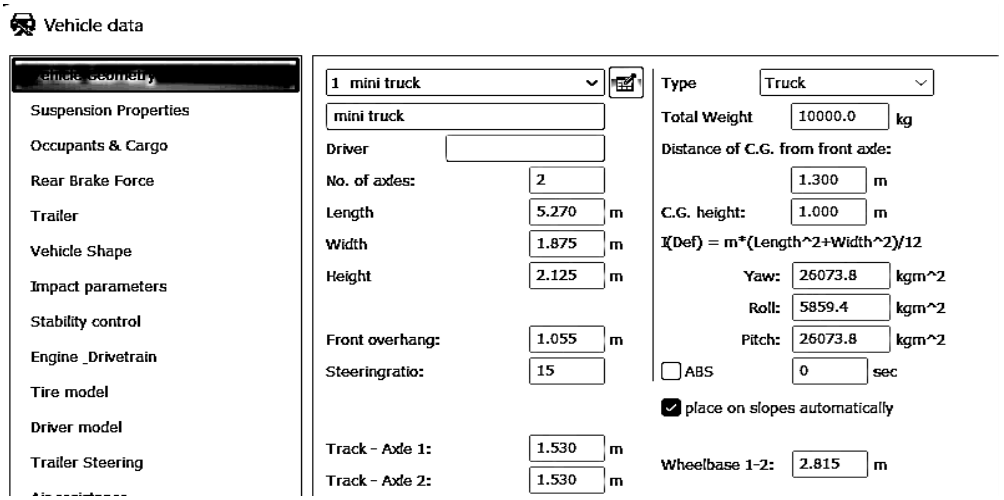

Figure 4.3 Vehicle Geometry and Parameter Input

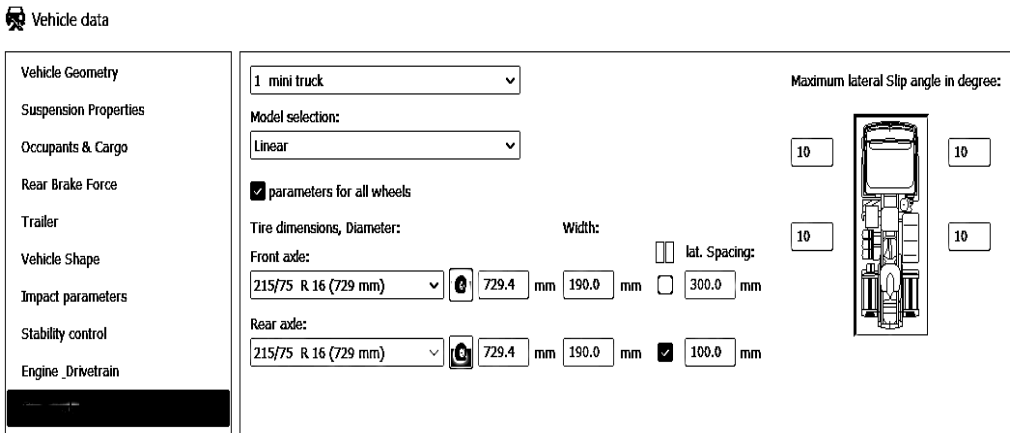

Figure 4.4 Tire Geometry and Parameter Input

4.3.2.2 Modeling of Multibody System

A multibody human model was integrated into PC-Crash environment to realistically model the occupant motion and response during and after the crash. The model comprised rigid body segments representing major anatomical regions, connected by articulated joints that permit flexion and movement consistent with human biomechanics. Each segment was assigned mass, dimensions, and a center of gravity based on standard anthropometric values; the total model represented a typical adult of 70 kg and 170 cm, consistent with available records.

Joints were modeled as ball-and-socket connections, permitting multi-directional motion and enabling simulation of tumbling, rolling, and sliding with high fidelity. Joint stiffness and damping values were set within physiologically realistic ranges using anthropometric data and PC-Crash's default biomechanical parameters. Contact friction coefficients were set at 0.6 for body-ground interaction and between 0.3 and 0.5 for body-vehicle contact, ensuring realistic post-impact occupant kinematics (Figure 4.5).

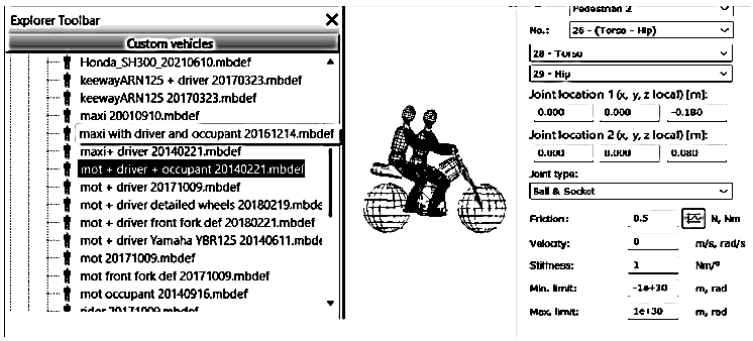

Figure 4.5 Multibody Model and Configuration

4.3.2.3 Dynamics Modeling

The collision scenario was simulated considering realistic driver dynamics by including sequential vehicle motions inputs including braking, acceleration and steering in the pre- and post-impact phases. For more accurate results, the simulation was divided into two stages: the first reconstructed pre-impact behavior based on police reports and representative driving behavior, and then simulated the post-impact dynamics to find final rest positions. In the absence of verified speed data, iterative trial simulations, initiated at

35km/h, were carried out to match physical evidence from the crash scene. The pre-impact maneuvers of the truck (including its acceleration, lane change and braking) and those of the motorcycle (including rider response and emergency braking) were parameterized based on available information. Vehicle trajectories were improved to represent realistic reaction times and motion behavior, as shown in Figure 4.6.

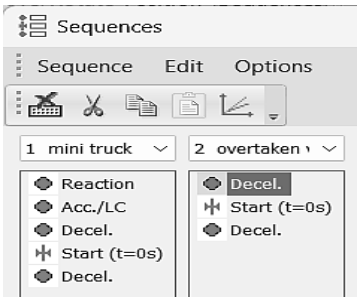

Figure 4.6 Pre-Impact Motion Sequence Control Box

The truck's pre-crash maneuver sequence included forward acceleration of 1.00 m/s², a rightward lane-change with a lateral rise distance of 4.0 m, maximum lateral acceleration of 4 m/s², and a steering angular velocity of 5.0 deg/s over a pre-impact duration of 3.25 seconds as in Figure 4.7(a). Brake control was parameterized based on crash data, with realistic braking distances and per-wheel braking factors of 3.75m/s^2 braking force applied without wheel lockup as in Figure 4.7(b). The steering path was coded to follow observed paths before and after collision and this allowed the exact reconstruction of the truck motion during the collision incident.

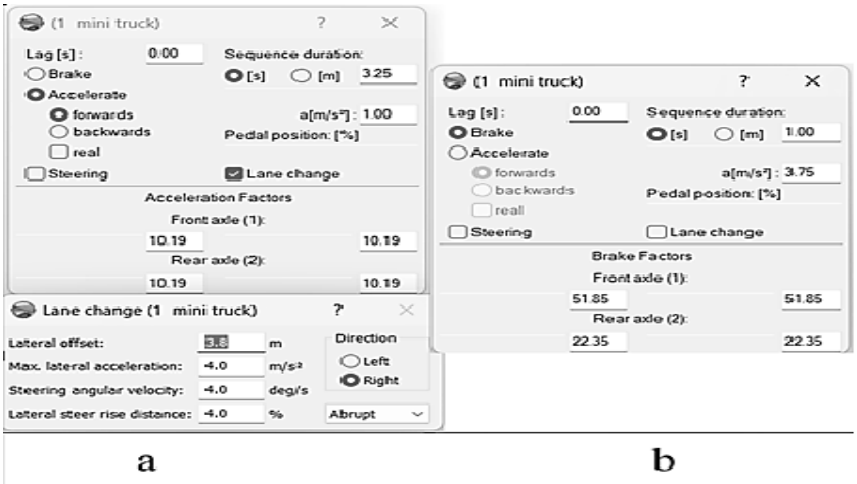

Figure 4.7 A) Pre-Impact Acceleration Lane Change Sequence B) Pre Impact Braking Sequence

4.3.3 Impact

The impact phase of the reconstruction involved positioning the motorcycle multibody system and the truck model at the identified point of impact (POI) to simulate the collision event. The pre-impact speeds of the truck and motorcycle were established at 34 km/h and 18 km/h respectively, derived from the iterative calibration process described in Section 4.3.2.3. These values were applied as the initial conditions at the moment of contact between the two vehicles.

The simulation incorporated a coefficient of restitution of e = 0.1 and an inter-vehicle friction coefficient of μ = 0.6, representing average road and contact surface conditions consistent with PC-Crash standard values for this class of collision. Through multiple iterative simulation runs, post-impact velocities and final rest positions were systematically compared against physical scene evidence after each iteration, with the objective of matching simulated vehicle kinematics and final orientations as closely as possible to the documentation recorded in the police report.

In PC-Crash, a collision is modeled as a sequence of repeated impacts spaced 30 to 100 milliseconds apart, as each point of contact between the vehicles is treated as a discrete stage. The motorcycle was represented as a full multibody system incorporating rider biomechanics, constituting the final model configuration used throughout the impact simulation. This enabled a realistic depiction of human body response during and after the impact event. The location of the point of impact derived from this process is shown in Figure 4.8.

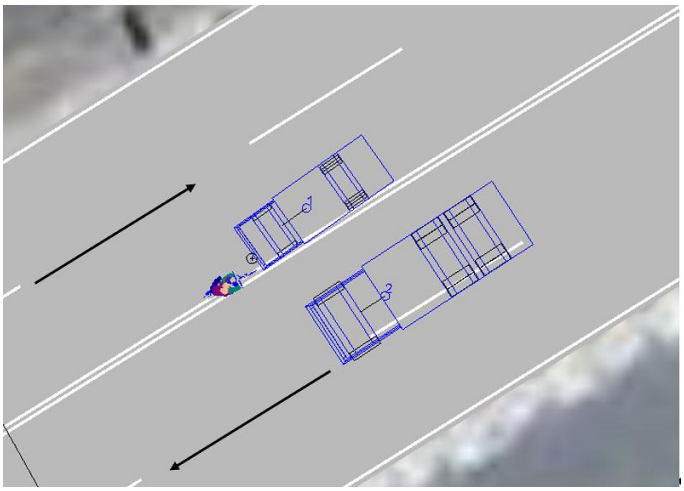

Figure 4.8 Location of Impact Point

The calibrated impact simulation delivered outputs including linear and angular accelerations, impact forces, energy transfer, post-impact velocities, and final rest positions. These results collectively characterize the severity and underlying dynamics of the collision and formed the kinematic basis for the subsequent finite element head impact analysis in LS-DYNA.

4.3.4 Calibration of the PC-Crash Model

Model calibration was conducted to ensure that simulation outputs accurately represented the recorded crash sequence. Following initial PC-Crash simulation runs, model parameters were adjusted iteratively to align vehicle trajectories, impact configurations and rest positions with physical evidence form the crash scene. In the absence of experimental data, calibration was performed against police reports, case files and roadway measurements. Key calibration references included the impact location, final rest positions of both vehicles, and roadway markings. Calibration confidence was further supported by the consistency between the simulated occupant ejection trajectory and the documented post-impact positions of the rider and pillion passenger recorded in the police report.

4.3.5.1 Scene Initialization

The crash scene in PC-Crash was spatially calibrated using scaled, georeferenced satellite imagery imported to reconstruct roadway layout and verify reference distances as in Figure 4.9. Road geometry and key spatial markers were aligned with certified measurement datasets to establish a precise geospatial framework. This step ensured that the scale, orientation, and geometry matched the real crash site.

Figure 4.9 Google Maps Satellite View of Crash Site for Spatial Calibration (Accessed August 2025)

4.3.5.2 Vehicle Motion

Vehicle trajectories were refined to achieve precise spatial and temporal alignment with the documented collision point. The truck's simulated path was adjusted to incorporate an overtaking maneuver constrained by existing roadway geometry a lateral translation of approximately 3.5 m representing a sudden lane change initiated to pass a slower-moving vehicle traveling at 35 km/h on a road with a posted speed limit of 50 km/h. This adjustment ensured that the relative positions, approach vectors, and timing of both vehicles converged accurately at the collision point (represented with circle) in Figure 4.10, consistent with physical and documentary evidence.

Figure 4.10 Vehicle Motion Prior to Collision

4.3.5.3 Post-crash Positions

The calibration accuracy was assessed by comparing simulated post-impact rest positions against the estimated values recorded in the official police report. The police report documented the truck coming to rest at approximately 11.0 m from the collision point and the rider being projected approximately 12.4 m from the impact location. The calibrated simulation produced corresponding rest positions of 10.8 m for the truck and 12.1 m for the rider, yielding absolute errors of 0.2 m and 0.3 m respectively, equivalent to percentage errors of 1.8% and 2.4%. These deviations fall well within the ±5% tolerance commonly accepted for PC-Crash reconstruction qualitative consistency check in the literature, confirming satisfactory calibration of the impact parameters. The final simulated rest positions of both vehicles are shown in Figure 4.11.

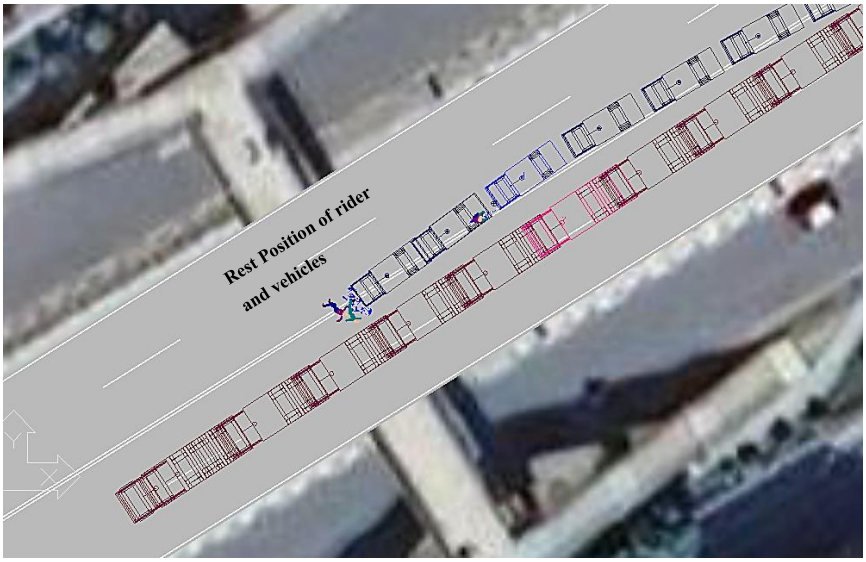

Figure 4.11 Post-crash Positions

4.3.5.4 Damage Zone Analysis

Impact zones on both vehicles were compared with police report descriptions to verify the accuracy of simulated contact points and severity levels. Truck sustained moderate damage to the left headlight, whereas the motorcycle exhibited extensive frontal damage. As shown in Figure 4.12, the contact force magnitudes on the motorcycle components were significantly higher than those on truck, indicating greater damage severity consistent with the physical evidence. Despite limited photographic documentation, the simulated damage

locations and force intensities closely matched the reported collision details, thereby supporting the validity of the reconstruction.

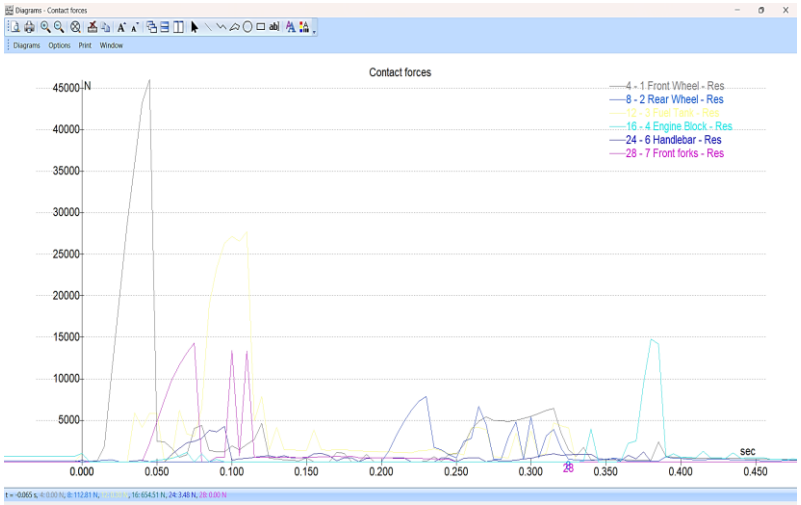

Figure 4.12 Contact Forces for Motorcycle Components

The calibrated PC-Crash model successfully reproduced the essential kinematics of the crash event vehicle trajectories, impact location, post-impact rest positions, and damage distribution with outcomes consistent with available physical and documentary evidence. The primary calibration limitation was the absence of precise post-impact position measurements in the police report, requiring estimation based on crash dynamics principles.

4.3.5 Extracted Output Parameters

After successful calibration of PC-Crash model, the most important kinematic and dynamic output parameters that controlled the motorcycle-truck crash were systematically extracted. These parameters are input parameters of LS-DYNA finite element simulation. The results of the extraction are the angle of collision approach, the velocities of the vehicles at the point of collision, multibody acceleration during and after the impact, and the force magnitudes of different multibody parts. All the parameters are discussed below, with references to the respective PC-Crash output plots.

4.3.5.1 Collision Approach Angle

The collision angle diagram obtained out of PC-Crash as in Figure 4.13 proves that it was not a perfectly head-on collision. The motorcycle approached the truck at a lateral deflection angle of ~25° relative to the truck's longitudinal axis. This oblique approach geometry is important in that it defines how the resulting impact velocity should be decomposed into axial and lateral components prior to being used as a boundary condition in the finite element model.

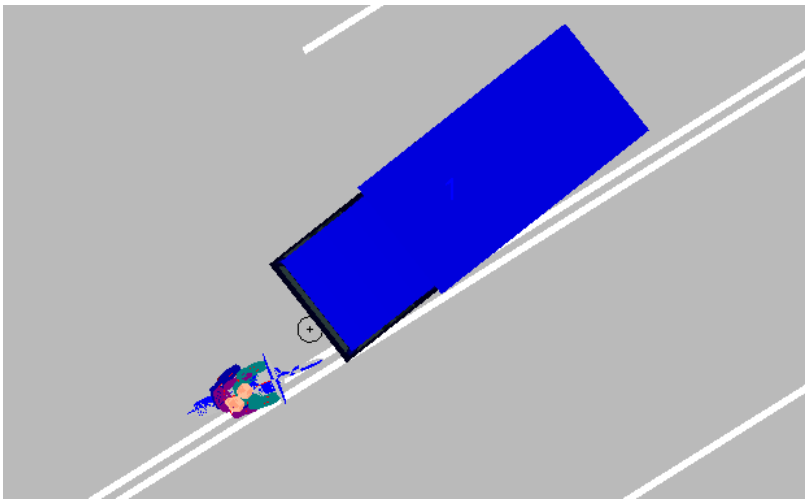

Figure 4.13 Approach Collision Angle at Point of Impact

4.3.5.2 Vehicle Velocities at Impact

The velocity time-history plot for the mini-truck, presented in Figure 4.14, shows the vehicle speed from the pre-impact phase through the collision and into the post-impact phase. The mini-truck was moving at a speed of about 34 km/h at the time of impact. The velocity profile shows a comparatively smaller reduction in speed immediately after contact, which is consistent with the truck's significantly greater mass relative to the motorcycle. It is interesting to note that the post-impact velocity of the rider based on the multibody simulation Figure 4.15(21 Head for rider and 41 Head for Pillion rider) was relatively high right after collision, which means that a lot of kinetic energy was passed on to the rider during the collision. These velocity outputs are inputs parameter to the LS-DYNA headform simulation, which determines the loading conditions in which the helmet and head response of each occupant is then analyzed.

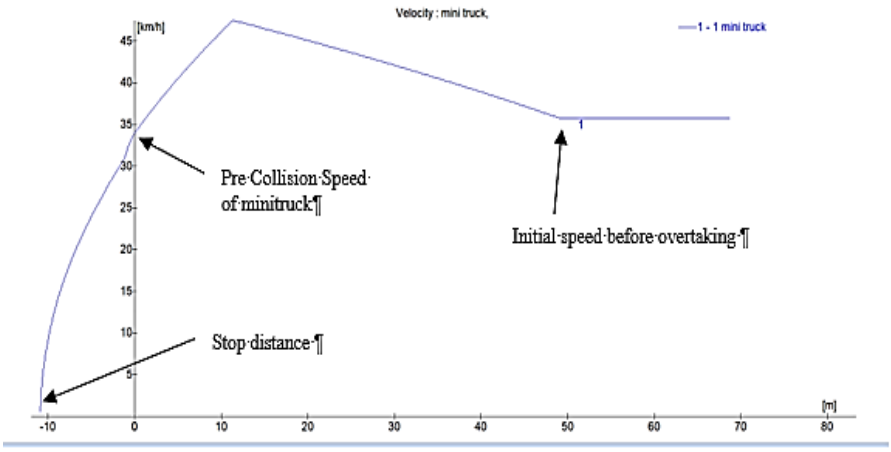

Figure 4.14 Velocity Profile of Mini-truck

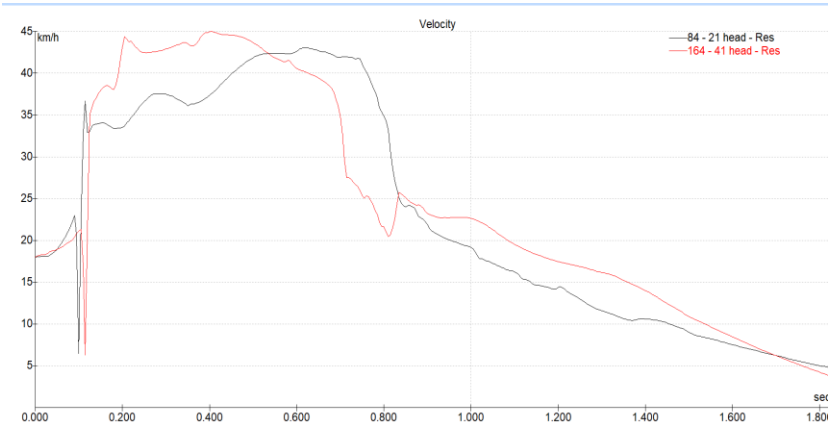

Figure 4.15 Velocity Profile of Multibody Head After Collision

4.3.5.3 Multibody Head Acceleration

The time-history plots of acceleration of the rider and the pillion passenger as in Figure 4.16 take the acceleration of each occupant during and shortly after the impact. The acceleration of the head of the rider (21 Head) was recorded to have a maximum value of about 2409m/s^2 and the acceleration of the head of the pillion passenger (41 Head) was recorded as having a maximum value of about 1208 m/s^2 during the impact pulse. The two acceleration pulses can be described as typically sharp and short in nature, and they represent the sudden change in momentum of the collision to both occupants. The relative magnitude of the two pulses is also in line with the relative location of the two occupants on the motorcycle and how the impact energy was transmitted into the vehicle structure to the occupants.

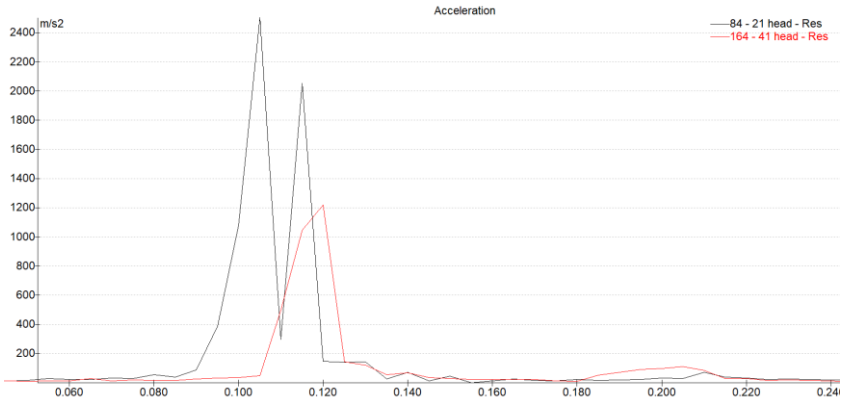

Figure 4.16 Acceleration Profile

4.3.5.4 Contact Forces on Multibody Head Models

The time-history of contact force on the rider and pillion passenger, as in Figure 4.17 illustrates how the time-dependent force on the head of each occupant varies during the collision. The maximum force on the head of the riders (21 Head) was found to be approximately 10850 N and the maximum force on the head of the pillion passengers (41 Head) was found to be approximately 7220N at an approximate time 100 ms after initial contact. In both scenarios, the force profile increases steeply with the beginning of contact and falls off quickly when the occupants lose touch with the impact surface. The size of the peak force of the two occupants on the motorcycle shows where they were on the motorcycle and the distribution of the impact load over the motorcycle structure to the two bodies. The maximum forces are also quite large and the focus is on a short period of time, which is consistent with the severity of collision and the large post impact velocities that were encountered by both occupants during the multibody simulation.

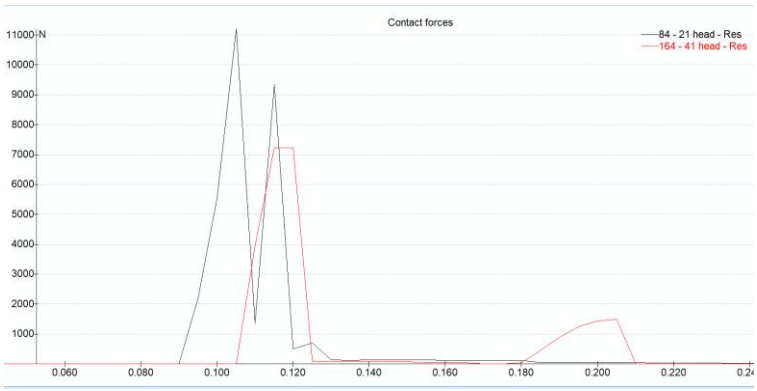

Figure 4.17 Contact Force Profile

LS-DYNA simulation impact speed was calculated by performing a vector decomposition of the two opposite vehicle velocities. Truck was moving with 34 km/h along the primary reference axis, and Two-wheeler was coming at 18 km/h with a 25-degree angular deviation, which is an effective heading of 155 mini-truck. By performing the vector subtraction in both horizontal and vertical directions, the relative velocity was calculated to be about 50.8 km/h(≈14mm/ms) and it was at 6.9degree of the original direction of mini-truck as in the Table 4.1. This final velocity was then prescribed as the impact velocity in the LS-DYNA finite element model to determine the kinematic conditions of the instant the frontal collision occurs.

Table 4.1 Extracted Parameters From PC-Crash for LS- DYNA Modeling

Parameter	**PC Crash Output**	**LS-DYNA Input**
Head Impact Velocity	50.8kmph(≈14mm/ms)	Initial velocity of headform
Approach Angle	25° oblique	Impact direction vector
Contact Surface	Truck front panel	Target surface geometry

4.4 Finite Element Modeling

This section presents the finite element (FE) modeling of the head impact event, developed to quantify head injury assessment resulting from the motorcycle-truck collision reconstructed in Section 4.2. The FE model employed a standardized headform assembly from the LS-DYNA pedestrian impactor library, with initial conditions derived from the validated PC-Crash kinematics. The modeling procedure followed the sequence described in CHAPTER 3: (Section 3.5): CAD preparation, meshing, material definition, contact specification, boundary condition assignment, and solver execution.

4.4.1 CAD Model Preparation

The CAD geometries of the headform, helmet and truck impact surface were prepared to achieve a balance between geometric realism and computational efficiency. The standardized LS-DYNA headform impactor model was adopted directly from the software's pedestrian impact library, which is extensively validated and eliminates the need for new geometry development. The model comprises four structural components: the outer skin layer, the acceleration block housing the virtual accelerometer, the skull shell, and the rigid base plate (Figure 4.18). The truck impact surface was modeled as a rigid flat shell,

accurately representing its substantially greater stiffness relative to the headform. Minor geometric inconsistencies and surface gaps were corrected to produce clean, watertight geometries suitable for stable meshing.

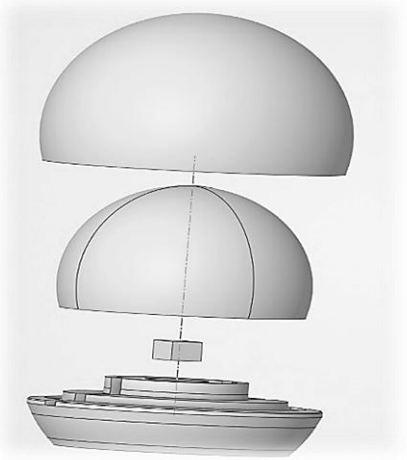

Figure 4.18 CAD Model of Headform Components

The selection of the LS-DYNA standardized headform impactor was based on four considerations. First, it is a well-validated model with demonstrated accuracy in replicating realistic head impact response across published studies. Second, it ensures consistency and direct comparability with existing literature employing the same model. Third, it improves computational efficiency by eliminating custom geometry development and associated error risk. Fourth, its geometric and mass distribution properties are suitable for the dynamic impact conditions of this analysis.

4.4.2 Meshing Models

All parts, including the headform, and impact surfaces were meshed using Ansys LS-PrePost as in Figure 4.19. Special attention was devoted to the consistency, element quality, and suitability of the mesh for dynamic impact simulations. A spatially graded meshing strategy was applied: finer mesh density was used in regions of interest particularly the outer skin and contact surfaces to accurately resolve local stress concentrations and deformation patterns; coarser meshes were applied to less critical regions to maintain computational efficiency. The truck body was meshed with structured refinement at the contact zone, while the remainder of the rigid surface was coarsened. Standard element

quality checks including aspect ratio, skewness, and Jacobian evaluations were performed prior to simulation to ensure numerical stability

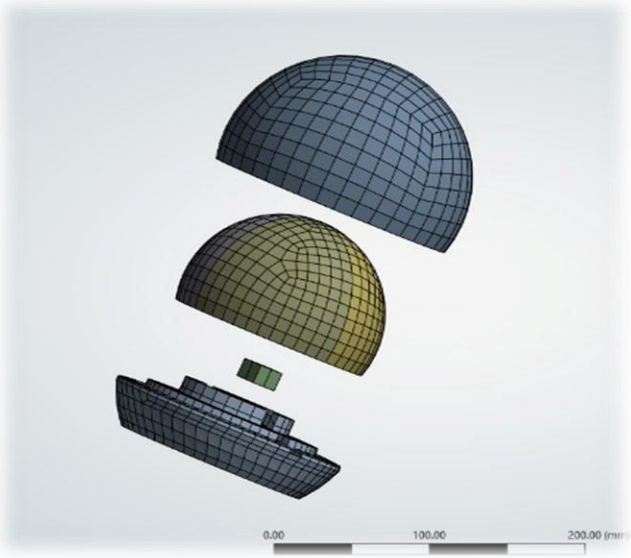

Figure 4.19 FE Model of Headform

4.4.3 Material Models, Element Formulation and Contact Definitions

Material models, element formulations, and contact definitions were assigned to each component in LS-DYNA to accurately represent their mechanical behavior under dynamic impact loading. The parameters applied are described for the headform, helmet and truck section respectively below.

4.4.3.1 Headform Material Properties

The headform impactor is divided into four distinct sections, including the skin, acceleration block, skull, and base plate used by Nguyen & Dinh (2025) and provided by Dynamore, each assigned a constitutive model appropriate to its functional role in the assembly as shown in Table 4.2. The outer skin is modeled using a viscoelastic material formulation to represent its compliant, energy-dissipating behavior under impact. The acceleration block, which houses the virtual accelerometer, is assigned an elastic material model to maintain structural stability and protect measurement integrity. The skull shell uses a linear elastic model accounting for elastic deformation and potential yielding under

dynamic loading. The base plate is modeled as a rigid body, providing high structural stiffness to maintain assembly integrity throughout the simulation.

Table 4.2 Material Properties of Headform

Material	Density(kg/m3)	Young's modulus (Gpa)	Poisson's ratio
Skin	1088	-	0.493
Acceleration Block	3150	207	0.28
Skull	2906	207	0.28
Backplate	3150	207	0.28

4.4.3.2 Helmet

The helmet model consists of two components: the outer shell and EPS foam liner., each assigned material properties representative of their respective mechanical behavior under dynamic impact loading. The foam liner is modeled using solid element type of LSDYNA3D element library outer shell is modeled using thick shell element type similar to model used by Thai et al. (2021). Table 4.3 shows modeling details of complete helmet system considered. This formulation is appropriate for capturing the initial stiffness response of each layer during the impact event.

Table 4.3 Material Properties for Helmet

Material	Density(kg/m3)	Young's modulus (Gpa)	Poisson's ratio
EPS padding	60	0.00206	-
Outer shell	1200	4	0.37

4.4.3.3 Truck Section

The truck impact section was simulated as a metal sheet plate modeled using 3.5 mm thick shell elements with MAT_PIECEWISE_LINEAR_PLASTICITY material keyword in LS-DYNA. The boundary conditions applied to the finite element bonnet model are critical parameters that directly govern its structural response during impact. The truck bonnet is modelled using aluminum, assigned an elastic-plastic material (Bourdet et al., 2011; Tinard et al., 2009). The corresponding mechanical properties are reported in

Table 4.4

Table 4.4 Material Properties of Truck Section

Material	Truck Section
Density(kg/m3)	2700
Young's modulus (Gpa)	70
Poisson's ratio	0.33

4.4.3.4 Contact Conditions

Appropriate contact definitions are essential for numerically stable and physically realistic impact simulation. The model employs two types of contact interaction, as shown in Figure 4.20 summarized in Table 4.5. AUTOMATIC_SURFACE_TO_SURFACE contact is applied globally across all interacting surfaces to capture the headform-truck impact response. TIED_SURFACE_TO_SURFACE_OFFSET constraints are used at bonded interfaces between headform components specifically between the skin and skull, skin and base plate, base plate and acceleration block, and skull and base plate ensuring structural continuity without allowing unphysical separation at these interfaces.

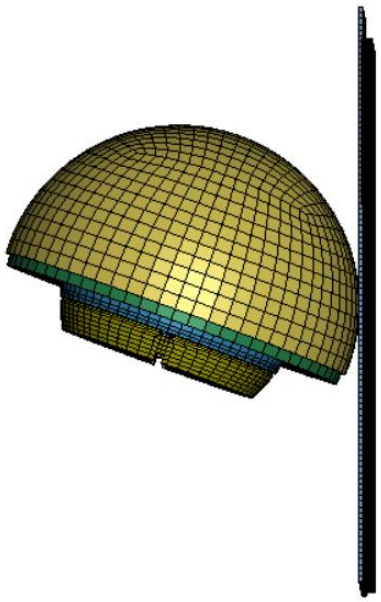

Figure 4.20 FE Model with Contact Plane

Table 4.5 Contact Conditions

Contact Conditions	Parts
AUTOMATIC_SURFACE_TO_SURFACE	All surfaces
TIED _SURFACE_TO_SURFACE_OFFSET	Skin to Skull
TIED _SURFACE_TO_SURFACE_OFFSET	Skin to Backplate
TIED _SURFACE_TO_SURFACE_OFFSET	Backplate to AccBlock
AUTOMATIC_SURFACE_TO_SURFACE	Skin to Padding
AUTOMATIC_SURFACE_TO_SURFACE	Padding to Outer Shell
AUTOMATIC_SURFACE_TO_SURFACE	Outer shell to Truck shell

4.4.4 Initial and Boundary Condition

Rather than simulating the entire vehicle-to-head collision sequence, the headform assembly were assigned an initial velocity of 14mm/ms corresponding to impact conditions calculated from PC-Crash simulations. This was done by assigning the headform translational velocity of 14mm/ms using INITIAL_VELOCITY_GENERATION keyword in LS-DYNA. The truck impact surface was modeled as metal sheet plate using MAT_PIECEWISE_LINEAR_PLASTICITY keyword, with boundary conditions set to fully constrain the body. All PC-Crash output files provided velocity magnitude and direction, which were directly used to ensure the simulation closely represented the crash case.

4.4.5 Solver Setup and Processing

The simulation was executed using LS-DYNA's explicit solver (LS-DYNA R16.1 Student Version) with Shared Memory Parallel (SMP) processing, appropriate for the short-duration, high-rate dynamics of the head impact event. The simulation duration was set to encompass the complete impact pulse, including the peak acceleration response and subsequent rebound phase on the order of 25 to 30 milliseconds. The computational time step was governed automatically by LS-DYNA's Courant stability criterion, calculated from the minimum element characteristic length and material wave speed. Output data including nodal accelerations, contact forces, and element stresses were requested at sufficiently fine intervals to resolve the temporal profile of the acceleration pulse with adequate resolution.

4.4.6 Simulation Results

Two LS-DYNA simulations were conducted sequentially. The first is the unprotected head impact scenario, in which the headform strikes the truck surface without any helmet at 50.8kmph(≈14mm/ms) establishing the baseline injury reference. The second is the helmeted head impact scenario, conducted under identical kinematic initial conditions but with the two-component helmet model assembled on the headform. The results of each simulation are presented below, followed by a comparative analysis in Section 4.4.6.3.

4.4.6.1 Unprotected Head Impact

The initial simulation represents the unprotected head impact scenario, the headform impacting the rigid truck surface without a helmet protection at an initial velocity of 14mm/ms derived from the PC-Crash reconstruction output. This scenario establishes the reference condition against which the helmeted impact simulation will be compared in the subsequent phase of the study.

A Head Acceleration Response

The acceleration response was then obtained using the accelerometer block node and graphed versus time in LS-PrePost. The acceleration-time history was sharp and well defined and the impact pulse was characteristic of a high velocity headform hitting a rigid surface. The peak and average resultant head acceleration recorded from the baseline simulation was 190g and 151g as shown in Figure 4.21., which is consistent with published results for unprotected headform impacts at comparable velocities against rigid surfaces (T. Nguyen & Dinh, 2025; Radzuan et al., 2024).

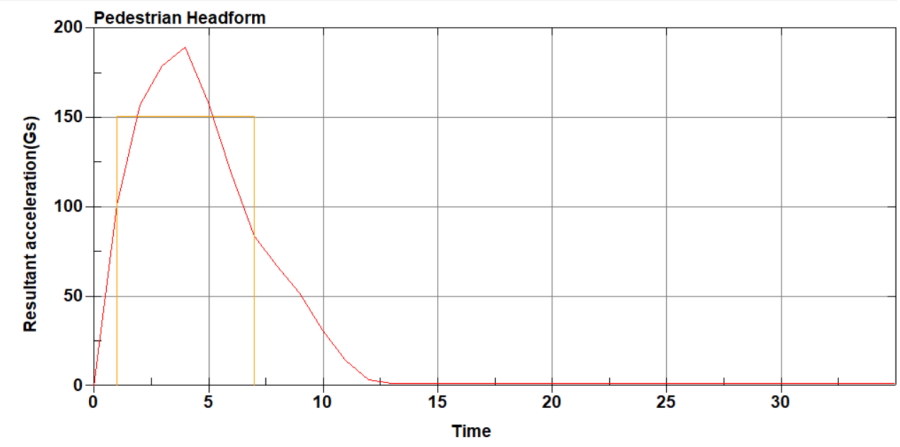

Figure 4.21 Resultant Head Acceleration Vs Time Graph

B Head Injury Criteria

HIC_{15} was computed from the resultant acceleration-time history using the standard formulation established in Section 2.3. The calculation identified the 15-millisecond time window within the acceleration pulse that produced the maximum HIC value. The HIC_{15} value obtained from the baseline simulation was 1403 as in Figure 4.22.

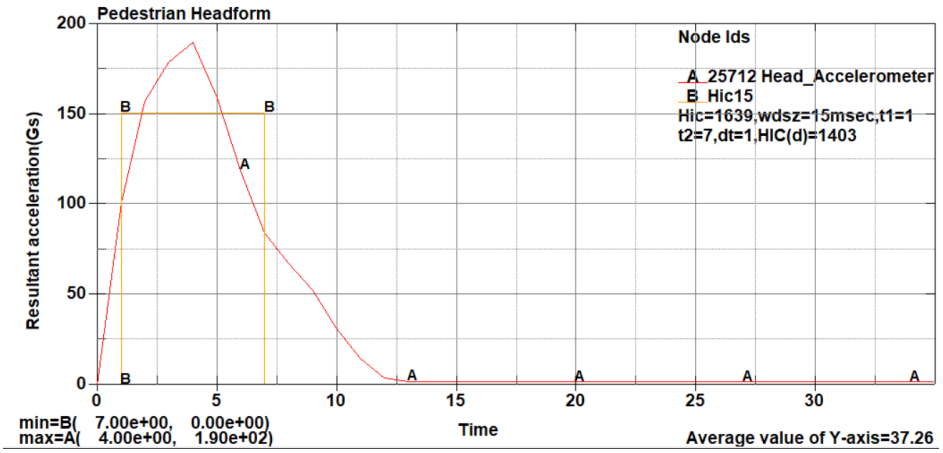

Figure 4.22 HIC_{15} Value for Head Impact

Referencing the AIS-based injury severity thresholds presented in Table 2.1, a HIC_{15} value of 1403 corresponds to Severe Injury (AIS 4). This indicates that an unprotected head impact at the reconstructed crash conditions produces significant but sub-critical head injury severity. This result is numerically consistent with the recorded clinical case outcome: the pillion rider survived the collision with severe cranial and bodily trauma, which aligns with an AIS 4 prediction rather than a Critical /Fatal outcome. The correspondence between the simulation result and the documented clinical injury level provides qualitative consistency check of the PC-Crash-derived kinematic inputs and the FE model configuration.

C Deformation and Stress Distribution

Nodal displacement output from the baseline simulation confirmed localized indentation of the headform skin at the contact zone, concentrated at the point of initial contact between the headform and the truck surface. The von Mises stress distribution reached a maximum of 0.0045 GPa at the headform-truck contact interface, as shown in Figure 4.23, which remains below the yield strength of all materials used. Secondary stress concentrations were

observed at the skin-skull interface, attributable to the compliance mismatch between the viscoelastic skin and the stiffer elastic skull, producing local stress amplification under dynamic loading. These stress patterns are consistent with the expected mechanical response of the headform assembly under impact and confirm that the contact definitions and material assignments are producing physically coherent results.

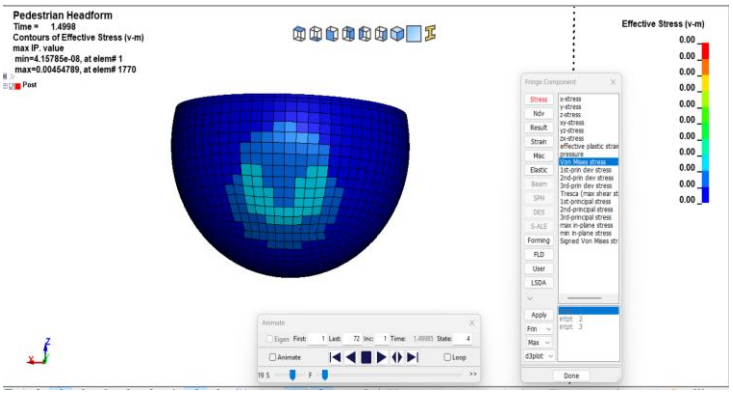

Figure 4.23 Von Mises Stress

D Energy Balance Validation

Simulation energy balance was verified by monitoring the ratio of hourglass energy to total internal energy during the period of time of the simulation (Miller et al., 2016). The maximum hourglass energy during simulation was found to be 5.57J as in the Figure 4.24 against the total internal energy of 303J resulting hourglass to internal energy ratio below 2%, within the accepted threshold of 5% for reduced integration element formulations. The kinetic energy of the headform changed rapidly at the impact point to internal energy in the deforming skin and contact energy at the impact interface as expected of the energy partitioning in a rigid-surface impact event. This confirms the numerical stability and physical validity of the baseline simulation.

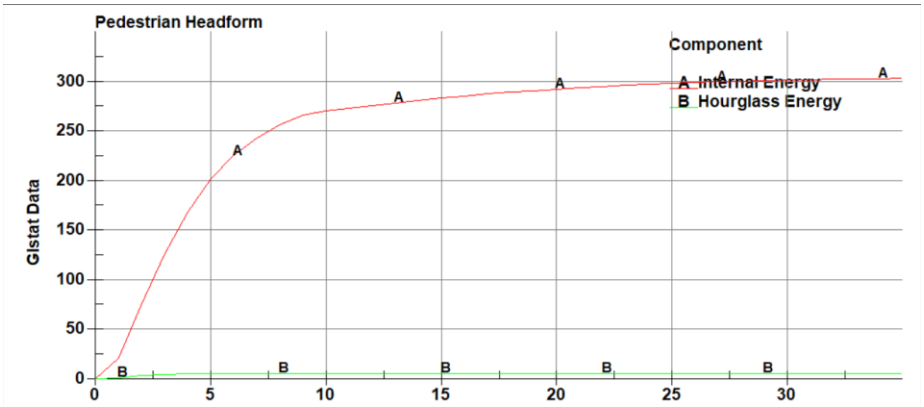

Figure 4.24 Total Hourglass Energy During Head Impact

The baseline simulation results presented in Table 4.6 indicate that FEM consistently predicts higher values than PC-Crash, as it more accurately captures detailed contact mechanics, material deformation, and stress wave propagation that are not resolved in multibody models.

Table 4.6 Summary of Baseline Simulation Results

Parameter	FEM simulation Values	PC- Crash output values
Impact velocity	50.8kmph	• Truck 34 kmph • Two-wheeler 18kmph
Peak resultant acceleration (g)	190	125
HIC_{15}	1403	1172
Energy balance -hourglass ratio	<2%	NA

4.4.6.2 Helmeted Head Impact Simulation

The helmeted head impact simulation was executed under the same initial conditions as the baseline simulation with an impact velocity of 14mm/ms against the fully constrained truck surface with the two-component helmet model (outer shell assigned MAT_PLASTIC_KINEMATICS and EPS foam liner assigned MAT_CRUSHABLE_FOAM formulations as described in Section 4.3.3) positioned on the headform assembly. The simulation ran to completion without numerical instability, confirming that the helmet-headform contact definitions and material assignments are functioning correctly within the LS-DYNA model.

A Head Acceleration Response

Introduction of the helmet fundamentally altered the shape of the acceleration-time pulse. The polycarbonate outer shell distributed the initial contact load over a larger area while the EPS foam liner underwent progressive compressive crushing, converting kinetic energy into internal strain energy at a controlled rate. This produced a broader, lower-amplitude acceleration pulse compared to the unprotected case. The peak resultant head acceleration from the helmeted simulation was 103g, representing a 46% reduction relative to the 190g baseline as shown in Figure 4.25. Pulse duration extended to approximately 10-15 ms, reflecting the prolonged energy absorption phase during foam compression before full densification. This temporal spreading significantly reduces HIC_{15} even at the same total impact energy.

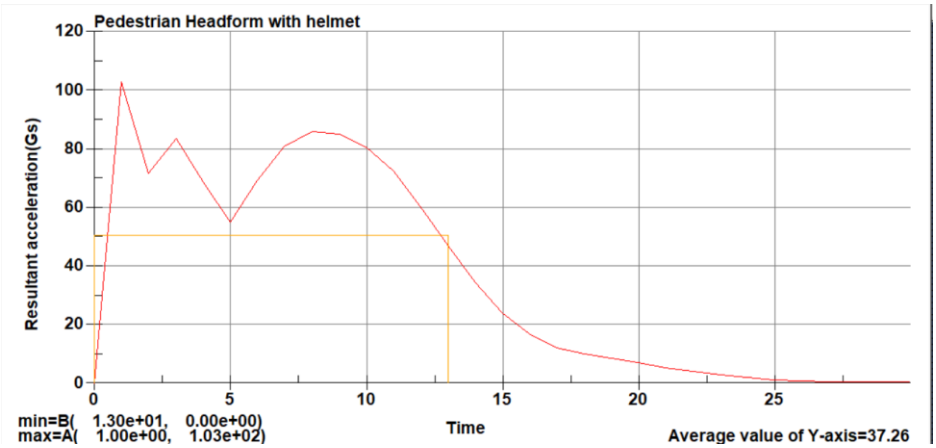

Figure 4.25 Resultant Head Acceleration Vs Time Graph

B Head Injury Criteria and Injury Severity

The helmeted simulation provided an HIC_{15} of 689 which is AIS 2 (Moderate) injury classification a 50.8% decrease compared with the baseline HIC_{15} of 1403 and two level less severe than the unprotected case. The stress response supports the attenuation of the risk of injury: the peak von Mises stress at the headform surface reduced by 42% to about 0.0026GPa, due to the energy absorption and spatial redistribution processes carried out by the polycarbonate shell and EPS foam liner before the force was passed onto the headform assembly. The hourglass energy test was met during the simulation with the helmet, thus establishing numerical stability that is equivalent to that of the baseline case.

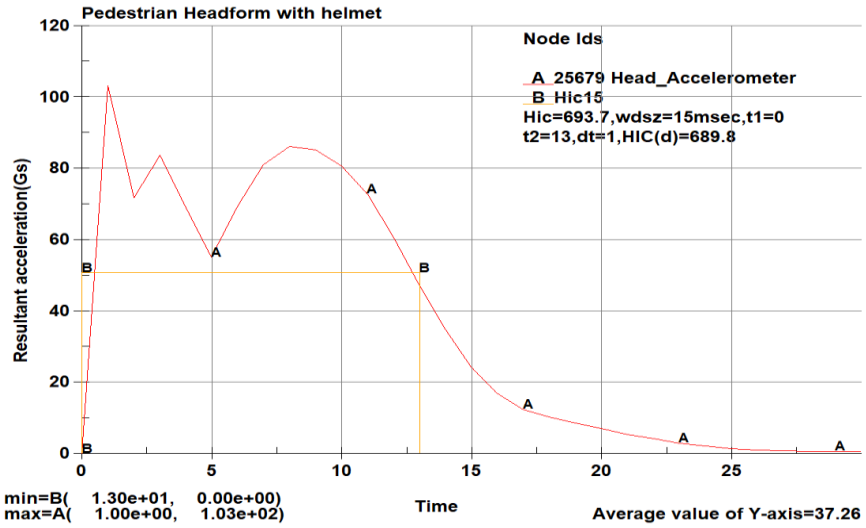

Figure 4.26 HIC_{15} Value for Helmeted Impact

4.4.6.3 Comparative Analysis and Discussion

A comparative assessment was conducted systematically on two LS-DYNA explicit FE simulations: an unprotected baseline and a head impact scenario with a helmet. The two simulations were run with the same boundary conditions, material models, definition of contacts, solver settings and fixed initial impact speed of 14mm/ms which is based on reconstruction of PC-Crash. The results of the analysis are presented in Table 4.7 and compared under acceleration-time response and peak kinematics, HIC_{15} and AIS injury severity, energy absorption and von Mises stress attenuation, and biomechanical consistency vs. the reported clinical outcomes.

Table 4.7 Comparison of Output Value

Parameter	Unprotected	Protected	Reduction
Impact velocity (mm/ms)	14	14	—
Peak resultant acc (g)	190	103	46%
HIC_{15}	1403	689	50.8
AIS classification	AIS 4 (Severe)	AIS2 (Moderate)	2 AIS levels
Max. von Mises stress (GPa)	0.0045	0.0026	42%
Acceleration pulse duration (approx.)	3-4 ms	10-15 ms	3-4× longer

A Acceleration Time Pulse

Unprotected headform-to-truck-surface contact produces a high-impedance impulse: peak and average resultant acceleration of 190g and 151g is reached within 3-4 ms, with no compliant intermediate layer to extend contact duration or redistribute the momentum exchange. Helmet interposition restructures the contact mechanics: the polycarbonate shell ($E = 3$ GPa, $\rho = 30$ kg/m³) spatially redistributes the contact force, and the EPS liner ($E = 2.06$ MPa, $\rho = 60$ kg/m³) dissipates kinetic energy through progressive compressive crushing, extending contact duration from 3-4 ms to 10-15 ms and reducing peak acceleration to 103g (−46%) and average acceleration to 50g(-67%). When the helmet spreads the same impact force over a longer duration at a lower peak, this mathematical penalty is reduced significantly more so than the reduction in acceleration alone would imply.

B HIC_{15} Analysis and Injury Severity Classification

HIC_{15} was calculated using the filtered resultant acceleration-time history at the accelerator block node, using the traditional formulation as defined in Section 2.3. The calculation finds the time range [t1, t2] which is limited by $(t_2 - t_1) \leq 15$ ms in which the HIC integral of the complete acceleration history is maximized. In the case of the unprotected simulation this critical window overlaps with the narrow, high-amplitude pulse thus resulting HIC_{15} value as 1403. This value is in the Severe Injury category (AIS 4), which is in the range of 1250-1750 of HIC_{15} , as referred to in Table 2.1, which is based on the AIS-based severity thresholds. In the case of the helmeted simulation, the larger, flatter-topped pulse brings the integral much lower, and gives HIC_{15} value as 689 resulting in the predicted outcome being in the range of the Moderate Injury band (AIS 2). The same impact conditions reduce HIC_{15} by 50.8% and the severity of two AIS levels, Severe (AIS 4) to Moderate (AIS 2) when interposed with a helmet, otherwise.

The magnitude of this reduction is consistent with published experimental and numerical benchmarks. Lloyd (2025) reported HIC reductions of up to 92% in standardized drop-test experiments using Hybrid III headforms with certified helmets, while Mohd Jawi et al. (2021) and Ho et al. (2025) documented HIC_{15} reductions upto 80% in finite element studies of motorcycle-car frontal collisions in Southeast Asian traffic conditions

C Impact Energy Absorption and Stress Attenuation

In the unprotected scenario, the headform's kinetic energy is quickly transferred to the rigid boundary within a 3-4ms impact, generating a peak von Mises stress of 0.0045 GPa at the contact area. Stress concentrations also occur at the skin-skull interface due to the stiffness difference between the viscoelastic skin and the rigid skull. However, the stresses remain below the material yield limits, indicating elastic-viscoelastic deformation. In the helmeted scenario, the polycarbonate shell spreads the impact force while the EPS foam liner absorbs much of the energy through compression. This layered structure reduces the stress transmitted to the headform, lowering the peak von Mises stress to about 0.0026 GPa, which is a 42% reduction compared to the unprotected case. The hourglass energy ratio remains below 5%, confirming stable and reliable simulation results.

4.4.7 Analysis of Impact Speed on Head Injury criteria

The sensitivity analysis was performed in a parametric manner by changing the impact speed between 11mm/ms to 16mm/ms, which is a realistic range of operating speeds in mixed urban traffic conditions. This range was selected to evaluate the influence of collision severity on head kinematics and to capture both medium and high-energy impact scenarios within the numerical framework.

The extracted results were subsequently plotted for comparative evaluation across the defined impact velocity range. The resultant peak head acceleration was used to represent the maximum instantaneous inertial loading experienced by the head during collision as in Figure 4.27, while the average head acceleration was computed to characterize the overall sustained dynamic response over the impact duration represented in Figure 4.28. Moreover, the Head Injury Criterion (HIC) values in Figure 4.29 were computed based on the resultant acceleration-time histories to include the magnitude and duration of exposure to acceleration over a specified time window, thus giving a more injury-relevant measure of potential traumatic risk. The Figure 4.30 that HIC increases nonlinearly with increasing impact speed. At lower speeds, the change in HIC is gradual, while at higher speeds, small increases in velocity result in significantly larger increases in HIC. This indicates a strong sensitivity of injury severity to speed at higher impact conditions.

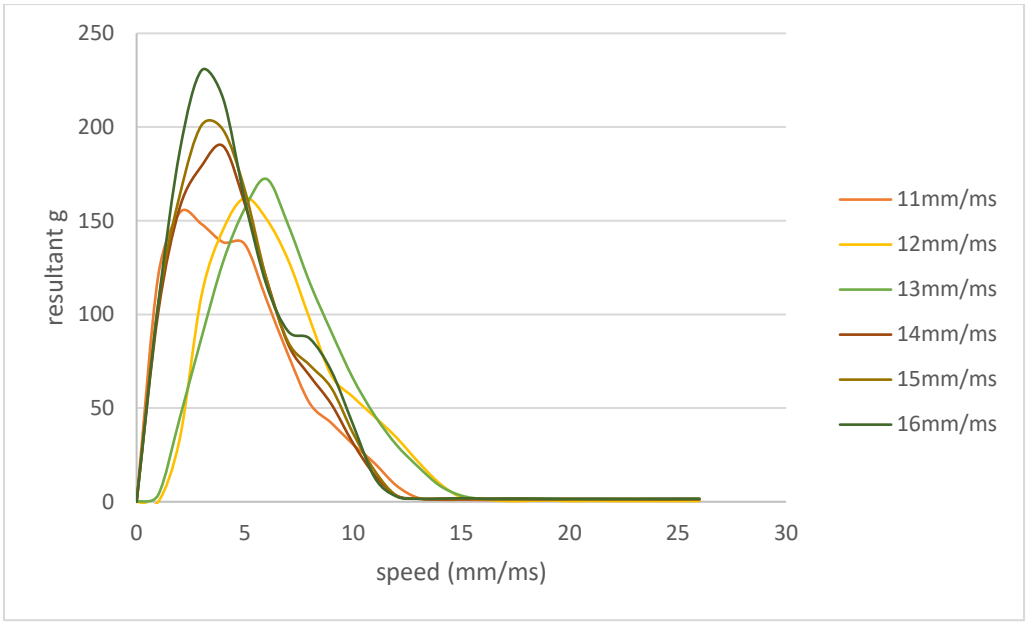

Figure 4.27 Collision Acceleration Graph for Different Velocities

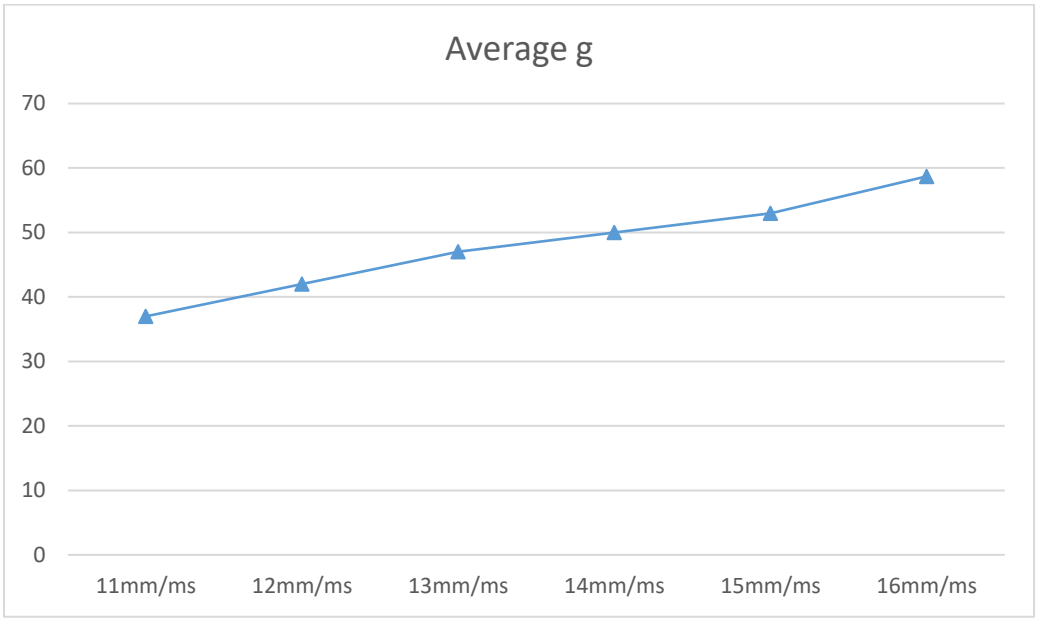

Figure 4.28 Average Value of Resultant Acceleration

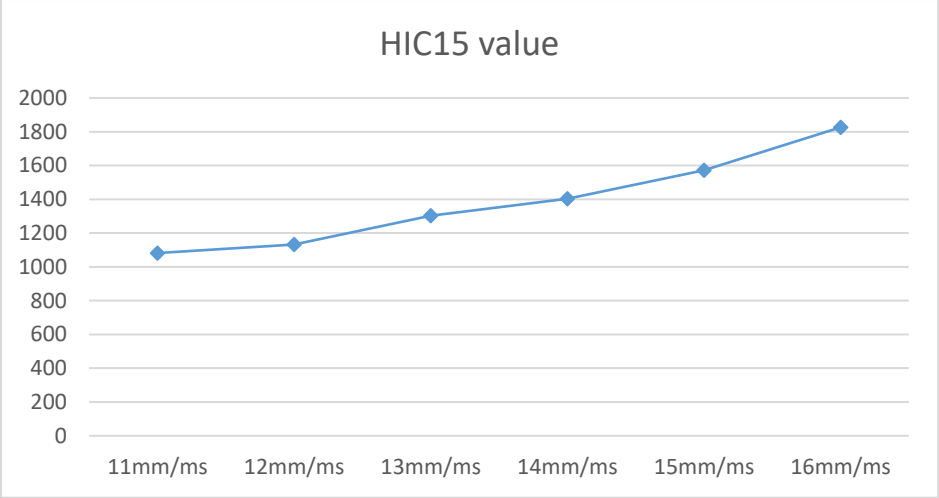

Figure 4.29 HIC_{15} Values

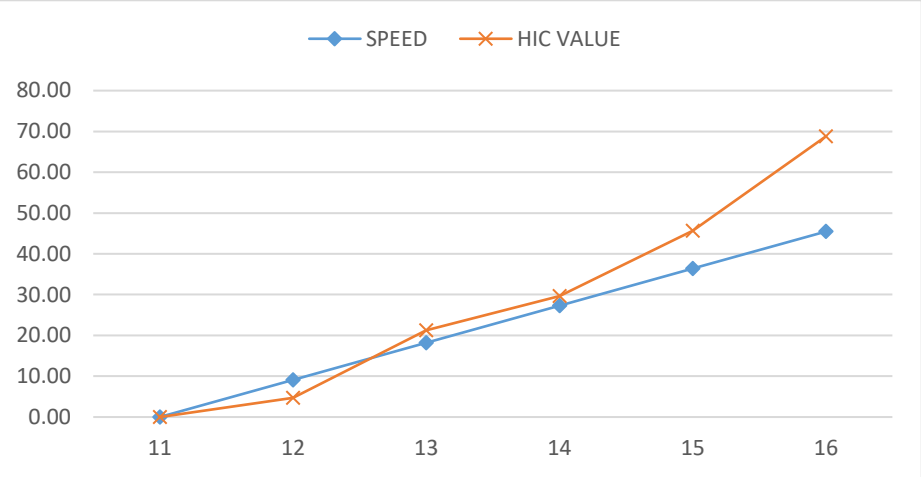

Figure 4.30 Variation of HIC Value with Impact Speed Variation

The parametric analysis of the simulated impact events indicates that the helmeted setup always reduces the Head Injury Criterion (HIC) compared to the unhelmeted baseline throughout the entire range of velocities studied. Although HIC 15 values show a monotonic rise with the magnitude of impact in both cohorts as in Figure 4.31, the helmeted condition systematically provides lower injury indices at each discrete velocity level, which supports a long-term protective effect. However, the data indicates that the relative protective efficacy of the helmet system is inversely proportional to the impact velocity as represented in Figure 4.32. This noted convergence of injury measures at increased velocities indicates a decreasing marginal protection, these results are similar to (Ho Trong

et al., 2026) which can be explained by the Expanded Polystyrene (EPS) liner approaching its densification limit, beyond which the shift to high-stiffness response prevents additional energy dissipation. As a result, although the study quantitatively confirms the protective effect of the helmet in reducing the severity of head injuries, it also demonstrates the importance of impact velocity on the mechanical limits of protective liner performance.

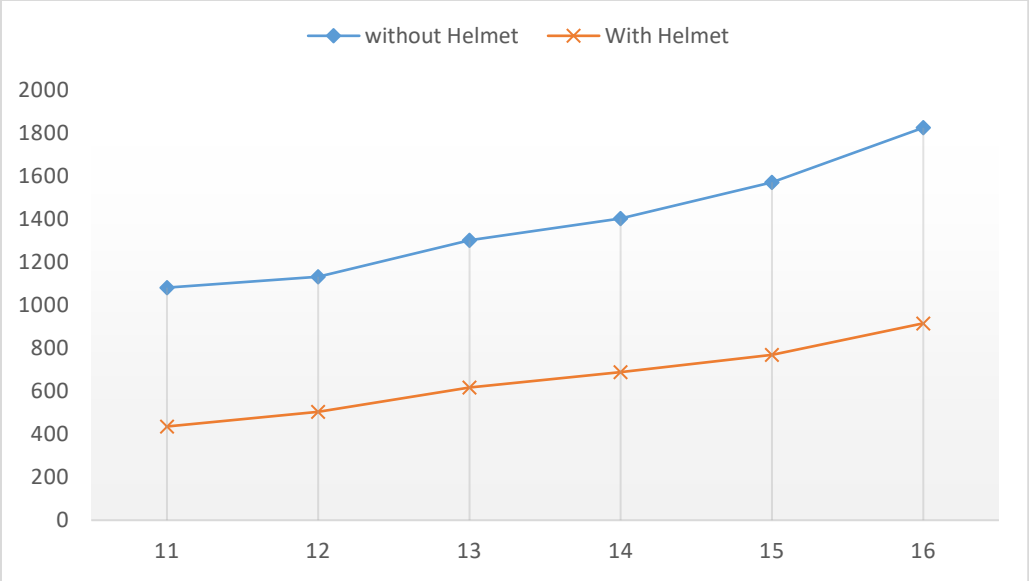

Figure 4.31 Comparison of HIC_{15} Values Across Impact Speeds for Unhelmeted and Helmeted Conditions

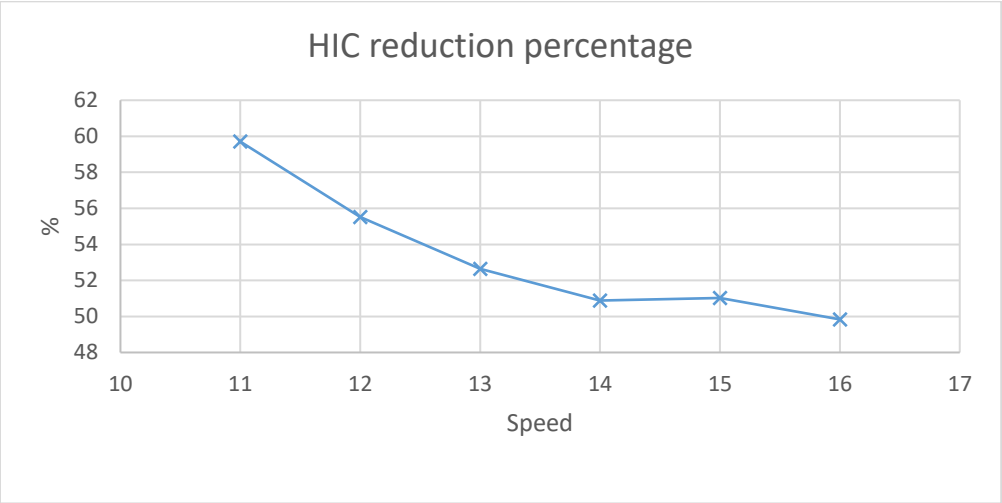

Figure 4.32 Percentage Reduction on HIC_{15} Attributes to Helmet Use t Different Speed

CHAPTER 5: CONCLUSIONS

5.1 General

This study presents a detailed analytical investigation of a real-world motorcycle-truck collision using an integrated two-stage simulation framework. The initial phase involves the use of PC-Crash in the macroscopic reconstruction of crashes, and the second phase involves the use of LS-DYNA in the microscopic finite element analysis of head injuries. Filling a significant gap in the literature on Nepalese road safety, the methodology creates a physically consistent connection between vehicle-based collision dynamics and head injury analysis of occupants through a case-specific approach. Kinematic boundary conditions are rigorously transferred from the reconstruction phase to the finite element model, enabling a quantitative evaluation of head injury mechanisms under both unhelmeted and helmeted conditions.

5.1.1 PC-Crash Crash Reconstruction

A physics-based reconstruction of the selected motorcycle-truck collision was effectively reconstructed with PC-Crash. The incident involved a two-occupant motorcycle a rider who sustained fatal head injuries and a pillion passenger who survived with severe cranial trauma in a collision with a heavy truck on an urban road. Primary input data were sourced from police incident records, supplemented by road geometry extracted from Google Maps satellite imagery and vehicle parameters retrieved from the PC-Crash vehicle database. The reconstruction was subjected to iterative calibration, with simulated post-impact vehicle trajectories, rest positions, and damage correspondence systematically adjusted until convergence with the available physical evidence was achieved. The calibrated model yielded the following key results:

- Pre-impact truck speed 34kmph and motorcycle speed 18kmph
- The trucks pre-crash maneuver involved forward acceleration at 1m/s2 followed by a rightward abrupt lane change with lateral rise distance of 4m and maximum lateral acceleration of 4m/s2, initiated to overtake a slow-moving vehicle

- Point of impact is almost 0.6m towards two- wheelers designated lane from double solid white line marking
- Post impact rest positions: truck approximately 10m and two-wheeler and riders approximately 12m beyond the crash point, were consistent with available police report documentation
- Contact force analysis confirmed the motorcycle sustained significantly higher impact forces than the truck, consistent with vehicle damage report evidence on case record.

Calibrated PC-Crash model has a proven kinematic base, and simulated crash trajectories, configurations of impacts, and patterns of damages have been found to be very close to recorded crash evidence. Outputs of pre-impact velocity and direction of the calibrated model were moved directly to LS-DYNA as initial conditions of the finite element simulation.

5.1.2 LS-DYNA Simulations

This study employed finite element simulation in LS-DYNA to assess the risk of head injury risk in unhelmeted and helmeted pillion rider head impact scenarios against a truck surface. A standardized LS-DYNA pedestrian headform impactor was used from the software library, comprising four components: outer skin (viscoelastic). The truck surface was modeled as a steel shell (MAT_PIECEWISE_LINEAR_PLASTICITY). For the helmeted configuration, a two-component helmet assembly was positioned over the headform -the outer shell modeled using MAT_PLASTIC_KINEMATIC to represent polycarbonate material capturing elastic-plastic deformation, and the inner EPS foam liner modeled using MAT_CRUSHABLE_FOAM, characterized by a volumetric stress-strain curve governing progressive compressive crushing and energy dissipation. contact interfaces defined using CONTACT_TIED_SURFACE_TO_SURFACE at the liner-headform interface and CONTACT_AUTOMATIC_SURFACE_TO_SURFACE at the truck surface. Both configurations were simulated at an identical impact velocity of 14mm/ms. Injury severity was assessed using peak resultant head acceleration, and HIC_{15}, benchmarked against the AIS scale and corroborated against the reported clinical outcome. The key results obtained from the simulation analyses are presented below to summarize the overall findings of this study.

- The unhelmeted simulation produced severe head injury with peak resultant acceleration of 190g with HIC_{15} value of 1403 correspond to AIS4(severe), consistent with clinically documented severe cranial trauma.
- The impact pulse was short and sharp at 3-4ms, indicating direct, unmitigated high velocity contact with the truck surface with no energy dissipation or absorption.
- Helmeted simulation significantly reduced predicted injury severity. Peak resultant acceleration reduced to 103g and HIC_{15} to 689, decreasing injury prediction by two AIS categories: Severe (AIS 4) to Moderate (AIS 2).
- The helmet extended the impact pulse to 10–12 ms, as the polycarbonate shell distributed contact load spatially and the EPS liner absorbed energy through progressive volumetric crushing.
- All measured metrics confirmed significant and consistent protective effect. Peak acceleration was decreased by 46%, HIC_{15} by 50.8% and von Mises stress by 42% (0.0045 Gpa to 0.0026 Gpa) compared to the unhelmeted baseline simulation.

5.2 Key Conclusions

Based on the integrated simulation framework and subsequent quantitative injury analysis, the following conclusions are drawn.

5.2.1 Effectiveness of the Integrated Simulation Approach

The integration of PC-Crash and LS-DYNA provides a technically feasible framework for linking crash dynamics and biomechanical injury assessment in the Nepalese context. The systematic transfer of boundary conditions between the two simulation platforms enabled a case-specific analysis of head injury mechanisms that would not be possible through traditional reconstruction methods alone. As a single-case proof-of-concept, the results are indicative rather than generalizable, and the framework should be treated as a methodological demonstration pending replication across multiple cases. The correspondence between the simulated unhelmeted HIC_{15} value (AIS 4) and the documented clinical outcome (severe cranial trauma, survived) provides qualitative confidence in the simulation inputs.

5.2.2 Strong Dependence of Injury Severity on Impact Conditions.

Head injury metrics, including peak resultant acceleration and HIC_{15}, are highly sensitive to impact velocity and contact surface conditions. Due to the nonlinear biomechanical response of the headform assembly, even moderate increases in impact speed result in disproportionately large increases in HIC_{15}, driven by the 2.5-power dependence of the metric on acceleration. This trend was confirmed through parametric analysis over impact velocities of 11–16 mm/ms, where HIC_{15} increased monotonically with speed in both configurations.

5.2.3 Indicative Evidence for Helmet Protective Effect

Helmets do not completely prevent serious injury, even though they greatly decrease the severity of injuries. The parametric analysis shows that the protective effectiveness decreases at higher impact velocities, as the EPS liner approaches its densification limit. Beyond this, the liner becomes highly stiffness-response, and it ceases to be able to absorb progressive energy, which sets a physical limit on how much protection the helmet can provide.

5.2.4 Relevance to the Nepalese Road Safety Context

This study provides simulation-based, case-specific evidence linking helmet use to reduced head injury in a motorcycle–truck collision within the Nepalese context. It demonstrates that the police records serve as a viable source of data to reconstruct a crash when there are no centralized crash databases. The methodology establishes a replicable framework for future multi-case investigations in Nepal and South Asia. Conclusions pertaining to helmet enforcement and safety policy should be treated as indicative of potential benefits, not as independent evidence sufficient for policy direction.

5.3 Limitations of This Study

Despite its contributions, this study has several limitations that should be considered when interpreting the results. To begin with, the analysis relies on a single crash case, which restricts its statistical generalizability. Second, there was no experimental validation, which limited the possibility to quantitatively confirm the results of the simulation. Third, the headform and the geometric models employed in the model are simplified and the material

models of the biological tissues and the helmet components are idealized. Fourth, the analysis did not include rotational head injury measures such as the Brain Rotational Injury Criterion (BrIC) or angular acceleration metrics. This is a substantive gap given that the reconstructed crash involves a 25° oblique approach angle, which is known to induce rotational head kinematics particularly associated with diffuse axonal injury a mechanism not captured by HIC_{15}, which is based solely on linear acceleration. Parametric analysis was limited to different impact speed. The effect of different impact angle on head injury matric was not investigated. Moreover, the helmet model does not include a retention system (chin strap, fit), visor and proper wear condition. The helmet material model was not calibrated against Nepal Standard certified helmets. Material properties from international research on helmet testing were used as surrogates, which may not represent the actual mechanical performance of helmets in use in Nepal. This may lead to differences in protective performance substantially from the simulated results.

5.4 Recommendation for Future Works

A few recommendations can be made in order to make this study more comprehensive and applicable. The approach must be applied to several crash cases to get more statistically valid and generalizable outcomes. Other injury measures like rotational acceleration and brain strain measures should be incorporated to provide a more holistic evaluation of head injuries.

The helmet model can be improved by incorporating more advanced material properties, such as rate-dependent and crushable foam behavior, calibrated using standard impact test data. Moreover, a more comprehensive parametric sensitivity analysis of the impact speed, angle, and the properties of the helmet materials on the injury outcomes would enhance the predictive power of the framework.

REFERENCES

Ahmed, I., Islam, T., Ali, G., & Nawaz, M. M. (2016). Pillion riders' cloth related injuries and helmet wearing patterns: A study of Lahore, Pakistan. *International Journal of Injury Control and Safety Promotion*, *23*(4), 388–394. https://doi.org/10.1080/17457300.2015.1047866

Ainy, E., Khorshidi, A., Monfared, A. B., Soori, H., & Haddadi, M. (2016). Epidemiological Pattern of Road Traffic Injuries among Occupants' Vehicles in 2012. *Journal of Transportation Technologies*, *6*(5), Article 5. https://doi.org/10.4236/jtts.2016.65025

Al-Zubaidi, H., Tamakloe, R., Al-Bdairi, N. S. S., Alnedawi, A., & Obaid, I. (2022). Exploring senior motorcyclist injury severity crashes: Random parameter model with heterogeneity in mean and variance. *IATSS Research*, *47*. https://doi.org/10.1016/j.iatssr.2022.12.001

Ankarath, S., Giannoudis, P. V., Barlow, I., Bellamy, M. C., Matthews, S. J., & Smith, R. M. (2002). Injury patterns associated with mortality following motorcycle crashes. *Injury*, *33*(6), 473–477. https://doi.org/10.1016/S0020-1383(02)00048-7

Asian Transport Observatory. (2025). Nepal Road Safety Profile 2025. https://asiantransportobservatory.org/analytical-outputs/roadsafetyprofiles/nepal-road-safety-profile-2025/

Bhatta, S., Pathak, P., Khadka, A., Parkin, J., Pilkington, P., Joshi, S. K., Joshi, S., & Mytton, J. (2024). Injury risks for different road users in Nepal: A secondary analysis of routinely collected crash data. *Global Health Research*, (1), 77–87. https://doi.org/10.3310/DWTR9883

Bourdet, N., Deck, C., & Willinger, R. (2011). *CAR BONNET EVALUATION AGAINST PEDESTRIAN HEAD IMPACT BASED ON A LUMPED MODELING APPROACH*.

Brown, L., Morris, A., Thomas, P., Ekambaram, K., Margaritis, D., Davidse, R., Usami, D. S., Robibaro, M., Persia, L., Buttler, I., Ziakopoulos, A., Theofilatos, A., Yannis, G., Martin, A., & Wadji, F. (2021). Investigation of accidents involving powered two wheelers and bicycles – A European in-depth study. *Journal of Safety Research*, *76*, 135–145. https://doi.org/10.1016/j.jsr.2020.12.015

Chaichan, S., Asawalertsaeng, T., Veerapongtongchai, P., Chattakul, P., Khamsai, S., Pongkulkiat, P., Chotmongkol, V., Limpawattana, P., Chindaprasirt, J., Senthong, V., Ngamjarus, C., Sittichanbuncha, Y., Kitkhuandee, A., & Sawanyawisuth, K. (2020). Are full-face helmets the most effective in preventing head and neck injury in motorcycle accidents? A *meta*-analysis. *Preventive Medicine Reports*, *19*, 101118. https://doi.org/10.1016/j.pmedr.2020.101118

Chang, F., Li, M., Xu, P., Zhou, H., Haque, M. M., & Huang, H. (2016). Injury Severity of Motorcycle Riders Involved in Traffic Crashes in Hunan, China: A Mixed Ordered Logit Approach. *International Journal of Environmental Research and Public Health*, *13*(7), 714. https://doi.org/10.3390/ijerph13070714

Department of Transport Management, GoN. (2025). *Annual Progress Report 2025* [DoTM Annual Progress Report]. Government of Nepal, Department of Transport Management. https://dotm.gov.np/content/27/annual-progress-report-2081-82/

Dr. Steffan Datentechnik. (2023). *PC-Crash Manual* (Version 14.1) [Computer software].

Faduyile, F., Emiogun, F., Soyemi, S., Oyewole, O., Okeke, U., & Williams, O. (2017). Pattern of Injuries in Fatal Motorcycle Accidents Seen in Lagos State University

Teaching Hospital: An Autopsy-Based Study. *Open Access Macedonian Journal of Medical Sciences*, *5*(2), 112–116. https://doi.org/10.3889/oamjms.2017.025

Fernandes. (2012). *Analysis of injuries resulting from impacts with motorcycle helmets*. https://www.proquest.com/docview/2891960231

Gabella, B., Reiner, K. L., Hoffman, R. E., Cook, M., & Stallones, L. (1994). *RELATIONSHIP OF HELMET USE AND HEAD INJURIES AMONG MOTORCYCLE CRASH VICTIMS IN EL PASO COUNTY, COLORADO, 1989-1990*.

Ghimire, J., C, L. K., Kafle, K. R., & Adhikari, B. (2025). Road Safety in Numbers: Using Data to Illustrate the Nepal's Scenarios. *American Journal of Traffic and Transportation Engineering*, *10*(5), 120–134. https://doi.org/10.11648/j.ajtte.20251005.13

Government of nepal. (1993). https://lawcommission.gov.np/content/13303/riding-and-transportation-arrangements-act--2049/

Harish, A. (2019, January 8). Implicit vs. Explicit FEM: What Is the Difference? *SimScale*. https://www.simscale.com/blog/implicit-vs-explicit-fem/

Ho, T., Ly, H., Nguyen, V.-T., & Quang, T. (2025). Analysis of head injuries of motorcyclist colliding with cars in traffic conditions in Vietnam. *Journal of Physics: Conference Series*, *2949*, 012036. https://doi.org/10.1088/1742-6596/2949/1/012036

Ho Trong, D., Ly Hung, A., & Nguyen Van, T. (2026). Effects of Half-Face Helmets on Motorcyclist Head Injuries: A Finite Element Simulation Study with Experimental Validation. *International Journal of Automotive Science And Technology*, *10*(1), 112–122. https://doi.org/10.30939/ijastech..1831183

iRAP. (2021). Safety Insights Explorer. *iRAP*. https://irap.org/safety-insights-explorer/

Johansson, A., & Nilsson, C. (2025). *Modeling Handball-Induced Head Injuries: Developing a Model of a Handball for Evaluating Concussion Risk and the Effectiveness of Protective Gear for Handball Players*. http://hdl.handle.net/20.500.12380/309876

Keall, M. D., & Newstead, S. (2012). Analysis of factors that increase motorcycle rider risk compared to car driver risk. *Accident Analysis & Prevention*, *49*, 23–29. https://doi.org/10.1016/j.aap.2011.07.001

Khadka, A., Parkin, J., Pilkington, P., Joshi, S. K., & Mytton, J. (2022). Completeness of police reporting of traffic crashes in Nepal: Evaluation using a community crash recording system. *Traffic Injury Prevention*, *23*(2), 79–84. https://doi.org/10.1080/15389588.2021.2012766

Kimpara, H., Nakahira, Y., Iwamoto, M., Miki, K., Ichihara, K., Kawano, S., & Taguchi, T. (2006). *Investigation of Anteroposterior Head-Neck Responses during Severe Frontal Impacts Using a Brain-Spinal Cord Complex FE Model*. The Stapp Association. 50th Stapp Car Crash Conference. https://doi.org/10.4271/2006-22-0019

Kirkpatrick, S. W., MacNeill, R., & Bocchieri, R. T. (2003). *Development of an LS-DYNA Occupant Model for use in Crash Analyses of Roadside Safety Features*.

Kononen, D., Flannagan, C., & Wang, S. (2011). Identification and validation of a logistic regression model for predicting serious injuries associated with motor vehicle crashes. *Accident; Analysis and Prevention*, *43*, 112–122. https://doi.org/10.1016/j.aap.2010.07.018

Kual, A., Sinha, U. S., Pathak, Y. K., Singh, A., Kapoor, A. K., Sharma, S., & Singh, S. (2005). Fatal Road Traffic Accidents, Study Of Distribution, Nature and Type of

Injury. *Journal of Indian Academy of Forensic Medicine*, *27*(2), 71–76. https://doi.org/10.1177/0971097320050203

Kudlich, H. (1966). *Beitrag zur mechanik des kraftfahrzeug-verkehrsunfalls*. na.

Larsen, C. F., & Hardt-Madsen, M. (1988). *FATAL MOTORCYCLE ACCIDENTS IN THE COUNTY OF FUNRN (DENMARK)*.

Lin, M.-R., & Kraus, J. F. (2009). A review of risk factors and patterns of motorcycle injuries. *Accident Analysis & Prevention*, *41*(4), 710–722. https://doi.org/10.1016/j.aap.2009.03.010

Lloyd, J. (2025). Traumatic Head and Brain Injuries in Helmeted Motorcycle Crashes. *Stapp Car Crash Journal*, *69*(1), 162–180. https://doi.org/10.4271/2025-22-0006

Lopez-Valdes, F., García, D., Pedrero, D., & Moreno, J. (2005). *Accidents of Motorcyclists Against Roadside Infrastructure* (pp. 163–170). https://doi.org/10.1007/1-4020-3796-1_17

LS DYNA user manual, L. D. (2021). Manuals. *LSDYNA*. https://lsdyna.ansys.com/manuals/

Marković, N., Pešić, D. R., Antić, B., & Vujanić, M. (2016). The analysis of influence of individual and environmental factors on 2-wheeled users' injuries. *Traffic Injury Prevention*, *17*(6), 610–617. https://doi.org/10.1080/15389588.2015.1132314

Mätzsch, T., & Karlsson, B. (1986). Moped and Motorcycle Accidents Similarities and Discrepancies. *The Journal of Trauma*, *26*, 538–543. https://doi.org/10.1097/00005373-198606000-00008

Miller, L. E., Urban, J. E., & Stitzel, J. D. (2016). Development and validation of an atlas-based finite element brain model. *Biomechanics and Modeling in Mechanobiology*, *15*(5), 1201–1214. https://doi.org/10.1007/s10237-015-0754-1

Mohd Jawi, Z., Tan, K. S., Risby, M. S., Ng, C. P., Loh, W. P., Abu Kassim, K. A., & Ahmad, Y. (2021). Rider's Head Injury Risks in Relation to Dynamics of Motorcycle in Frontal Crashes. *Journal of the Society of Automotive Engineers Malaysia*, *5*, 72–87. https://doi.org/10.56381/jsaem.v5i1.154

Moser, A., Steffan, H., & Kasanický, G. (1999). *The Pedestrian Model in PC-Crash—The Introduction of a Multi Body System and its Validation*. SAE International. International Congress & Exposition. https://doi.org/10.4271/1999-01-0445

N. Ottosson, & H. Petersson. (1992). *N. Ottosson and H. Petersson. Introduction to the FINITE ELEMENT METHOD. Prentice Hall Europe, 1992.* Bing.

Naqvi, H., & Tiwari, G. (2017). Factors Contributing to Motorcycle Fatal Crashes on National Highways in India. *Transportation Research Procedia*, *25*, 2089–2102. https://doi.org/10.1016/j.trpro.2017.05.402

Narayan Yoganandan, Alan M. Nahum, & John W. Melvin,. (2015). *Accidental Injury: Biomechanics and Prevention | Springer Nature Link*. https://doi.org/https://doi.org/10.1007/978-1-4939-1732-7 (Original work published Springer New York, NY)

Nepal Traffic Police. (2024). https://traffic.nepalpolice.gov.np/publication/5/

Nguyen, D. V. M., Vu, A. T., Polders, E., Ross, V., Brijs, T., Wets, G., & Brijs, K. (2021). Modeling the injury severity of small-displacement motorcycle crashes in Hanoi City, Vietnam. *Safety Science*, *142*, 105371. https://doi.org/10.1016/j.ssci.2021.105371

Nguyen, T., & Dinh, T. (2025). Research on modeling and simulation of car-pedestrian collision using ansys LS-DYNA software. *EUREKA: Physics and Engineering*, 175–182. https://doi.org/10.21303/2461-4262.2025.003677

Okereke, M., & Keates, S. (2018). *Finite Element Applications*. Springer International Publishing. https://doi.org/10.1007/978-3-319-67125-3

Orsi, C., Stendardo, A., Marinoni, A., Gilchrist, M. D., Otte, D., Chliaoutakis, J., Lajunen, T., Özkan, T., Pereira, J. D., Tzamalouka, G., & Morandi, A. (2012). Motorcycle riders' perception of helmet use: Complaints and dissatisfaction. *Accident Analysis & Prevention*, *44*(1), 111–117. https://doi.org/10.1016/j.aap.2010.12.029

Parab, M. S., Mallela, S., Bala, S., & Noronha, N. (2020). *Pedestrian Head Impact, Automated Post Simulation Results Aggregation, Visualization and Analysis Using d3VIEW* (SAE Technical Paper Nos. 2020-01–1330). SAE International. https://doi.org/10.4271/2020-01-1330

Pérez-Zuriaga, A. M., Dols, J., Nespereira, M., García, A., & Sajurjo-de-No, A. (2023). Analysis of the consequences of car to micromobility user side impact crashes. *Journal of Safety Research*, *87*, 168–175. https://doi.org/10.1016/j.jsr.2023.09.014

Qiu, J., Su, S., Duan, A., Feng, C., Xie, J., Li, K., & Yin, Z. (2020). Preliminary injury risk estimation for occupants involved in frontal crashes by combining computer simulations and real crashes. *Science Progress*, *103*(2), 0036850420908750. https://doi.org/10.1177/0036850420908750

Radzuan, N. Q., Hassan, M. H. A., Omar, M. N., & Abu Kassim, K. A. (2024). The Protective Performance of Different Types of Motorcycle Helmets in Terms of HIC and BrIC. In M. H. A. Hassan, M. N. Omar, N. H. Johari, & Y. Zhong (Eds.), *Proceedings of the 2nd Human Engineering Symposium* (pp. 249–262). Springer Nature. https://doi.org/10.1007/978-981-99-6890-9_20

Ramli, R., Oxley, J., Noor, F. M., Abdullah, N. K., Mahmood, M. S., Tajuddin, A. K., & McClure, R. (2014). Fatal injuries among motorcyclists in Klang Valley, Malaysia.

Journal of Forensic and Legal Medicine, *26*, 39–45. https://doi.org/10.1016/j.jflm.2014.06.007

Rifaat, S., Tay, R., & De Barros, A. (2012). Severity of motorcycle crashes in Calgary. *Accident; Analysis and Prevention*, *49*, 44–49. https://doi.org/10.1016/j.aap.2011.02.025

Ruan, J., El-Jawahri, R., Chai, L., Barbat, S., & Prasad, P. (2003, October 27). Prediction and Analysis of Human Thoracic Impact Responses and Injuries in Cadaver Impacts Using a Full Human Body Finite Element Model. *SAE Technical Paper Series*. 47th Stapp Car Crash Conference (2003). https://doi.org/10.4271/2003-22-0014

Santos, K., Silva, N. M., Dias, J. P., & Amado, C. (2023). A methodology for crash investigation of motorcycle-cars collisions combining accident reconstruction, finite elements, and experimental tests. *Engineering Failure Analysis*, *152*, 107505. https://doi.org/10.1016/j.engfailanal.2023.107505

Seyfi, M. A., Aghabayk, K., Karimi Mamaghan, A. M., & Shiwakoti, N. (2023). Modeling the Motorcycle Crash Severity on Nonintersection Urban Roadways in the Australian State of Victoria Using a Random Parameters Logit Model. *Journal of Advanced Transportation*, *2023*(1), 2250590. https://doi.org/10.1155/2023/2250590

Shaheed, M. S., & Gkritza, K. (2014). A latent class analysis of single-vehicle motorcycle crash severity outcomes. *Analytic Methods in Accident Research*, *2*, 30–38. https://doi.org/10.1016/j.amar.2014.03.002

Shankar, V., & Mannering, F. (1996). An exploratory multinomial logit analysis of single-vehicle motorcycle accident severity. *Journal of Safety Research*, *27*(3), 183–194. https://doi.org/10.1016/0022-4375(96)00010-2

Shunfeng Li,. (2022). *Methodologies for the Reliable and Efficient Design of Helmet Against Head Injury* [Doctor of Philosophy in the Faculty of Science and Engineering, The University of Manchester (United Kingdom)]. https://www.proquest.com/docview/3059442282

Siebert, F. W., Hellmann, L., Pant, P. R., Lin, H., & Et., A. (2021). Disparity of motorcycle helmet use in Nepal – Weak law enforcement or riders' reluctance? *Transportation Research Part F: Traffic Psychology and Behaviour*. https://doi.org/10.1016/j.trf.2021.04.005

Slibar, A. (1966). Die mechanischen Grundsätze des Stoßvorganges freier und geführter Körper und ihre Anwendung auf den Stoßvorgang von Fahrzeugen. *Archiv Für Unfallforschung*, *2*(1), 31.

Steffan, H., & Moser, A. (2011). PC-Crash, a simulation program for vehicle accidents. *Technical Manuel, Mac Innis Engineering*.

Sulaie, S. A. (2025). Sensitivity Analysis of Factors Affecting Consequences Due to Traffic Crashes: A Bayesian Network Modelling. *Journal of Road Safety*, *36*(1). https://doi.org/10.33492/JRS-D-25-1-2442769

Tay, R., & Rifaat, S. (2007). Factors contributing to the severity of intersection crashes. *Journal of Advanced Transportation*, *41*, 245–265. https://doi.org/10.1002/atr.5670410303

Thai, T., Ly, H., Vo, B., Do, H.-T., & Nguyen, L. (2021). Design and modeling motorcycle helmets using numerical simulation. In *AIP Conference Proceedings* (Vol. 2420). https://doi.org/10.1063/5.0068424

Thompson, D. C., Rivara, F., & Thompson, R. (1999). *Helmets for preventing head and facial injuries in bicyclists* -. https://www.cochranelibrary.com/cdsr/doi/10.1002/14651858.CD001855/full

Tinard, V., Deck, C., Meyer, F., Bourdet, N., & Willinger, R. (2009). Influence of pedestrian head surrogate and boudary conditions on head injury risk prediction. *International Journal of Crashworthiness*, *14*, 259–268. https://doi.org/10.1080/13588260802434046

Unal, V., Unal, E. O., Koral, F., Cetinkaya, Z., & Koc, S. (2018). Deaths from Motorcycle Accidents: An Autopsy Study from Turkey. *Arab Journal of Forensic Sciences & Forensic Medicine*, *1*(7), 893–901. https://doi.org/10.26735/16586794.2018.016

Urquhart, S. J. (2015a). *The Forensic Reconstruction of Road Traffic Accidents*.

Urquhart, S. J. (2015b). *The Forensic Reconstruction of Road Traffic Accidents*.

Van Elslande, P., & Elvik, R. (2012). Powered two-wheelers within the traffic system. *Accident Analysis & Prevention*, *49*, 1–4. https://doi.org/10.1016/j.aap.2012.09.007

van Elslande, P., Fournier, J.-Y., & Parraud, C. (2015). Powered Two-wheelers In Urban Environment: A Detailed Accident Analysis. *International Journal of Safety and Security Engineering*, *5*(4), pp.322-335. https://doi.org/10.2495/SAFE-V5-N4-322-335

Wan, X., Liu, Y., Gao, W., Xu, W., Zhao, Q., & Bai, Z. (2020). Comparison Study of Collision between Car and Different Two-Wheelers Based on PC-Crash Simulation. *2020 12th International Conference on Measuring Technology and Mechatronics Automation (ICMTMA)*, 1030–1038. https://doi.org/10.1109/ICMTMA50254.2020.00222

Wang, C., Quddus, M., & Ison, S. (2011). A spatio-temporal analysis of the impact of congestion on traffic safety on major roads in the UK. *Transportmetrica*, *2011*. https://doi.org/10.1080/18128602.2010.538871

Wang, Q. C., Xie, Z. K., Liu, W. G., & Xiao, H. T. (2012). Research on Simulation and Reconstruction of Vehicle-Pedestrian Collision Based on Multi-Body Dynamics.

Advanced Materials Research, *487*, 307–311. https://doi.org/10.4028/www.scientific.net/AMR.487.307

Waseem, M., Ahmed, A., & Saeed, T. U. (2019). Factors affecting motorcyclists' injury severities: An empirical assessment using random parameters logit model with heterogeneity in means and variances. *Accident Analysis & Prevention*, *123*, 12–19. https://doi.org/10.1016/j.aap.2018.10.022

WHO. (2023). *Global status report on road safety 2023*. https://www.who.int/publications/i/item/9789240086517

Wisutwattanasak, P., Se, C., Sum, S., Champahom, T., Ratanavaraha, V., & Jomnonkwao, S. (2026). Temporal instability of highway pedestrian crash severity: Comparative analysis of machine learning models. *Transportation Research Interdisciplinary Perspectives*, *37*, 101935. https://doi.org/10.1016/j.trip.2026.101935

Wyatt, J. P., O'Donnell, J., Beard, D., & Busuttil, A. (1999). Injury analyses of fatal motorcycle collisions in south-east Scotland. *Forensic Science International*, *104*(2–3), 127–132. https://doi.org/10.1016/S0379-0738(99)00104-8

Yaqoob Md, U., Nadeem, Z., Mehmood, M., Batool, D., Irshad, T., Ali, S., Irshad, H., Aijaz, M., Maroof, S., Jafri, R., Ibrahim, S., Mehmood, R., & Hasan, S. (2016). Descriptive Pattern of Fractures among Motor Bike Riders Presenting in Jinnah Postgraduate Medical Centre, Karachi. *British Journal of Medicine and Medical Research*, *18*, 1–8. https://doi.org/10.9734/BJMMR/2016/28748

APPENDIX A: PC-Crash Simulation Outputs and Hic15 Calculation

A.1 PC-Crash Simulation Runtime output at different time

T=0.00s

T=0.1s

T=0.25s

T=0.7s

T=1.0s

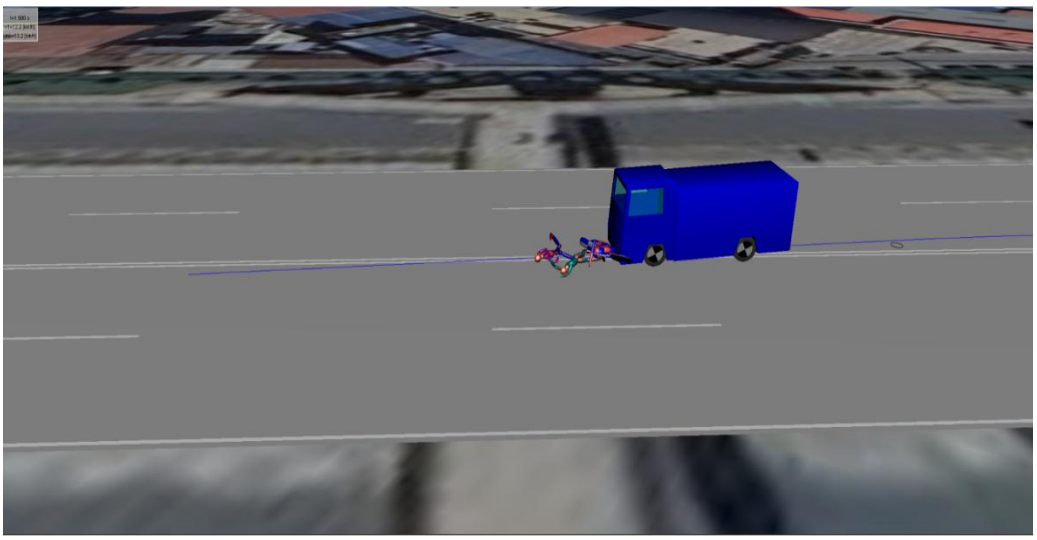

T=1.5s

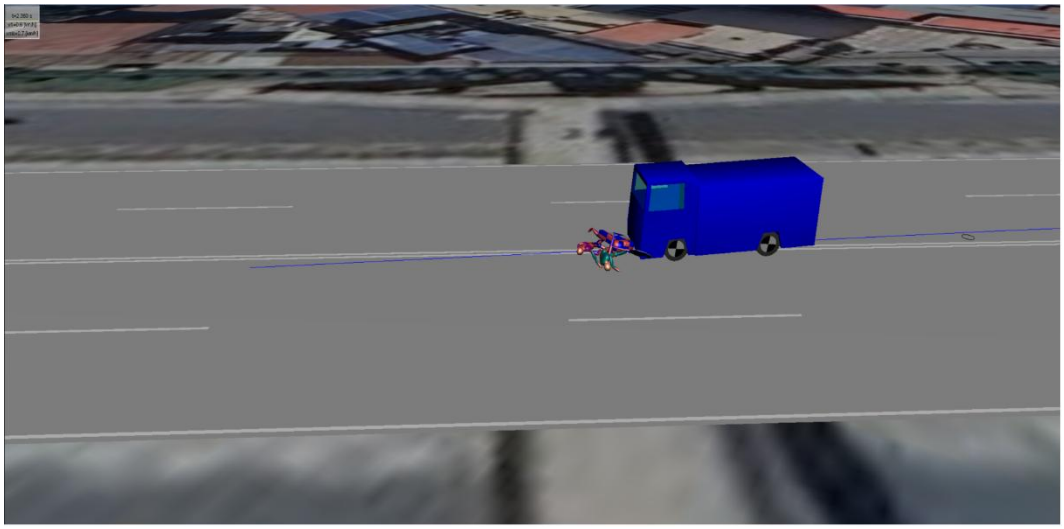

T=2.35s

A.2 Python code for Head Injury Criteria Calculation

```
import numpy as np
import pandas as pd
from scipy.integrate import trapezoid
from openpyxl import load_workbook
from openpyxl.styles import Font, PatternFill, Alignment, Border, Side



def compute_hic15(time: np.ndarray, accel_g: np.ndarray) -> dict:
    """
    Compute HIC₁₅ using sliding window (max 15 ms).
    Formula: HIC = (t2-t1) * [1/(t2-t1) * integral(a dt)]^2.5
    """
    if len(time) != len(accel_g):
        raise ValueError("time and acceleration arrays must have the same length.")
    if len(time) < 2:
        raise ValueError("At least 2 data points are required.")


    max_window_s = 0.015
    hic_max = 0.0
    best_t1 = time[0]
    best_t2 = time[0]
    n = len(time)
```

```
for i in range(n - 1):
    for j in range(i + 1, n):
        dt = time[j] - time[i]
        if dt > max_window_s + 1e-12:
            j -= 1
            break
        integral = trapezoid(accel_g[i:j+1], time[i:j+1])
        if dt > 0:
            hic = dt * (integral / dt) ** 2.5
            if hic > hic_max:
                hic_max = hic
                best_t1 = time[i]
                best_t2 = time[j]


return {
    "hic15"       : round(hic_max, 4),
    "t1"          : best_t1,
    "t2"          : best_t2,
    "duration_ms" : round((best_t2 - best_t1) * 1000, 4),
    "peak_accel"  : round(float(np.max(accel_g)), 4),
}
```

```
def read_data(filepath: str, time_col="Time", accel_col="Acceleration"):
    df = pd.read_excel(filepath, sheet_name=0)

    df.columns = [c.strip() for c in df.columns]

    def find_col(keyword):
        for c in df.columns:
            if keyword.lower() in c.lower():
                return c
        raise KeyError(f"Could not find column containing '{keyword}'. Available:
{list(df.columns)}")

    t_col = find_col(time_col)
    a_col = find_col(accel_col)
    df.dropna(subset=[t_col, a_col], inplace=True)
    df.sort_values(t_col, inplace=True)
    df.reset_index(drop=True, inplace=True)
    return df[t_col].to_numpy(dtype=float), df[a_col].to_numpy(dtype=float), df


# Read data
time_arr, accel_arr, df = read_data("hiccalculation (1).xlsx")
print(f"Loaded {len(time_arr)} data points  |  time range: {time_arr[0]:.4f} – {time_arr[-
1]:.4f} s")
```

```
# Compute HIC15

print("\nComputing HIC15 ...")

result = compute_hic15(time_arr, accel_arr)


# Print results

print("\n" + "="*44)

print("  HIC15  Results")

print("="*44)

print(f"  HIC15                : {result['hic15']}")

print(f"  Window start (t1)    : {result['t1']:.6f} s")

print(f"  Window end   (t2)    : {result['t2']:.6f} s")

print(f"  Window duration      : {result['duration_ms']:.4f} ms")

print(f"  Peak acceleration    : {result['peak_accel']} g")


print("="*44)
```

APPENDIX B: LS-DYNA Finite Element Head Simulation Output

B.1 Linear Head Acceleration output of Unhelmeted and Helmeted simulation at 11mm/ms

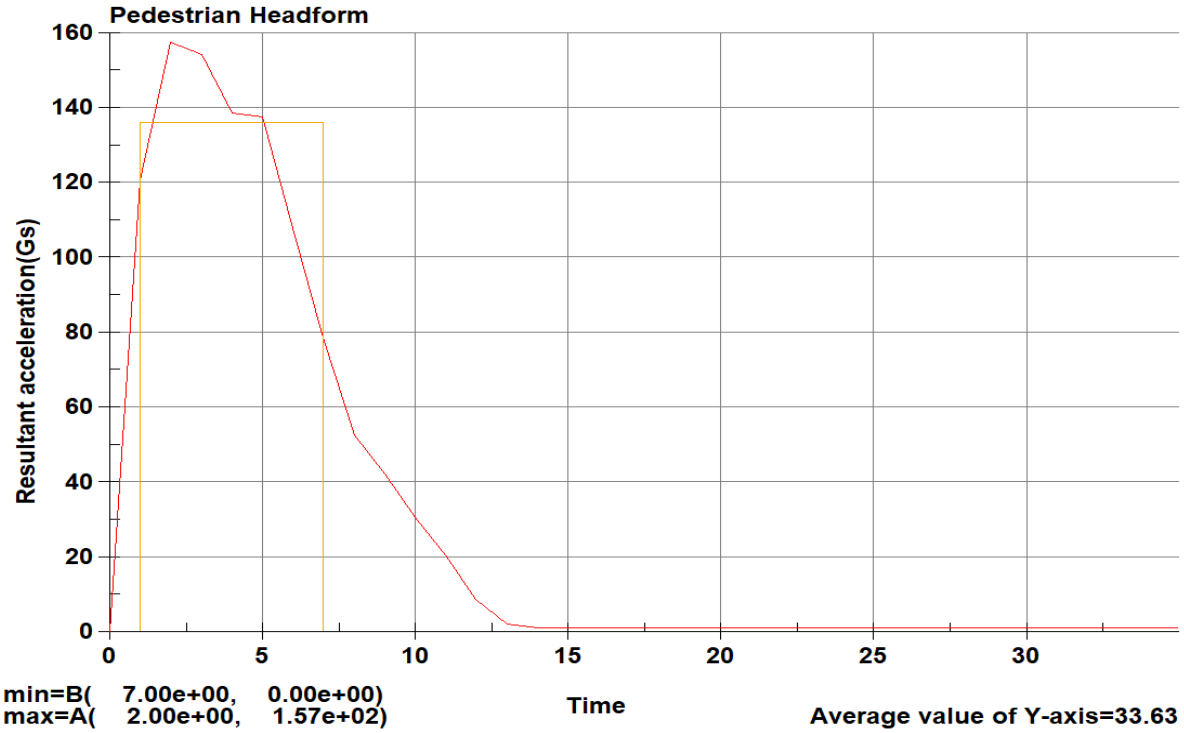

Head impact without Helmet

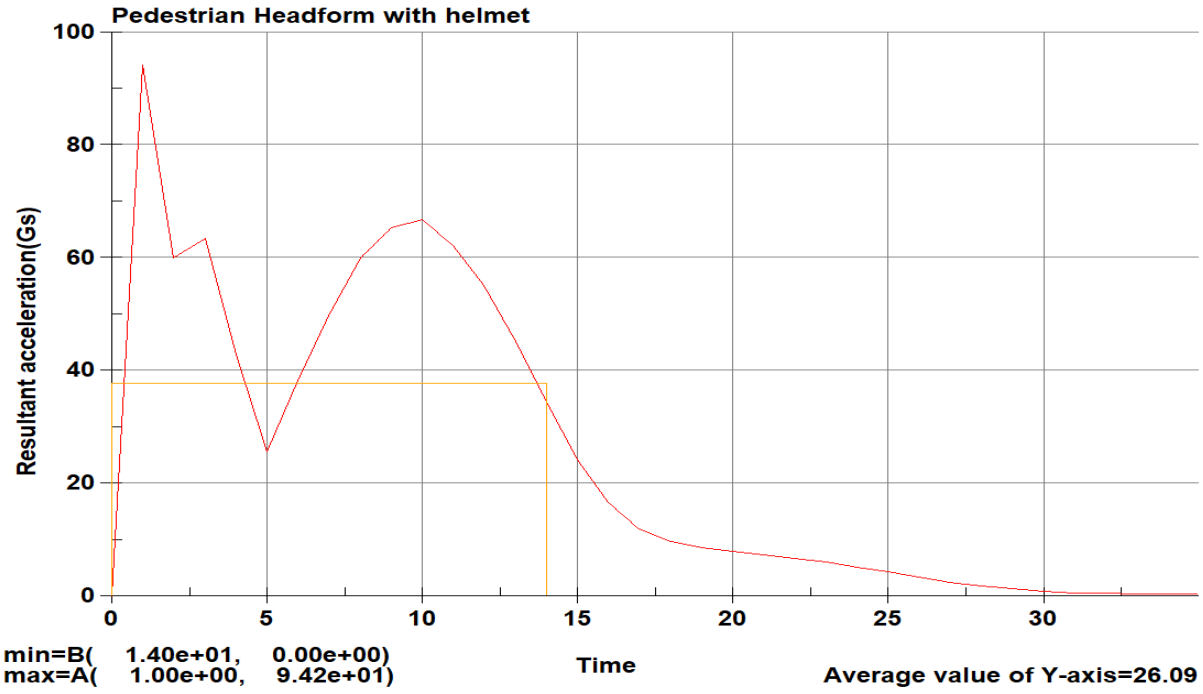

Head impact with Helmet

B.2 Linear Head Acceleration output of Unhelmeted and Helmeted simulation at 12mm/ms

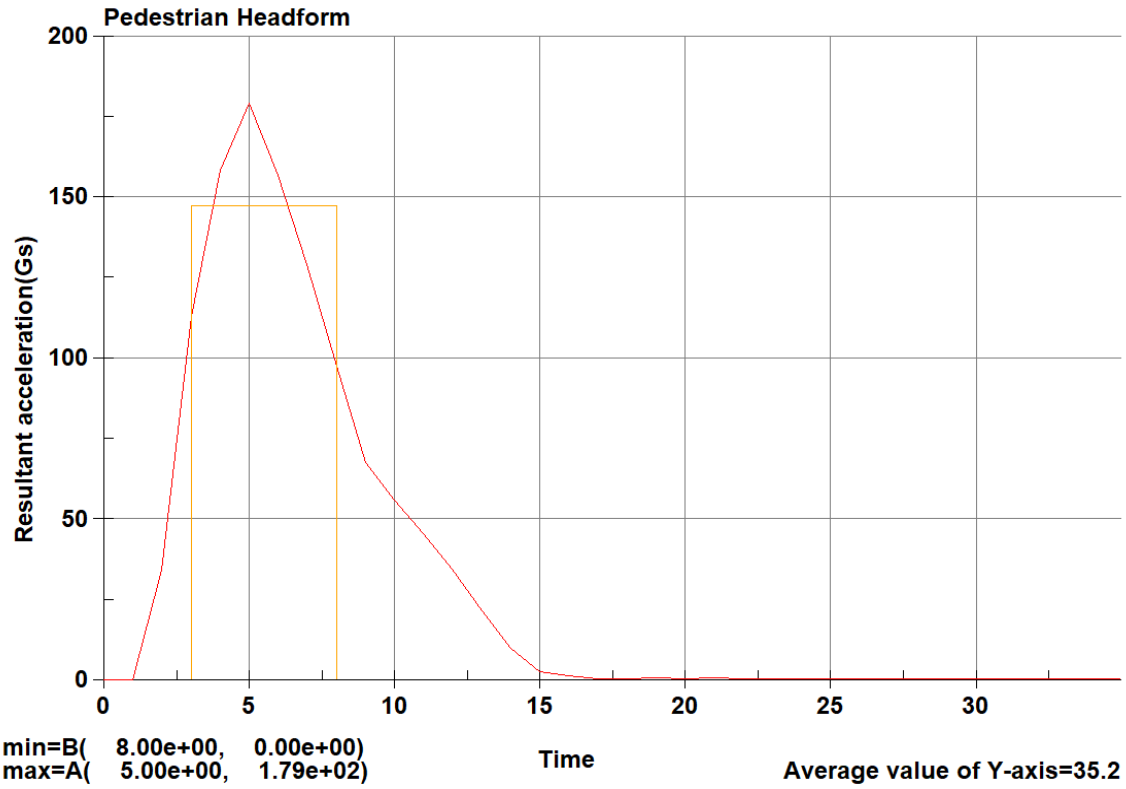

Head impact without Helmet

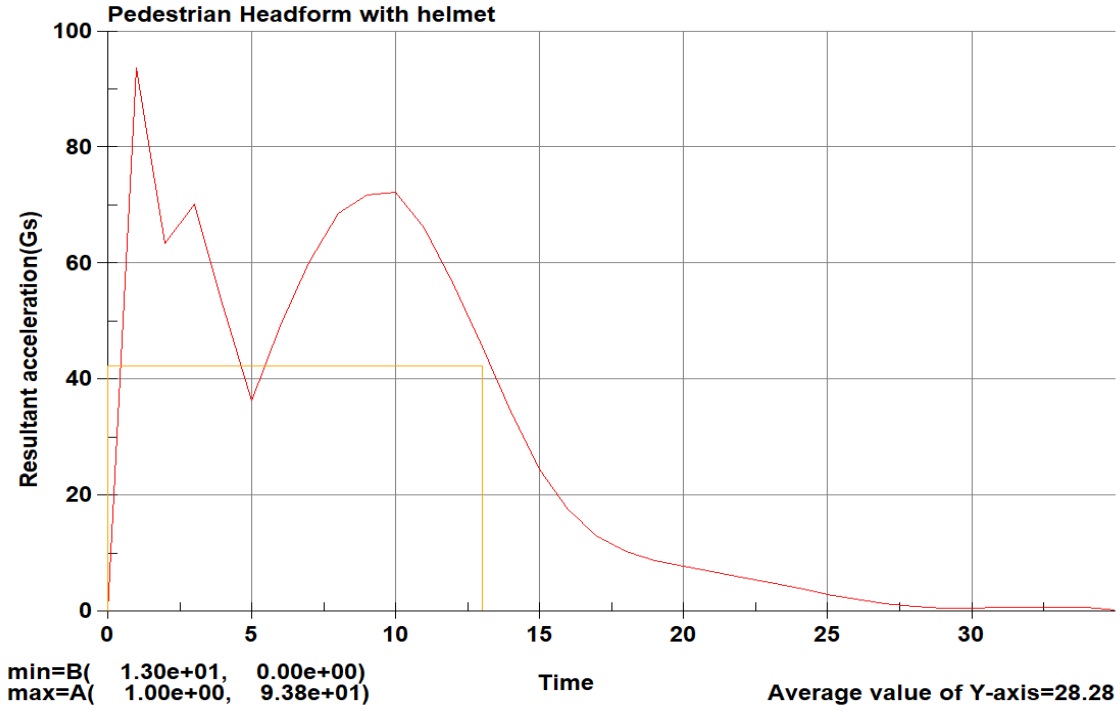

Head impact with Helmet

B.3 Linear Head Acceleration output of Unhelmeted and Helmeted simulation at 13mm/ms

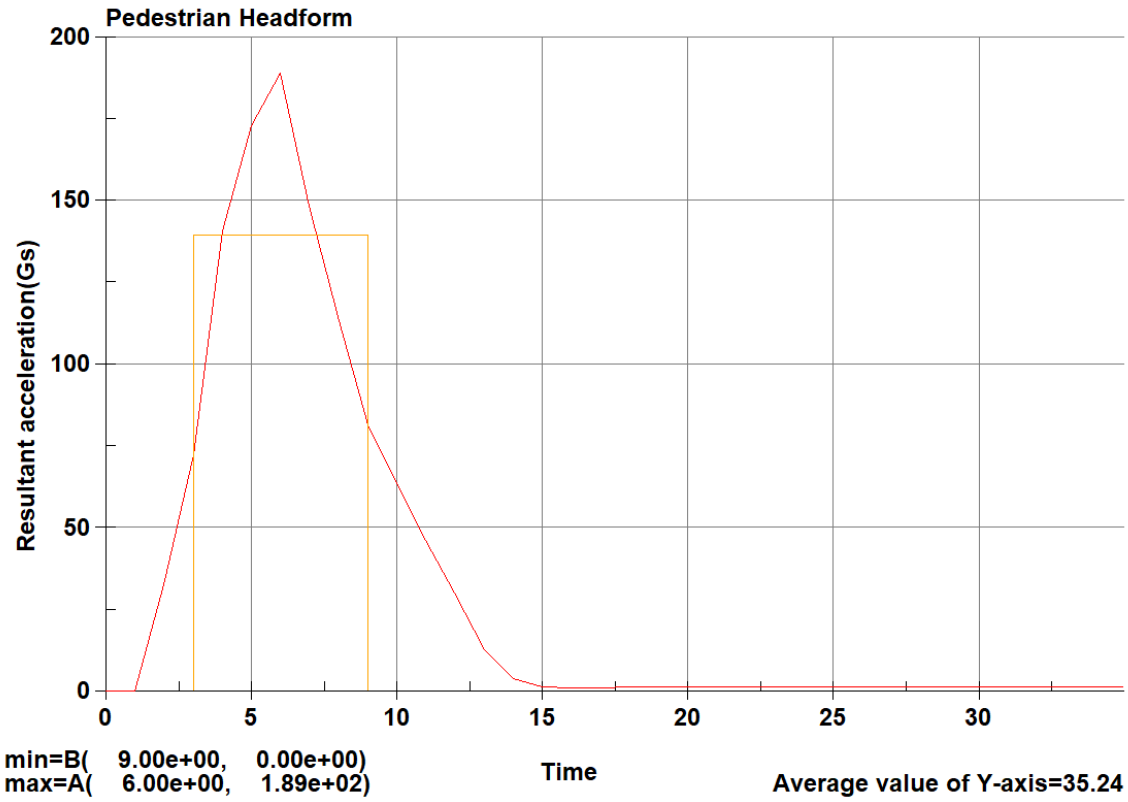

Head impact without Helmet

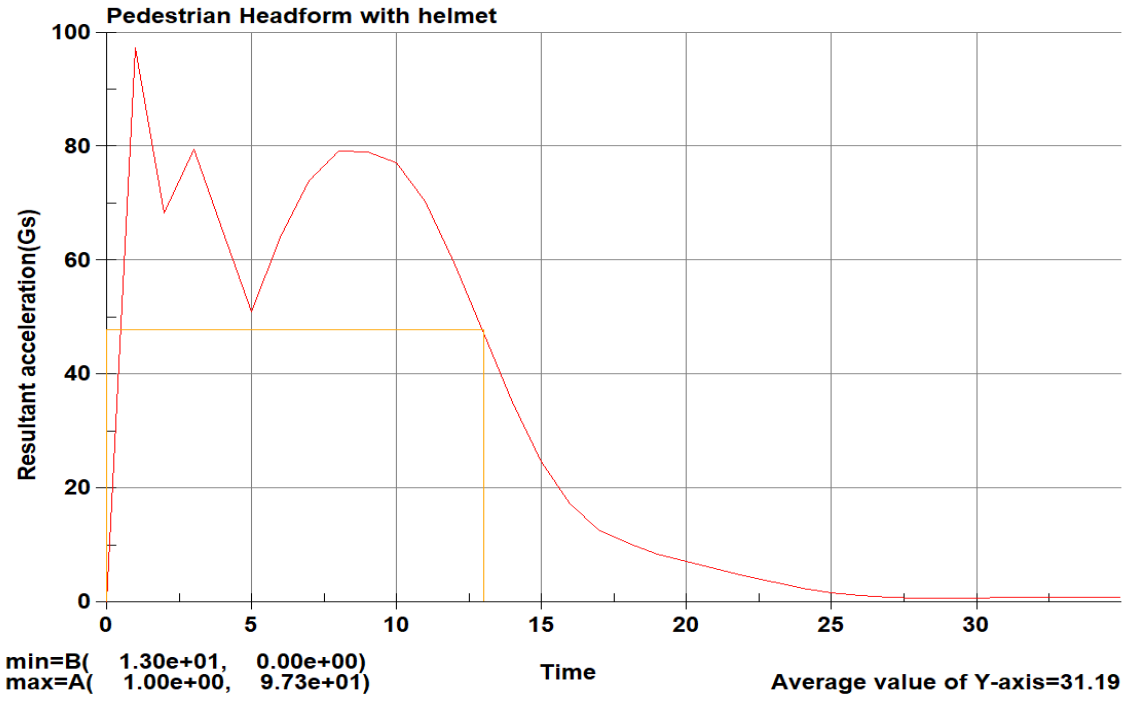

Head impact with Helmet

B.4 Linear Head Acceleration output of Unhelmeted and Helmeted simulation at 14mm/ms

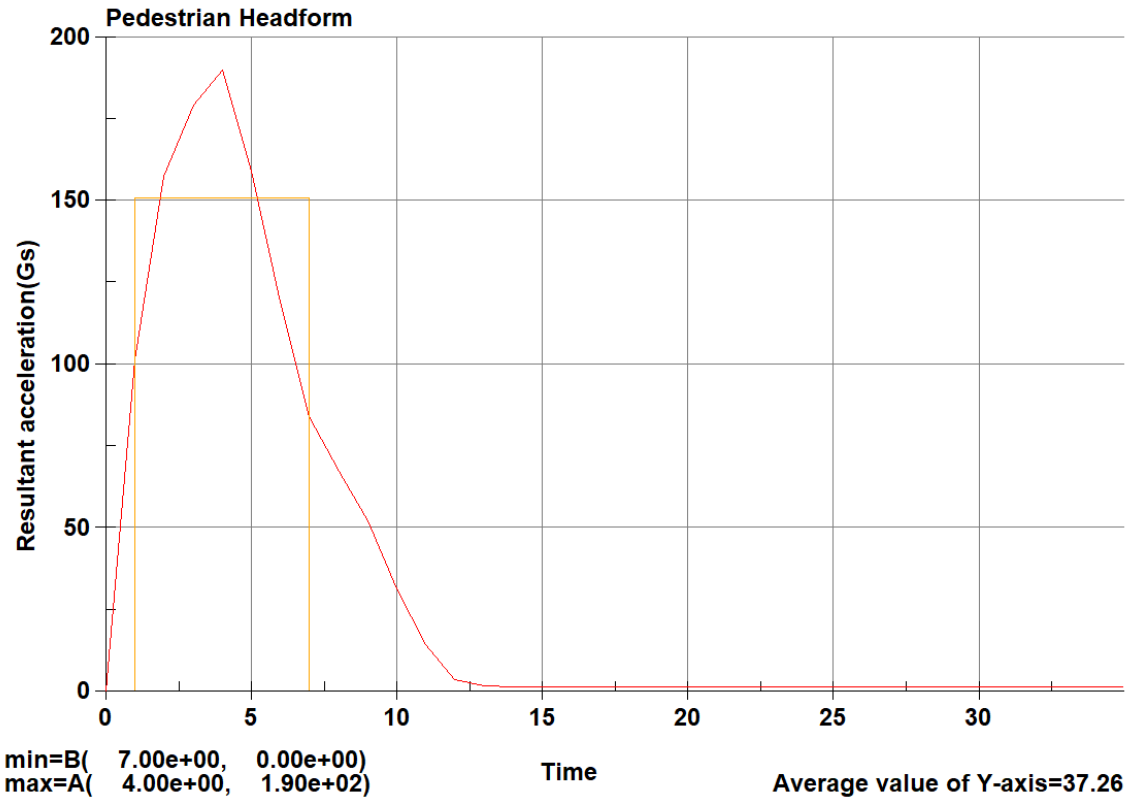

Head impact without Helmet

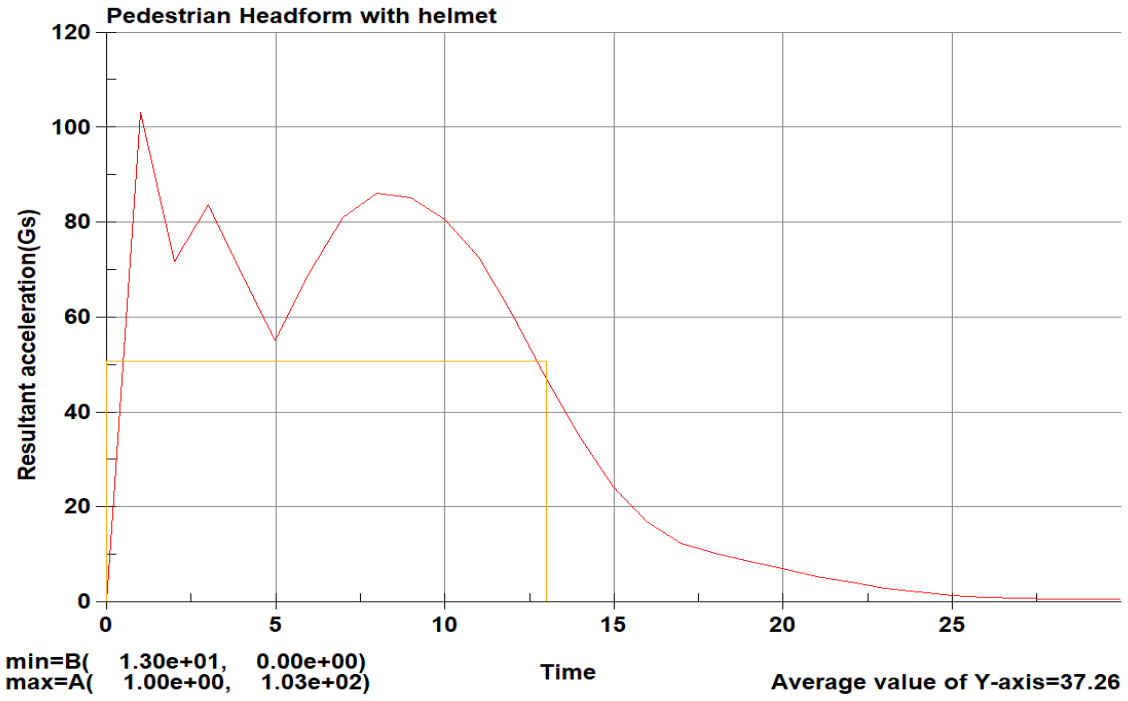

Head impact with Helmet

B.5 Linear Head Acceleration output of Unhelmeted and Helmeted simulation at 15mm/ms

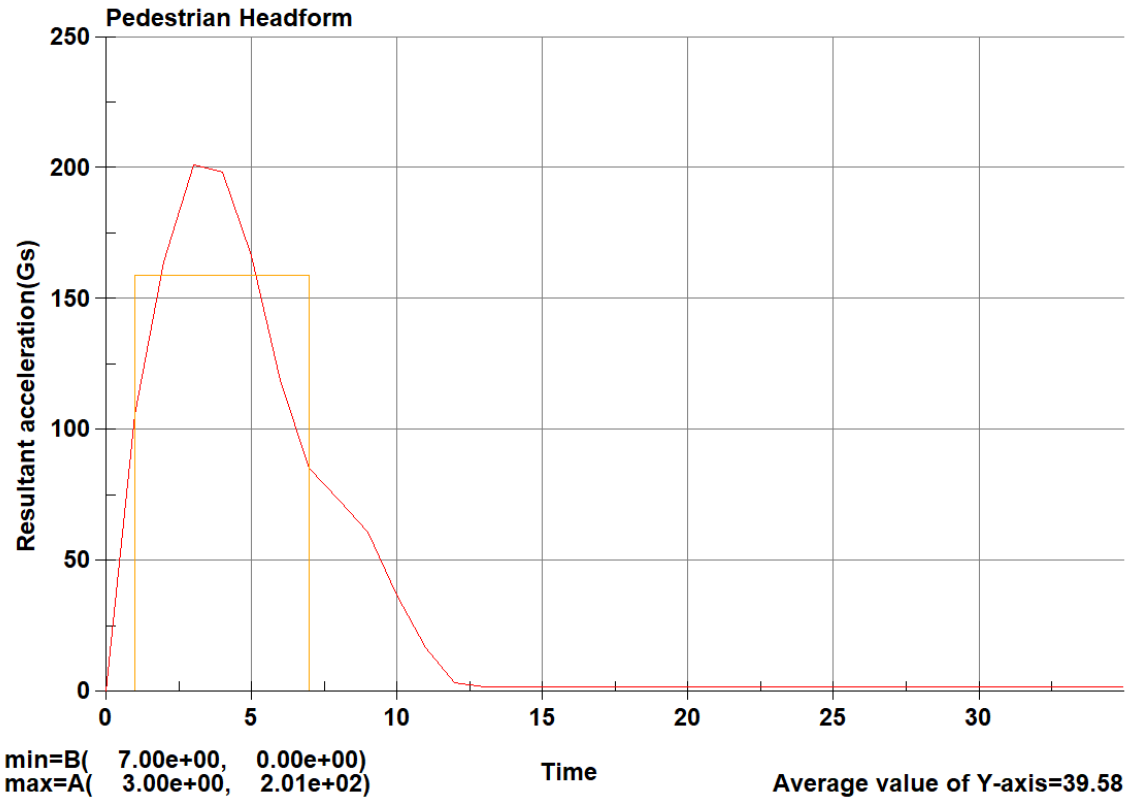

Head impact without Helmet

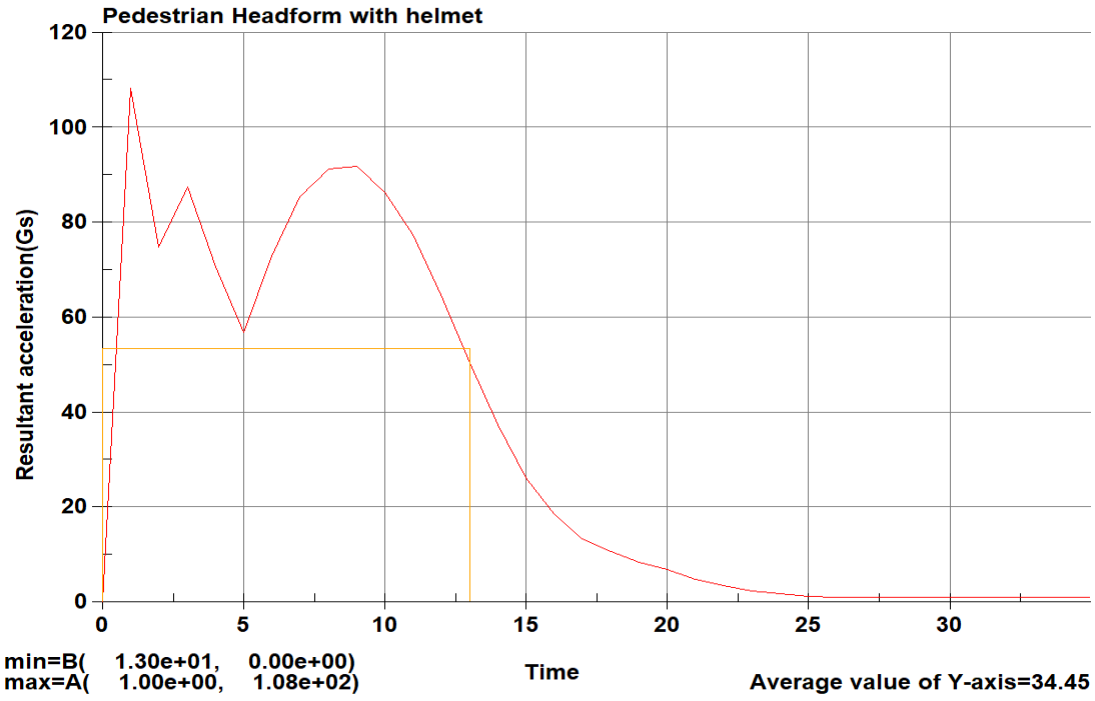

Head impact with Helmet

B.6 Liner Head Acceleration output of Unhelmeted and Helmeted simulation at 16mm/ms

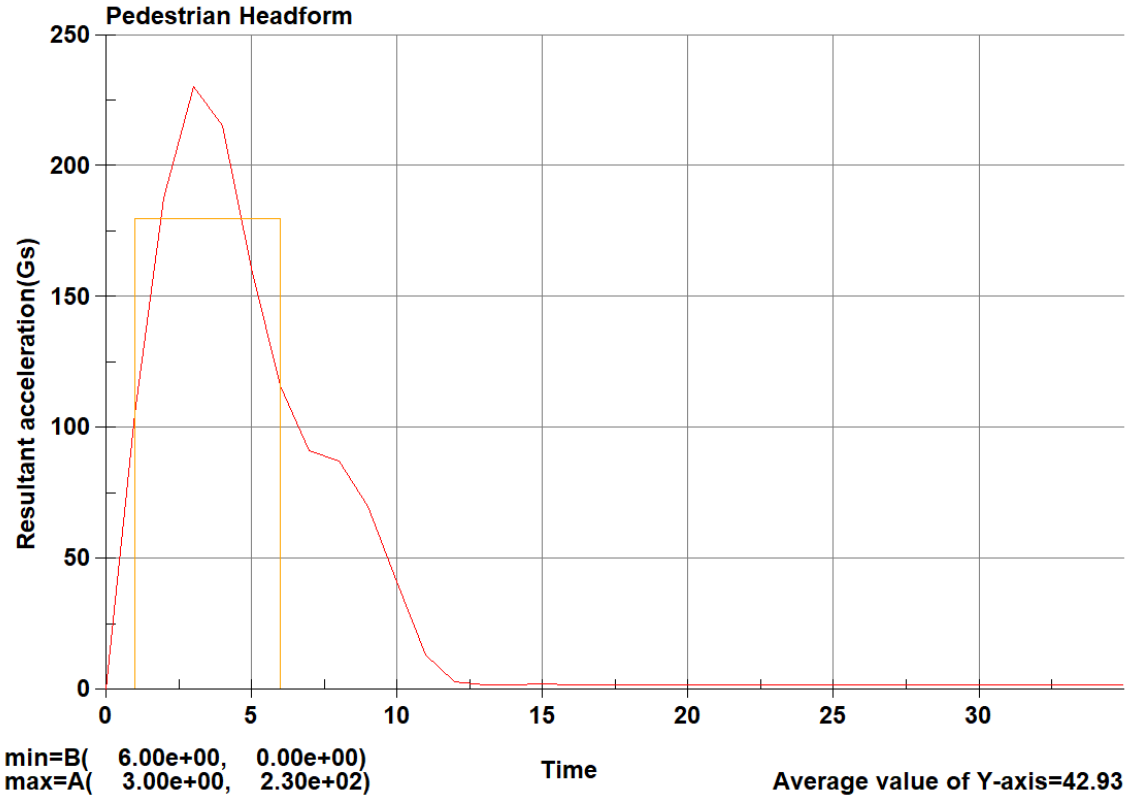

Head impact without Helmet

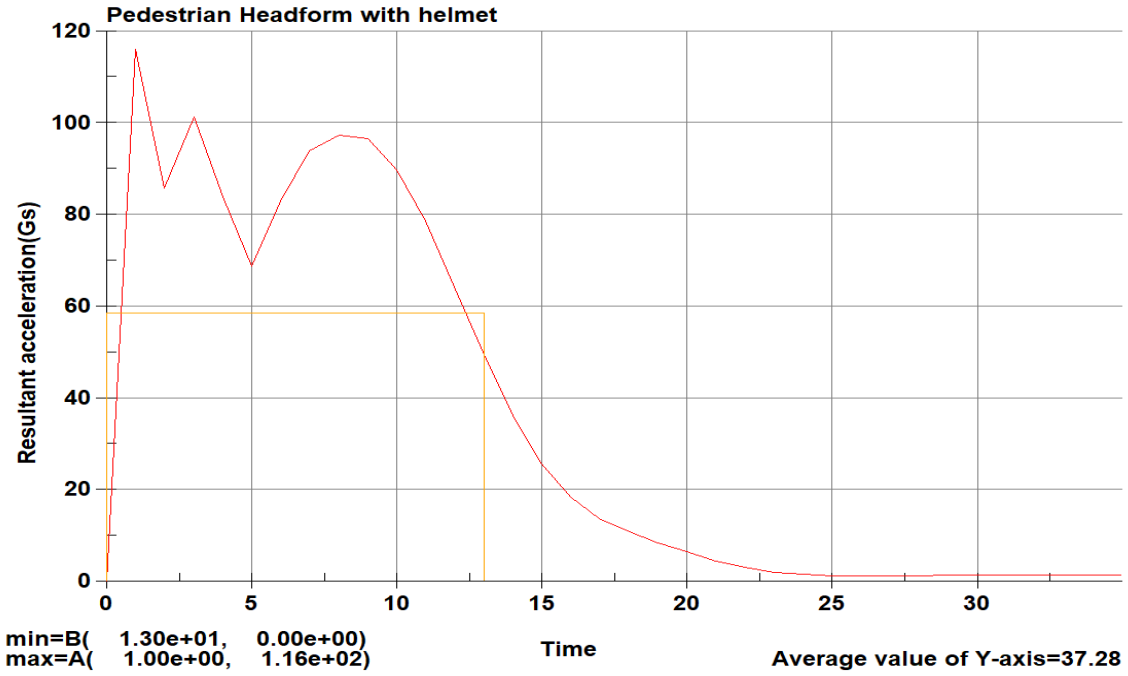

Head impact with Helmet

iThenticate®

Similarity Report ID: oid:3117:588058150

PAPER NAME

Crash Reconstruction and Head Injury Assessment in Motorcycle-Truck Collisions : A Case Study

AUTHOR

Hem Paudel

WORD COUNT

20800 Words

CHARACTER COUNT

120508 Characters

PAGE COUNT

82 Pages

FILE SIZE

2.5MB

SUBMISSION DATE

May 8, 2026 11:10 PM GMT+5:45

REPORT DATE

May 8, 2026 11:11 PM GMT+5:45

2% Overall Similarity

The combined total of all matches, including overlapping sources, for each database.

- 2% Internet database
- 1% Publications database
- Crossref database
- Crossref Posted Content database
- 0% Submitted Works database

Excluded from Similarity Report

- Bibliographic material
- Quoted material
- Cited material
- Small Matches (Less then 10 words)

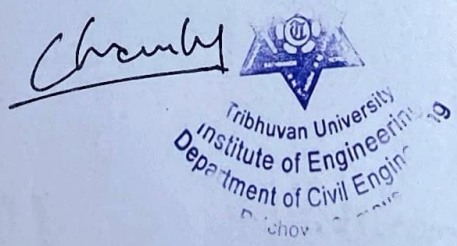

Summary

Regd. No. 70730/066/067

PAN Regd. No. 304131411

LALITPUR ENGINEERING COLLEGE

(Affiliated to TU)

Chakupat, Patandhoka, Lalitpur

Ref.: 411-082-83

Date: April 30, 2026

To Whom It May Concern

This is to certify that the paper titled "**Crash Reconstruction of Mixed-Vehicle Collision Using PC-Crash**" submitted by **Hem Paudel** as the first author has been accepted for publication after the peer-review process. The paper was also formally presented at the **LEC Conference 2026**, held on **31 January 2026** at Lalitpur Engineering College.

Kindly note that the final revision of accepted manuscripts and the formal publication process is currently underway. Inclusion of the accepted manuscript in the LEC Journal "InJET-InDEV, Vol. 2, Issue 2" is contingent upon the author's timely response to editorial revisions requested by the proceedings committee.

Conference Name: 2nd International Conference on Engineering Technology and Infrastructure Development (LEC Conference 2026)

Venue: Lalitpur Engineering College, Lalitpur, Nepal

Date of Presentation: 31 January 2026

Journal Name: InJET-InDEV, Vol. 2, Issue 2

Publication Status: Accepted with minor revision; Publication in progress

Dr. Surendra Bahadur Tamrakar

Principal

Lalitpur Engineering College

Tel: 01-5268215 / 5268216, E-mail: info@lec.edu.np, Url: www.lec.edu.np

International Conference on Engineering Technology and Infrastructure Development
Jan 2026

Crash Reconstruction of Mixed-Vehicle Collision Using PC-Crash

Hem Paudel[1], Rojee Pradhananga [2]

[1]*Department of Civil Engineering , Pulchowk Campus , Institute of Engineering , Lalitpur , 079mstre007.hem@pcampus.edu.np*
[2]*Department of Civil Engineering , Pulchowk Campus , Institute of Engineering , Lalitpur rojee.pradhananga@pcampus.edu.np*

Abstract

Road traffic crashes are a leading cause of injury and property damage worldwide, which has disclosed the need of taking systematic and precise reconstruction techniques. This paper presents the simulation of real-world road crash between a minitruck and a motorcycle using PC-Crash Software. The reconstruction followed a structured four stage workflow, i.e. the reconstruction of the accident scene, Vehicle modeling, crash simulation, and iterative validation. Calibrated simulations established pre-impact speeds of 34 km/h for the minitruck and 18 km/h for the motorcycle, with post-impact rest positions and vehicle orientations showing strong correspondence with physical scene evidence. Most significant dynamic parameters such as head acceleration, contact force and energies were obtained to describe the severity of collisions. The motorcycle was modeled as a complete multibody system including the biomechanical aspects of the rider, which allowed to simulate the realistic behavior of a human body during the impact event. The results show that PC- Crash can be very appropriate in reconstruction of mixed-vehicle collisions within the context of low- and middle-income countries like Nepal, where crash databases are not centralized, and field evidence is represented by police documentation.

Keywords: Crash Reconstruction, PC-Crash, Vehicle Dynamics, Road Safety,

1. Introduction

Traffic safety is a major concern in the present global context. Road crashes are one of the most important factors of injury, death and property damage, impacting millions of lives globally. As per WHO (2023), road traffic crashes claimed the lives of 1.19 million people in 2021, equivalent to 15 deaths per 100,000 population. Low- and middle-income countries account for the deaths of most people in road traffic collisions (about 92%), largely because of inadequate road safety infrastructure and the enforcement of traffic laws. In 2024, Nepal registered 242,441 vehicles, with motorcycles alone accounting for 80.9% of total registrations due to their affordability and suitability for the country's challenging terrain(Department of Transport Management, GoN, 2025). Nearly 160,000 road traffic crashes occurred in Nepal from 2015 to 2024, killing 23,900 people and leaving 50,000 seriously injured (Ghimire et al., 2025; Nepal Traffic Police, 2024) -an average of seven deaths and 83 injuries each day. Estimated economic impact is 1.5 - 2% of GDP, more than national health expenditure for 2021. With these trends, it is now essential to use systematic crash analysis and computational simulation tools like PC-Crash to gain insight into collision patterns, severity of injuries, and to identify targeted safety interventions.

Crash reconstruction is an essential element of road safety research, which offers systematic and technical basis to the study of collision mechanics, identifying contributing factors, and informing both engineering interventions and policy decisions. In high-risk traffic environments for two wheelers such as Nepal, reliable reconstruction methodologies are critical for understanding crash occurrences and designing targeted safety interventions. Conventional analytical or field-based reconstructions are constrained by missing scene evidence, measurement errors, and the lack of capability to test alternative collision hypotheses. These restrictions are especially acute in mixed-vehicle collisions where significant disparities in mass, geometry, and structural stiffness can generate complex pre- and post-impact dynamics that are difficult to resolve through manual calculation alone. These restrictions lead to the necessity of the development of sophisticated simulation tools that can provide detailed, repeatable and physically reliable analysis.

PC-Crash, developed by Dr. Steffan Datentechnik GmbH (DSD), is a complex vehicle dynamics and crash reconstruction software designed to meet the need for more accurate computational analysis of road traffic crashes (Steffan & Moser, 2011). The software incorporates multi-body dynamics and the impulse-based collision model of Kudlich and Slibar which calculates the momentum exchange between vehicles based on pre-impact kinematic conditions and vehicle geometry, along with a parameter set of restitution coefficients and friction parameters (Moser et al., 1999). The application of PC-Crash for research, forensic investigations, and educational uses may be suitable, due to its ability to show crash sequences and to simulate the input of measured field data and the analysis of different variations of scenarios.

Considerable studies have utilized PC-Crash to test different types of collisions proving its applicability in both vehicle-vehicle and vehicle-vulnerable road user studies. Zhang et al.(2014) developed a systematic approach for PC-Crash to simulate vehicle to vehicle interactions and they found that the pre-impact velocity and stiffness coefficients of the collision model of Kudlich (1966) and Slibar (1966) can be iterated to replicate post-impact vehicle kinematics with reasonable accuracy. Zou and Zhang (2013) explained the uncertainty in the simulation outputs, Kong-kang (2008) validated the applicability of PC-Crash as a quantitative crash reconstruction tool by showing its capability to reproduce pedestrian throw distance and impact dynamics in the case of vehicle-pedestrian collisions, provided that input parameters are carefully set. Zou et al. (2010) extended this study by identifying statistical regularities in vehicle-pedestrian collision simulations, and then Zou et al. (2011) compared pedestrian trajectory modeling in PC-Crash with physical evidence, further demonstrating the reliability of PC-Crash as a forensic reconstruction tool. Studies involving motorcycles have also progressed. Zhao et al. (2022) used PC-Crash to reconstruct cyclist and electric bicycles crashes explaining how multibody models were able to produce physically representative injury estimates. Similarly, wang (2019) used detailed human body models to study injury responses of riders on motorcycles and the injury patterns among motorcycles and e-bike riders have been studied through national accident databases and PC-Crash simulation

Although this wide range of applications is available, the available literature is based on either the targeted types of impacts, such as mostly side impacts, or on a single type of vehicle and little has been done on the data constrained phenomena of the low- and middle-income states including Nepal. The field of mixed-vehicle crashes between light commercial vehicles and motorcycles is a relatively under-researched area of the crash reconstruction field, especially when lacking a centralized crash database and instrumental recording devices for crash investigations.

2. Crash Case Introduction

The crash occurred in the morning of 2022 on Kathmandu Ring Road between a fully loaded minitruck and a motorcycle with a rider and a pillion passenger. A fully loaded minitruck was moving along the road, tried to overtake slow moving vehicle by moving into the right lane when it collided with a two-wheeler causing considerable structural of damages to both vehicles. Both two-wheeler occupants sustained severe injuries while the minitruck driver sustained no injuries. Reconstruction was limited to secondary documentary evidence sources, with official police reports used to set up the PC-Crash simulation including the vehicle specifications,

damage patterns, rest positions, skid mark geometry and scene measurements as boundary conditions and validation benchmarks. Measurements and photographic records of the scenes were done by the authorized police officers totally; the researchers did not conduct any measurements independently in the field. The case is noteworthy in that it involves a common but under-studied collision type in Nepal, and that it proves forensically credible reconstruction is possible in a very evidence-limited setting, with important implications for road safety practice where instrumental crash recording is underdeveloped.

3. Methodology

3.1 Data collection

In the lack of a centralized crash database in Nepal, data were collected to support this study using official police records. These sources provided essential information, including type of crash, time of occurrence, vehicle identifications, rider details, helmet usage, injury descriptions. Where available, supplementary data on road geometry, vehicle deformation and collision points were included. Missing vehicle specifications were sourced from verified manufacturer documentation and official technical databases. All scene documents were conducted by the officials; the researchers performed no independent field surveys. The collected data were reviewed for internal consistency and completeness prior to use, ensuring the dataset was sufficient to support a credible reconstruction.

3.2 Vehicle modeling

The information in the official records about the vehicles was compared to the PC-Crash database and in the case, it had no exact models, similar vehicles were adjusted with parameters like mass, dimensions, and wheelbase altered in such a way that they reflected the actual car dynamics as in the Figure 1 a. The diversity of vehicle library at PC-Crash could simulate the physical characteristics and behavior of motion so that collision re-creation would be accurate and visually realistic. Similarly multibody human vehicle model was integrated into PC-Crash environment to realistically model the occupant motion and response throughout the crash incident. The model comprised rigid body segments representing major anatomical regions, connected by articulated joints that permit flexion and movement consistent with human biomechanics (Moser et al., 1999) as shown in Figure 1 b . Each segment was assigned mass, dimensions, and a center of gravity based on standard anthropometric values; the total model represented a typical adult of 70 kg and 170 cm, consistent with available records.

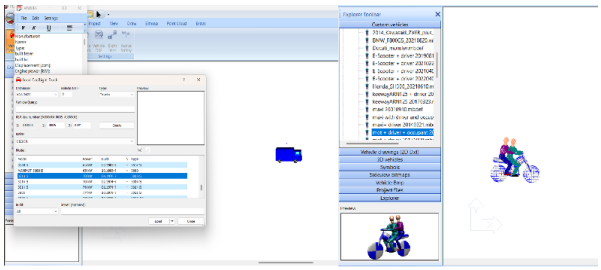

a. Truck model b. Multibody Model

Figure 1 Vehicle model selection from database

3.3 Vehicle setup and data

The motorcycle and minitruck were modeled in PC-Crash using DSD database vehicles that best matched the requirements available in the official records. Critical parameters of vehicle dynamics, such as curb weight, center of gravity, ABS setup, wheelbase, and axle geometry were tuned to produce realistic motion behavior, without

altering standard geometry or suspension inputs. The minitruck was then suspended more rigidly and engine power and torque values were added to reflect the pre-impact acceleration of the mini truck. Linear tire models defined tire properties, such as type, dimensions and spacing, to provide computationally stable and reliable braking performance as shown in Figure 2

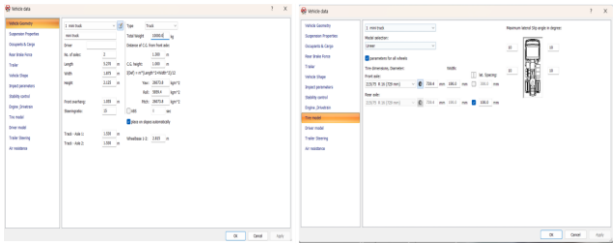

Figure 2: Vehicle parameter input box

3.4 Dynamics modeling

In PC-Crash, the collision event occurred by means of a single and permanently evolving simulation that blended the pre-impact and post-impact vehicle motions. The realistic driver dynamics were included by specifying the sequential control inputs of acceleration, braking and steering during the entire event and thus provided an overall picture of vehicle behavior during the initial approach to the final rest positions.

In the absence of verifiable instrumental speed data, an iterative calibration strategy was adopted. Simulations were initialized at an initial velocity of 35 km/h as a conservative baseline and iteratively refined, converging on pre-impact speeds of 34 km/h for the truck and 18 km/h for the motorcycle. Input parameters were systematically refined across successive runs until the simulated vehicle final positions, motion trajectories, and deformation patterns converged with the physical evidence documented at the crash scene. Figure 3 shows the dynamic control inputs, comprising acceleration of the truck, lane change steering, and braking control and the motorcycle emergency response, which were tuned iteratively to reproduce realistic driver reaction behavior consistent with the documented scenario.

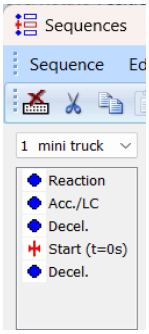

Figure 3: Impact motion sequence box

Lane-change maneuver of the minitruck was determined as a crucial aspect that affected the reconstruction accuracy. Longitudinal acceleration was set to 1.0 m/s 2 and a rightward lane change was performed within 3.25 s (Figure 4). Motion steering was simulated by 3.8 m lateral movement, which is equivalent to the largest lateral acceleration of 4.0 m/s2 and a steering angular velocity of 5.0 deg/s, representing a desperate move. The braking parameters chosen with the data of the RTA crash database were used in order to provide realistic braking deceleration and wheel-specific braking response, avoiding tire lockup or failure.

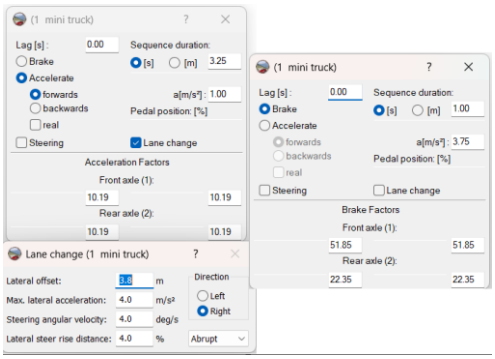

Figure 4: Pre-impact sequence box

3.5 Impact

At the impact phase, the motorcycle multibody system and truck model were placed at the identified POI to simulate the crash event. Initial contact conditions were assigned based on pre-impact speeds of 35 km/h for both vehicles. A coefficient of restitution of e = 0.1 and friction coefficient of μ= 0.6 (S. Wang et al., 2014) were applied to reflect typical road and contact surface conditions, consistent with PC-Crash standard values for this class of collision.

The simulation was run iteratively, with post-impact velocities and final rest positions compared against documented physical evidence after each simulation. Iterations continued until simulated post-impact kinematics and final rest orientations converged with the recorded scene evidence. The motorcycle was modeled as a complete multibody system with integrated rider biomechanics, allowing for a physically representative response of the human body during and following the impact. The POI location determined from this process is illustrated in Figure 5.

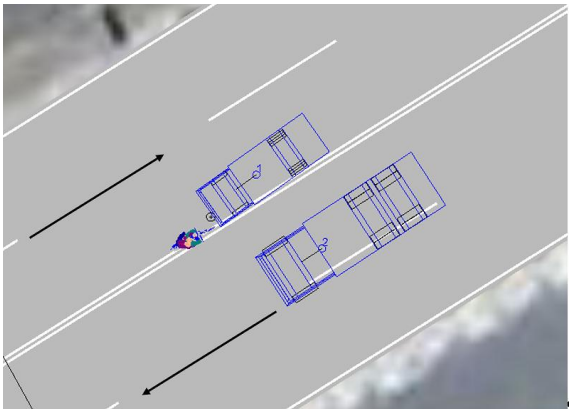

Figure 5: location of impact point

3.6 Validation

Validation of the reconstruction was carried out by systematically comparing the results of the simulation to the physical evidence found that was documented in the official police records. The accuracy of reconstructed model was assessed based on four main parameters;

3.6.1 Crash location and point of impact

The point of impact simulation was compared to physical evidence markers at the crash scene. The spatial coordinates obtained from the simulation were compared with the official police report to validate positional accuracy.

3.6.2 Vehicle motion

Vehicle paths were modified to achieve the proper spatial and temporal alignment at the collision site. The minitruck's trajectory included an overtaking move (lateral translation of about 3.5 m, or equivalent to a sudden lane change to overtake a slower vehicle). This adjustment enabled the relative position, approach vector and the timing of both cars to intersect correctly at the point of collision, as indicated by physical evidence and documentary evidence.

3.6.3 Post-crash position

The accuracy of the calibration was evaluated by comparing the resting positions obtained after the impact with the values in the official police report. The truck stopped at 11.0 m from the collision point and the rider was thrown 12.4 m from the impact point. The simulated rest position using the calibrated simulation was found to be 10.8 m and 12.1 m, which gave absolute errors of 0.2 m (1.8%) and 0.3 m (2.4 %), respectively. These deviations are within the allowable ±5% range of PC-Crash reconstruction, which proves the good validation of the impact parameters and simulation.

3.6.4 Damage zone analysis

Both vehicles impact areas were compared to descriptions in the police report to confirm simulated impact locations and damage severity. The motorcycle had extensive frontal damage and the truck had moderate damage to the headlight on the left side. The average magnitudes for the forces of contact for the motorcycle components were much greater than the forces for the minitruck components, and this was a reflection of the degree of damage as mentioned in post-crash vehicle inspection report. There was minimal photographic evidence but the locations of the damages and force levels were sufficiently close to what has been reported, which supports the validity of the reconstruction.

The lack of instrumental data sources (such as Event Data Recorder (EDR) outputs and speed camera videos) made it impossible to use independent velocity validation methodologies. Conversely, a systematic iterative calibration approach was used, where speed parameters for the pre-impact conditions were iterated based on convergence of evidentiary constraints from both spatial, orientational and damage. This multi-criteria calibration method thus served as the primary evidence-based validation model for the reconstructed collision scenario.

4. Result and Discussion

4.1 Overview

A physics-based kinematic and dynamic simulation of motorcycle-minitruck crash was performed in the PC-Crash multibody simulation environment. The incident described was a two-occupant motorcycle travelling on an urban carriageway when it collided with a minitruck, resulting in severe head injuries. The boundary condition inputs were obtained from official documentation, georeferenced satellite Google maps and the PC-Crash integrated vehicle dynamics database. The fidelity of the reconstruction was developed through a systematic iterative process of progressively refining pre-impact velocities, impact vectors and contact geometry until reconstruction results of post-impact trajectories, final rest positions and crush damage patterns matched available physical evidence.

4.2 Key reconstruction outcomes

The calibrated simulation resulted in pre-impact velocities of 34 km/ph and 18 km/ph for the minitruck and motorcycle, respectively. Pre collision kinematic analysis showed that the minitruck accelerated forward at a rate

of 1 m/s2 and then suddenly moved to change lanes to the right, resulting in a lateral offset of 4 m and a peak lateral acceleration of 4 m/s2 in an attempt to pass another slow-moving vehicle. The reconstructed impact point was 0.6 m into the motorcycle's designated travel lane from the solid double centerline marking, which confirmed lane boundary encroachment by the minitruck. Post-impact rest positions were about 10 m and 12 m away from the impact point for the minitruck and the motorcycle, respectively, which was consistent with police scene documentation. Contact force analysis showed that the impact forces recorded on the motorcycle were higher than those recorded on the minitruck, which was supported by case recorded vehicle damage evidence.

4.3 Discussion

The results validate the effective applicability of PC-Crash to mixed-vehicle collision reconstruction, when input parameters are carefully defined and systematically calibrated. Pre-impact velocities of 34 km/h for minitruck and 18 km/h for motorcycle, were determined using a multi-criteria iterative calibration procedure, in which outputs from the simulations were compared to spatial, orientational and damage-based physical evidence. The significant difference in contact forces between the two vehicles is physically consistent with the differences in mass and structural stiffness between the vehicles, and directly confirms the severity of the injuries sustained by the motorcycle occupants of the collision and the biomechanical vulnerability of motorcycle users in heavy goods vehicle collisions at urban speeds. The post impact rest positions, orientations of vehicle and rider, and ejected trajectory of the rider were all in close agreement between simulation and police documented and contributed to the confidence in the kinematic reconstruction. The collision dynamics described in the simulation are subject to uncertainty, mainly related to assumptions made about vehicle stiffness and the simplified tyre-ground interaction model used in PC-Crash, which are inherent limitations and should be taken into account when interpreting the estimated collision dynamics.

5. Conclusion

The given research has shown the effectiveness of PC-Crash to reconstruct and simulate mixed-vehicle crashes in data-limited situations. Besides accurately modelling the complete sequence of impact, such as pre-impact vehicle motion, the geometry of an impact point and the post-impact speed and rest positions, the simulation also converged on the final positions simulated within the range of about 0.3 to 0.5 meters over the recorded scene data. Mechanically consistent representations of the severity of the collision are provided by calibrated pre-impact speeds of 34 kmph of the minitruck and 18 kmph of the motorcycle along with extracted impact force and energy dissipation measures. The use of a multibody rider model also helped in the realistic simulation of the occupant kinematics during and after impact, thus giving significant information on the mechanisms of injury causation. This evidence supports the suitability of PC-Crash to forensic crash investigation and traffic safety evaluation. The method should be further strengthened by independent modeling of the pillion passenger, sensitivity analysis of the key input parameter. Future research should focus on validating reconstruction outputs using instrumentally measured crash data, where available

References

Department of Transport Management, GoN. (2025). *Annual Progress Report 2025* [DoTM Annual Progress Report]. Government of Nepal, Department of Transport Management. https://dotm.gov.np/content/27/annual-progress-report-2081-82/

Ghimire, J., C, L. K., Kafle, K. R., & Adhikari, B. (2025). Road Safety in Numbers: Using Data to Illustrate the Nepal's Scenarios. *American Journal of Traffic and Transportation Engineering*, *10*(5), 120–134. https://doi.org/10.11648/j.ajtte.20251005.13

Kong-kang, Z. (2008). Study of Simulation of Vehicle-Pedestrian Collision Accident Based on PC-Crash. *Tractor & Farm Transporter*. https://www.semanticscholar.org/paper/Study-of-Simulation-of-Vehicle-Pedestrian-Collision-Kong-kang/47c5d3d666e96cd73a5dbcdf425cae8c0610c322#citing-papers

Kudlich, H. (1966). *Beitrag zur mechanik des kraftfahrzeug-verkehrsunfalls*. na.

Moser, A., Steffan, H., & Kasanický, G. (1999). *The Pedestrian Model in PC-Crash—The Introduction of a Multi Body System and its Validation*. SAE International. International Congress & Exposition. https://doi.org/10.4271/1999-01-0445

Nepal Traffic Police. (2024). https://traffic.nepalpolice.gov.np/publication/5/

Slibar, A. (1966). Die mechanischen Grundsätze des Stoßvorganges freier und geführter Körper und ihre Anwendung auf den Stoßvorgang von Fahrzeugen. *Archiv Für Unfallforschung*, *2*(1), 31.

Steffan, H., & Moser, A. (2011). PC-Crash, a simulation program for vehicle accidents. *Technical Manuel, Mac Innis Engineering*.

Wang, longliang. (2019). *Research on Head Damage of Cyclists in Vehicle-Electric Two-wheeled Vehicle Collision Accident Based on THUMS Mode*.

Wang, S., Qian, Y., & Qu, X. (2014). Reconstruction of Car-Electric Bicycle Side Collision Based on PC-Crash. *Journal of Transportation Technologies*, *04*, 355–364. https://doi.org/10.4236/jtts.2014.44032

WHO. (2023). *Global status report on road safety 2023*. https://www.who.int/publications/i/item/9789240086517

Zhang, Y. G., Xu, J. M., Zou, T. F., & Liu, Y. (2014). A Method for Reconstructing Vehicle—Vehicle Impact Accidents Based on Pc-Crash. *Applied Mechanics and Materials*, *641–642*, 799–804. https://doi.org/10.4028/www.scientific.net/AMM.641-642.799

Zhao, L., Wu, H., Yang, N., & Wang, J. (2022). Cyclist head injuries Based on an electric bicycle to car accident reconstruction. *Computer Technology and Transportation ISCTT 2022; 7th International Conference on Information Science*, 1–4. https://ieeexplore.ieee.org/abstract/document/10071868

Zou. (2010). *Zou, T.F., Yu, Z. and Chai, M. (2010) Study on Laws of Vehicle-Pedestrian Accident Simulation Based on Pc-Crash Software. Journal of China Safety Science, 2, 54-58. - References—Scientific Research Publishing*. https://www.scirp.org/reference/referencespapers?referenceid=1324578

Zou, T., zhi, yu, & ming, cai. (2011). Car-Pedestrian Accident Reconstruction Based on Pc-Crash. *Journal of Vibration and Shock*, *30*(3), 215–219. https://jvs.sjtu.edu.cn/EN/Y2011/V30/I3/215

Zou, T.-F., & Zhang, Y.-G. (2013). Methods for analyzing uncertainty of results in accident simulation. *Zhendong Yu Chongji/Journal of Vibration and Shock*, *32*, 176-180+184.